SOLUÇÃO NUMÉRICA DE EQUAÇÕES DIFERENCIAIS ORDINÁRIAS USANDO INTEGRAÇÃO DA TRANSFORMADA DE LAPLACE

Ana Cecilia Rojas Mendoza

Dissertação apresentada
ao
Instituto de Matemática e Estatística
da
Universidade de São Paulo
para
obtenção do título
de
Mestre em Ciências

Programa: Matemática Aplicada

Orientador: Prof. Dr. Pedro da Silva Peixoto

O presente trabalho foi realizado com apoio da Coordenação de Aperfeiçoamento de Pessoal de Nível Superior - Brasil (CAPES) - Código de Financiamento 001

São Paulo, março de 2020

Numerical Solution of Ordinary Differential Equations Using Laplace Transform Integration

Esta versão da dissertação contém as correções e alterações sugeridas pela Comissão Julgadora durante a defesa da versão original do trabalho, realizada em 20/03/2020. Uma cópia da versão original está disponível no Instituto de Matemática e Estatística da Universidade de São Paulo.

Comissão Julgadora:

- Prof. Dr. Pedro da Silva Peixoto (orientador) - IME-USP
- Prof. Dr. Rudimar Luiz Nós - UTFPR
- Prof. Dr. André Pierro Camargo - UFABC

Agradecimentos

En primer lugar quiero agradecer a Dios, por darme la fuerza y paciencia necesarias para superar las dificultades en mi vida. Agradezco a mis padres, Haydeé y Roberto, por eseñarme la importancia de estudiar y superarse. A mi hermana Maruja, casi mi hija, le agradezco por ser mi amiga siempre. A mis queridos padrinos, Dalila y Luis, por ser como mis segundos padres y darme su cariño incondicional. Mi gratitud infinita a mis amigas de toda la vida: Maria Fernanda, Fiorella, Laly, Lyzeth, Lenny, Jocelyne, Claudia S. y Rossy, por acompañarme en mis días grises y claros, por hacerme reir y apoyarme durante esta caminata.

Un agradecimiento especial a Robert, que con poco de conocerme, fue mi guía y amigo a mi llegada a São Paulo. A Deissy y Lorena, dos grandes amigas, por su ánimo y aliento constante.

Com carinho especial, agradeço a todas as pessoas que se tornaram minha familía em São Paulo. Ao meu querido orientador Dr. Pedro da Silva Peixoto, cuja paciência, apoio e incentivo valiosos foram fundamentais para alcançar meu objetivo. À Larissa, a minha melhor amiga, pela sua companhia e paciência em tempos difíceis e felizes. À Bruna, pelos conselhos e carinho. À Luana, Polly, Jerusa, Vanessa e Simone por me fazer rir sempre. À Laura, porque mesmo estando longe, sempre se preocupa comigo. Ao Erick, meu irmão e melhor amigo, por estar sempre ao meu lado. Agradeço também ao Leonardo, Luan e Fernando, por esclarecer minhas dúvidas sempre que precisei.

Gostaria de agradecer também à Fabiana, Rodrigo e Nanda, três pessoas muito queridas que entraram na minha vida e me ajudaram no meu objetivo de melhorar minha qualidade de vida e minha autoestima. Além disso, expresso minha gratidão à Juliana, Nathália, Erika, Carol, Aninha, Isa e Mari. Sua companhia me ajudou a clarear minha mente e trabalhar melhor na minha dissertação.

Agradeço a todos os funcionários que trabalham no IME, secretárias, pessoal da biblioteca, da gráfica, segurança e limpeza, que fazem deste um local agradável para estudar.

Finalmente, quero agradecer à CAPES pelo apoio financeiro durante o mestrado, que foi muito importante para o desenvolvimento deste trabalho. À Universidade de São Paulo, por dar-me a oportunidade de evoluir como profissional fazendo o mestrado aqui. Agradeço, em geral, a todas as pessoas que de forma direta ou indireta tornaram a minha estadia mais agradável e feliz.

Abstract

ROJAS MENDOZA, ANA C. **Numerical Solution of Ordinary Differential Equations Using Laplace Transform Integration**. 2020.89 f. Dissertation (Master's degree) - Institute of Mathematics and Statistics, University of São Paulo, São Paulo, 2020.

Oscillatory problems modeled by differential equations are called *stiff* when the eigenvalues vary (simultaneously) in different orders of magnitude: high values cause rapid oscillations while small values cause slower oscillations. The time step size of the numerical methods used to integrate such models is usually restricted by stability requirements. An explicit method will need a relatively small time step, whereas with an implicit method it is possible to take larger time steps, but usually impacting the accuracy of the solution. The aim of this work is to obtain a numerical integration method that allows us to use larger time steps maintaining stability and precision. An alternative method to solve differential equations based on the Inverse Laplace Transform is developed. The numerical scheme is defined, taking advantage of the properties of the Laplace Transform and making some modifications on the integration contour. We analyze the method for different cases, including applied models, in order to establish a relationship between the integration parameters and to obtain optimal conditions to maintain stability, precision and the ability to use larger time steps. In addition, under certain conditions, we also analyze the ability of the method to act as a high-frequency component filter. The comparison of this method with the Fourth Order Runge Kutta Method, for different cases, reveals that it is possible to take much larger time steps without affecting stability and accuracy. Moreover, unlike the Runge Kutta Method, in the Laplace Integration Method each evaluation is independent of each other. This implies that the calculations can be executed in parallel, which could reduce the computation time.

Keywords: Laplace Transform, Inverse Laplace Transform, Time integration, Integration contour, Filtering.

Resumo

ROJAS MENDOZA, ANA C. **Solução Numérica de Equações Diferenciais Ordinárias usando Integração da Transformada de Laplace**. 2020. 89 f. Dissertação (Mestrado) - Instituto de Matemática e Estatística, Universidade de São Paulo, São Paulo, 2020.

Problemas oscilatórios modelados por equações diferenciais são chamados *rígidos* quando os autovalores variam (simultaneamente) em diferentes ordens de grandeza: valores elevados causam oscilações rápidas, enquanto valores pequenos causam oscilações mais lentas. O tamanho do passo de tempo dos métodos numéricos usados para integrar esses modelos geralmente é restrito pelos requisitos de estabilidade. Um método explícito precisará de um passo de tempo relativamente pequeno, enquanto que, com um método implícito é possível usar passos de tempo maiores, mas geralmente afetando a precisão da solução. O objetivo deste trabalho é obter um método de integração numérica que nos permita usar passos de tempo maiores, mantendo a estabilidade e a precisão. Um método alternativo para resolver equações diferenciais ordinárias baseado na Transformada Inversa de Laplace é desenvolvido. O esquema numérico é definido aplicando as propriedades da Transformada de Laplace e fazendo algumas modificações no contorno da integração. Analisamos o método para diferentes casos, incluindo modelos aplicados, a fim de estabelecer uma relação entre os parâmetros de integração e obter condições ideais para manter a estabilidade, a precisão e a capacidade de usar passos de tempo maiores. Analisamos também, sob certas condições, a capacidade do método de atuar como um filtro de componentes de alta frequência. A comparação desse método com o Método de Runge Kutta de quarta ordem, para diferentes casos, revela que é possível utilizar passos de tempo muito maiores sem afetar a estabilidade e a precisão. Além disso, ao contrário do Método de Runge Kutta, no método de integração de Laplace cada avaliação é independente. Isso implica que os cálculos podem ser executados em paralelo, o que poderia reduzir o tempo de computação.

Palavras-chave: Transformada de Laplace, Transformada Inversa de Laplace, Integração no tempo, Contorno de Integração, Filtragem.

Contents

List of Abbreviations ix

List of Figures xi

List of Tables xiii

1 Laplace Transform Theory 5
- 1.1 Existence and Uniqueness Requirements . . . 5
- 1.2 Properties . . . 8
- 1.3 Laplace Transform of some Functions . . . 10
- 1.4 Application to ODEs . . . 10
- 1.5 Inverse Laplace Transform . . . 11

2 Laplace Transform Integration Method 15
- 2.1 Numerical Inverse Laplace Transform . . . 15
- 2.2 Truncated Exponential . . . 18
- 2.3 Stability Criteria for Linear IVPs . . . 20
- 2.4 Numerical ODEs . . . 24

3 Numerical Results 29
- 3.1 Linear Case . . . 29
  - 3.1.1 Theory Validation: Effect of the Truncated Exponential . . . 29
  - 3.1.2 Linear ODEs . . . 31
- 3.2 Filter Case . . . 37
  - 3.2.1 Effect of the Truncated Exponential . . . 38
  - 3.2.2 Filtering . . . 39
- 3.3 Non-linear ODEs . . . 43
- 3.4 Stability Limitations of the LTIM . . . 47
  - 3.4.1 Numerical instability due to roundoff errors . . . 47

4 Comparison with Fourth Order Runge Kutta Method 51
- 4.1 Linear Initial Value Problem . . . 51
- 4.2 Non-linear Initial Value Problem . . . 53
  - 4.2.1 Swinging Spring System . . . 53

5 Conclusions 57

Bibliography **59**

Complex Analysis Review **63**

.1 Complex numbers 63

.2 Complex functions 65

.3 Analytic functions and Cauchy Riemann conditions 68

.4 Integrals in the complex plane 69

List of Abbreviations

ODE	*Ordinary Differential Equation*
IVP	*Initial Value Problem*
LT	*Laplace Transform*
ILT	*Inverse Laplace Transform*
LTIM	*Laplace Transform Integration Method*
RK4	*Fourth Order Runge Kutta Method*

List of Figures

1.1 Function with a jump discontinuity in $t = t_0$. 6
1.2 Bromwich integral domain. 11
1.3 Bromwich closed contour $C = C_R \cup L$. 12
1.4 Bromwich close contour for $\widehat{f}(s) = \frac{1}{s-a}$. 13
1.5 Alternative Bromwich close contour 13

2.1 Original contour vs Close contour C^* 15
2.2 Relation between ds and Δs_n. 16
2.3 C^* vs C_N^* 17

3.1 Error Comparison in $\|\cdot\|_\infty$ between the full and truncated exponential. 30
3.2 Error Comparison in $\|\cdot\|_\infty$ between the full and truncated exponential, using a smaller time step. 30
3.3 Solution for IVP 3.1 using the full and truncated exponential with 10 time steps and $N = 12$. 31
3.4 Exact solution vs Approximate solutions for $\gamma = 2.1$. 31
3.5 Exact solution vs Approximate solutions for $\gamma = 3.3$. 32
3.6 Number of s-points (N) vs Maximum Error with $dt = 0.0390625$. 32
3.7 Number of s-points (N) vs Maximum Error, $dt = 1.25$ 33
3.8 γ vs Maximum Error, $N = 12$ 33
3.9 γ vs Maximum Error, $N = 52$ 34
3.10 N vs Maximum Error, $\gamma = 2.1$ 34
3.11 N vs Maximum Error, $\gamma = 3.3$ 35
3.12 Damping function for the linear case. 37
3.13 Error Comparison ($in\|\cdot\|_\infty$) between the full and truncated exponential - Filter case. 38
3.14 Error Comparison in $\|\cdot\|_\infty$ between the full and truncated exponential - Filter case . 39
3.15 Exact filtered solution X_1^* vs Approximate filtered solutions with $dt = 0.15625$. . . . 40
3.16 Exact filtered solution X_1^* vs Approximate filtered solutions with $dt = 0.15625$. . . . 40
3.17 Exact filtered solution X_2^* vs Approximate filtered solutions with $dt = 0.15625$. . . . 41
3.18 Exact filtered solution X_2^* vs Approximate filtered solutions with $dt = 0.15625$. . . . 41
3.19 N vs Maximum Error for X_2^* with $dt = 0.15625$. 42
3.20 N vs Maximum Error for X^{*1} with $dt = 0.15625$. 42
3.21 Exact solution vs Approximate solutions with $dt = 0.3125$. 43
3.22 Exact solution vs Approximate solutions with $dt = 0.15625$ 43
3.23 N vs Maximum Error ($\|\cdot\|_\infty$) for $dt = 0.009766$. 44

3.24 N vs Maximum Error ($\|\cdot\|_\infty$) for $dt = 0.015625$ . . . 44
3.25 N vs Maximum Error ($\|\cdot\|_\infty$) . . . 45
3.26 N vs Maximum Error ($\|\cdot\|_\infty$) . . . 45
3.27 dt vs Maximum Error . . . 46
3.28 dt vs Maximum Error. . . . 47
3.29 γ vs Maximum Error. . . . 48
3.30 dt vs Maximum Error. . . . 48
3.31 γ vs Maximum Error. . . . 49
3.32 Stability Region of LTIM. . . . 50

4.1 Stability Region of RK4. . . . 51
4.2 Swinging Spring Pendulum. . . . 53
4.3 Angular Amplitude and Radial Amplitude. . . . 54
4.4 Angular Velocity and Radial Velocity. . . . 54
4.5 Error Comparison RK4 vs LTIM. . . . 55
4.6 Error Comparison RK4 vs LTIM - Zoom. . . . 55

1 Argand Plane. . . . 63
2 Complex circle of radius r. . . . 64
3 Roots of the unity - Example .1 . . . 66
4 Complex logarithm. . . . 68
5 On the left an example of a simple contour, on the right an example of a closed simple contour. . . . 69
6 Independence of the path, $C = C_1 + C_2$. . . . 70
7 Deformation of the paths. . . . 71
8 Contour C deformed into a circle C_δ. . . . 72
9 Annulus of convergence for Laurent series. . . . 74
10 Semicircle C_R . . . 75

List of Tables

1.1 Laplace Transforms - Spiegel (1965) 10

2.1 Time Steps for different values of N and a fix value of γ 23

3.1 Error Decay Order p for a fix $dt = 0.625$. 36
3.2 Error Decay Order p for a fix $\gamma = 3.3$. 36
3.3 Error Decay Order with respect to the time step 46
3.4 Analytical and Numerical dt for $N = 160$ 49

4.1 Fourth Order Runge Kutta vs LTIM I. 52
4.2 Fourth Order Runge Kuta vs LTIM - II. 52
4.3 Fourth Order Runge Kuta vs LTIM III. 52
4.4 On the left: Time steps and number of evaluations for Rk4. On the right: Time steps and number of evaluations for LTIM using $\gamma = 40$ and $N = 40$. 55

Introduction

Many problems in science and engineering lead to the necessity of solving systems of differential equations, which is not always an easy task. Differential equations are used to model problems that describe physical phenomena like Weather prediction, Motion of the Planets, Electrical Systems, Molecular Dynamics and Population Growth (Griffiths and Highman (2010), Randall (2013), Coiffer (2011), Logemann and Ryan (2013), Langer (1954), Ahmad and Ambrosetti (2014), Deng (2015)). These mathematical models are accompanied by a set of initial and boundary conditions given by the problem. Usually, the analytic solutions of these equations are hard to find or non-existent so numerical methods must be used (See Mayers and Süli (2003), Bishop and Isaacson (2003), Burlish and Stoer (2002)).

Naturally, some difficulties arise in the development of the numerical solution of differential equations. One of them is the simultaneous variation of the eigenvalues of the differential systems with different orders of magnitude. In oscillating systems, large eigenvalues produce rapid oscillatory solutions, while small eigenvalues produce slow oscillatory solutions. Depending on the method, the stability requirements compromise the size of the time step. Explicit methods need a relatively small time step in order to guarantee stability and accuracy and implicit methods will allow larger time steps, however, there is no guarantee of accuracy. The set of differential equations that produce this behavior is called *stiff equations*.
Some examples of stiff systems are those with wave propagation such as weather, climate, seismic imaging, and electrical systems. The methods designed to solve stiff equations allow to use larger time steps maintaining stability and precision, however there is a price to pay, the computational cost. Some of these time stepping strategies and methods are discussed in Busch *et al.* (2014), Aydin and Kizilkan (2012) and Rahman and Thohura (2013).

Another class of methods developed to solve initial value problems are the Exponential Integrator Methods (See Hochbruck and Ostermann (2010), Cox and Matthews (2002), Pope (1963)). The exponential integrator methods are based on the exact integration of the linear part of the differential system using matrix exponentials, with the aim of avoiding the stiffness of the problem, improving the stability properties for larger time steps and achieving accuracy.

An integration method that has similar characteristics to the exponential integrator methods is given by the Laplace Transform formula. The basic idea is to convert an Initial Value Problem in the time domain (or t-domain) into an equivalent algebraic problem in a frequency domain (or s-domain). Once the algebraic expression is obtained, the inverse transform will give the solution of the differential equation system.

The Laplace Transform, defined for a time function $f(t)$ as

$$\widehat{f}\,(s) = \mathfrak{L}\{f(t)\} = \int_0^\infty e^{-st} f\,(t)\,dt, \quad s \in \mathbb{C}, \tag{1}$$

is an important mathematical tool that has different applications in science and engineering fields, for example, Nuclear Physics, Control Theory and Signal processing (See Sawant (2018), Li *et al.*

(2010), Rani *et al.* (2019), Ngounda (2009), Ahmad and Javidi (2013), Al *et al.* (2016)). The Laplace Transform is useful to examine different aspects of a physical system. The real part of s in Equation (1) is related to the quantity of damping and decay of the system and the imaginary part is related to the frequency part of the system.

On the other hand, the Inverse Laplace Transform, may be defined using the Bromwich Integral:

$$f(t) = \mathfrak{L}^{-1}\left\{\widehat{f}\right\} = \frac{1}{2\pi i}\int_{\delta-i\infty}^{\delta+i\infty} e^{st}\widehat{f}(s)\,ds, \tag{2}$$

where δ must be greater than the real part of all the poles of $\widehat{f}(s)$ (Schiff (1999)). The numerical inversion of the Laplace Transform of a function represents a computational challenge, because it depends on the sensitivity of the inversion procedure. Since the inversion formula has an exponential term, it is important to be very careful with the value of st in Equation (2), as this can take very large values which may produce an increasing round off error and lead to divergence of the solution. Another aspect to consider is the presence of very fast oscillations on the solutions, which is the reason why different numerical integration methods failed (Bellman (1966), Craig and Thompson (1994)).
In the development of this work, it will be shown that making some modifications on the integration contour in Equation (2) it is possible to define a useful method that can numerically invert the Laplace Transform and apply it to solve differential equations.

The numerical inversion of the Laplace Transform has attracted the attention of many researchers. Lynch (1985) developed a numerical scheme based on the Laplace Inversion formula. The method is proposed as an initialization method to eliminate the high-frequency components from initial conditions. Later Struylaert and Isacker (1985) stated that the application of the numerical inverse transform is not restricted to initialization and applied the technique to solve a Baroclinic Model for atmosphere dynamics (See also Davies (1999), Ashan (2012), Clancy and Lynch (1994)). Clancy (2010) showed some of the properties and benefits of the method, also an application of this integration method to Shallow Water Equations is presented in Clancy and Lynch (2011), Clancy and Lynch (2015).

The main contribution of this work is to provide a study of the benefits and drawbacks of applying the Numerical Laplace Transform and its inverse to solve differential equation systems instead of the classic methods of differences. In addition, we make a comparison of the Laplace Transform Integration Method with the Fourth Order Runge Kutta Method for linear and non-linear cases. With this, we seek to be able to use a larger time step that reduces computational cost without affecting the stability and accuracy of the numerical solution.

Aims

The aim of this work is to explore the skills and limitations of the Laplace Transform Integration Method (LTIM) to solve Ordinary Differential Equations. We want to see the advantages of this method over classic differences methods such as the Fourth Order Runge Kutta Method. Some specific aims are

† Establish a relationship between the parameters involved in the inversion process looking for optimal conditions for larger time steps, accuracy, and stability,

† Analyse the capability of the method to act as a filter of high-frequency components,

† Compare the scheme with a classical method in application models.

Organization of the work

This work was organized as follow. Chapter 1 contains a brief compilation of the theory of the Laplace Transform such as: conditions of existence and uniqueness, properties, examples, and applications. Also, the Inverse Laplace Transform was defined and Appendix 5 includes the necessary background of complex analysis to understand and apply the inversion formula given by the Bromwich integral.

In Chapter 2 we describe and discuss the numerical scheme. We show the effects of replacing the exponential function on the formula by its truncated Taylor Series. In addition, we deduce the stability condition of the method. Finally, we present a general numerical scheme to solve initial value problems.

In Chapter 3 we present the numerical results obtained after applying the Laplace Transform Integration Method. The Chapter is divided into four sections. In section 3.1, we solved a Linear case. The behavior of the error corresponding to each parameter was analyzed and the relation between the parameters was established, using that information we calculated the error decay order. In section 3.2, we show how the LTIM works as a filter of high-frequency components. Next, in Section 3.3, we solved a non-linear IVP. We also observed the behavior of the error corresponding to each parameter to see how the non-linear part influences the relation between accuracy, stability, and computational cost. In Section 3.4, we point out some of the limitations related to the numerical stability of the method.

Chapter 4 presents a comparison between the Laplace Transform Integration Method and the Fourth Order Runge Kutta Method for different cases. Finally, we present the conclusions. Here we discuss some of the advantages and applications of the method, pointing out the contributions resulting from this research.

Chapter 1

Laplace Transform Theory

Laplace Transform theory, named in honor of the Marquis Pierre Simone Laplace (1749 - 1827), constitutes a very important tool in science, with impact in mathematics and physics, and engineering because it provides a method to solve Ordinary Differential Equations (ODE). The advantage of using the Laplace Transform (LT) is that it converts an ODE into an algebraic equation of the same order, which is usually easier to solve. Once the solution to the algebraic equation is found, the Inverse Laplace Transform will give us the time - domain solution. In this chapter we present a brief compilation of the Laplace Transform Theory. For more details we recommend to see Bellman (1966), Groove (1991), Schiff (1999), Smith (1966), Spiegel (1965).

1.1 Existence and Uniqueness Requirements

Definition 1.1 (Schiff, 1999)**.** *Suppose that f is a real or complex valued function of the variable $t \geq 0$. The* ***Laplace Transform of*** *f is given by:*

$$\widehat{f}(s) = \mathfrak{L}\{f(t)\} = \int_0^\infty e^{-st} f(t)\, dt, \tag{1.1}$$

where s is a complex number.

It is said that the Laplace Transform of the function $f(t)$ exists if the integral (1.1) converges for some s. Otherwise, it does not exists.

Example 1.1. *Let $f(t) \equiv 1$, for $t \geq 0$ and $s \in \mathbb{R}$. Then:*

$$\begin{aligned}
\mathfrak{L}\{f(t)\} &= \int_0^\infty e^{-st}(1)dt \\
&= \lim_{b\to\infty}\left[\frac{e^{-st}}{-s}\right]_0^b = \lim_{b\to\infty}\left[\frac{e^{-sb}}{-s} + \frac{1}{s}\right] \\
&= \begin{cases} \frac{1}{s}, & \text{if} \quad s > 0 \\ \\ \infty, & \text{if} \quad s \leq 0. \end{cases}
\end{aligned}$$

Here we have considered a real s, but if s is a complex number the process will be equivalent. Let's suppose that $s = x + iy$. Then:

$$
\begin{aligned}
\mathfrak{L}\{f(t)\} &= \int_0^{\infty} e^{-st}(1)dt \\
&= \lim_{b\to\infty}\left[\frac{e^{-st}}{-s}\right]_0^b = \lim_{b\to\infty}\left[\frac{e^{-(x+iy)t}}{-(x+iy)}\right]_0^b \\
&= \lim_{b\to\infty}\left[\frac{e^{-(x+iy)b}}{-(x+iy)} + \frac{1}{x+iy}\right] \\
&= \lim_{b\to\infty}\left[\frac{e^{-xb}\left(\cos(by) - i\sin(by)\right)}{-(x+iy)} + \frac{1}{x+iy}\right] \\
&= \frac{1}{x+iy} = \begin{cases} \frac{1}{s} \quad , & if \quad Re(s) = x > 0 \\ diverge, & if \quad Re(s) = x \leq 0. \end{cases}
\end{aligned}
$$

The Example 1.1 shows that, for suitable values of s, the Laplace transform of $f(t) \equiv 1$ exists. Now consider that $f(t) \equiv e^{t^2}$. In this case, for any choice of s the integral (1.1) will diverge because the function $f(t)$ grows without indefinitely. Thus, we need to establish sufficient conditions under which the transform exists.

Definition 1.2 (Schiff, 1999). *A function f has a **jump discontinuity** at a point t_0 if both limits*

$$
\begin{aligned}
\lim_{t\to t_0^-} f(t) &= f(t_0^-), \\
\lim_{t\to t_0^+} f(t) &= f(t_0^+),
\end{aligned}
$$

exist (as a finite number) and $f(t_0^-) \neq f(t_0^+)$. Here, t_0^- and t_0^+ mean that $t \longrightarrow t_0$ from the left and right, respectively, (see Figure 1.1).

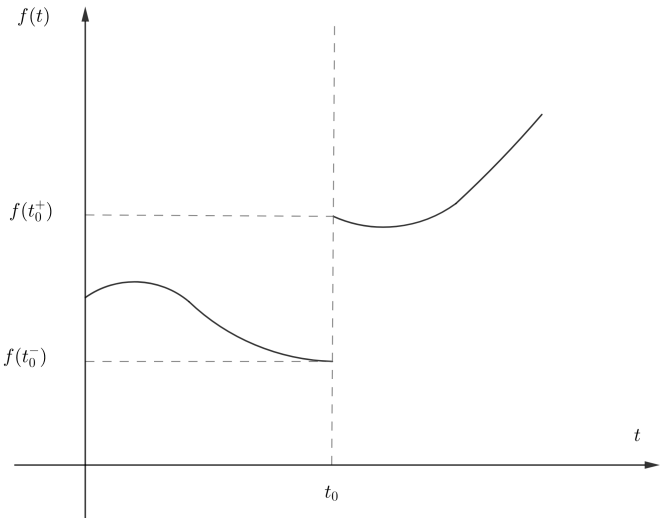

Figure 1.1: *Function with a jump discontinuity in $t = t_0$.*

Definition 1.3 (Schiff, 1999). *A function is **piecewise continuous** on the interval $[0, \infty)$ if:*

(i) $\lim_{t\to 0^+} f(t) = f(0^+)$ *exists;*

(ii) *f is continuous on every finite interval $(0,b)$ except possibly only at a finite number of points $\tau_1, \tau_2, ..., \tau_n$ in $(0,b)$ at which f has a jump discontinuity.*

Definition 1.4 (Schiff, 1999). *A function f has **exponential order** α if there exist constants $M > 0$ and α such that, for some $t_0 \geq 0$,*

$$|f(t)| \leq Me^{\alpha t}, \tag{1.2}$$

for $t \geq t_0$.

Example 1.2. *Some examples of exponential order functions are:*

(∗) *e^{at} has exponential order $\alpha = a$;*

(∗) *Bounded functions such as $\sin(t)$ and $\cos(t)$ have exponential order 0 because they are bounded by 1.*

Remark 1.1. *From now on, we will denote by $\mathcal{L}$ the class formed by those functions that satisfy definitions (1.3) and (1.4).*

Theorem 1.1 (Existence - Schiff, 1999). *If $f \in \mathcal{L}$, then the Laplace transform, $\mathfrak{L}\{f(t)\}$, exists for $Re(s) > \alpha$ and converges absolutely.*

Proof. First

$$|f(t)| \leq M_1 e^{\alpha t},$$

for $t \geq t_0$ and for some real α. Since $f \in \mathcal{L}$, then f is also piecewise continuous on $[0, t_0]$, thus, bounded in this interval, i.e.,

$$|f(t)| \leq M_2,$$

for $0 < t < t_0$. Notice that $e^{\alpha t}$ has a positive minimum on $[0, t_0]$, so a constant M can be chosen sufficiently large so that

$$|f(t)| \leq Me^{\alpha t},$$

for $t > 0$. Therefore,

$$\begin{aligned}
\int_0^\tau e^{-st} f(t)\, dt &\leq \int_0^\tau \left|e^{-st} f(t)\right| dt = \int_0^\tau \left|e^{-st}\right| |f(t)| dt \\
&= \int_0^\tau \left|e^{-(x+iy)t}\right| |f(t)| dt = \int_0^\tau e^{-xt} |f(t)| dt \\
&\leq M \int_0^\tau e^{-xt} e^{\alpha t} dt = M \int_0^\tau e^{-(x-\alpha)t} dt \\
&= \left[\frac{Me^{-(x-\alpha)t}}{-(x-\alpha)}\right]_0^\tau = \frac{Me^{-(x-\alpha)\tau}}{-(x-\alpha)} + \frac{M}{x-\alpha},
\end{aligned}$$

Letting $\tau \longrightarrow \infty$, $Re(s) = x > \alpha$, yield

$$\int_0^\tau \left|e^{-st} f(t)\right| dt \leq \frac{M}{x-\alpha}.$$

Thus the Laplace Transform converges absolutely (and hence converges) for $Re(s) = x > \alpha$. □

Theorem 1.2 (Uniqueness - Lerch Theorem)**.** *Let f and g two continuous functions and of exponential order such that $F(s) = \mathfrak{L}\{f(t)\}$ and $G(s) = \mathfrak{L}\{g(t)\}$. Suppose that there is an $s_0 \in \mathbb{C}$ such that $F(s) = G(s)$ for all $Re(s) > Re(s_0)$. Then, $f(t) - g(t)$ is a null function, i.e.:*

$$\int_0^a [f(t) - g(t)]\, dt = 0 \quad \forall a > 0. \tag{1.3}$$

Proof. If two functions $f(t)$ and $g(t)$ have the same LT, i.e., they satisfy:

$$\mathfrak{L}\{f(t)\} = \mathfrak{L}\{g(t)\},$$

or

$$\mathfrak{L}\{f(t)\} - \mathfrak{L}\{g(t)\} = 0,$$

we have, by the linearity of the Laplace transform, that,

$$\mathfrak{L}\{f(t) - g(t)\} = 0 \Rightarrow \int_0^\infty e^{-st}(f(t) - g(t))dt = 0.$$

Since the exponential function is always positive, the integral above indicates that $f(t)$ and $g(t)$ are essentially equal.

□

Lerch Theorem ensures that if two functions have the same LT then they are equal in $\mathcal{L}$. Hence, it will make sense to talk about the inverse transform $\mathfrak{L}^{-1}$ of a function considering that we have uniqueness in $\mathcal{L}$.

Example 1.3. *In this example we calculate the Laplace Transform of a function $f(t)$. Let $f(t) = e^{at}$, with real a . This function is continuous on $(0, \infty]$ and of exponential order a. Then:*

$$\begin{aligned}
\mathfrak{L}\left\{e^{at}\right\} &= \int_0^\infty e^{-st}e^{at}dt = \int_0^\infty e^{-(s-a)t}dt \\
&= \lim_{b\to\infty}\left[\frac{e^{-(s-a)t}}{-(s-a)}\right]_0^b = \lim_{b\to\infty}\left[\frac{e^{-(s-a)b}}{-(s-a)} + \frac{1}{s-a}\right] \\
&= \frac{1}{s-a}, \quad Re(s) > a.
\end{aligned}$$

If a is a complex number, then $Re(s) > Re(a)$.

1.2 Properties

In this section some basic, but very useful, properties of the Laplace Transform are mentioned (More details can be found in Schiff (1999)).

Linearity. If $f_1 \in \mathcal{L}$ for $Re(s) > \alpha$, $f_2 \in \mathcal{L}$ for $Re(s) > \beta$ then:

$$f_1 + f_2 \in \mathcal{L},$$

for $Re(s) > \max\{\alpha, \beta\}$ and,

$$\mathfrak{L}\{c_1 f_1(t) + c_2 f_2(t)\} = c_1\mathfrak{L}\{f_1(t)\} + c_2\mathfrak{L}\{f_2(t)\}. \tag{1.4}$$

for arbitrary real constants c_1, c_2.

Transform of a first order derivative. Suppose that $f \in \mathcal{L}$ and that f' is piecewise continuous in $[0,\infty)$. Then, for $Re(s) > \alpha$,

$$\mathfrak{L}\left\{f'(t)\right\} = s\mathfrak{L}\left\{f(t)\right\} - f(0). \tag{1.5}$$

Transform of an n-order derivative. Suppose that $f(t), f'(t), ..., f^{(n-1)}(t) \in \mathcal{L}$ on $[0,\infty)$, while $f^n(t)$ is piecewise continuous on $[0,\infty)$. Then,

$$\mathfrak{L}\left\{f^{(n)}(t)\right\} = s^n\mathfrak{L}\left\{f(t)\right\} - s^{n-1}f(0) - s^{n-2}f'(0) ... - sf^{(n-2)}(0) - f^{(n-1)}(0). \tag{1.6}$$

Transform of the convolution. Suppose that $f, g \in \mathcal{L}$. If $F(s) = \mathfrak{L}\left\{f(t)\right\}$ and $G(s) = \mathfrak{L}\left\{g(t)\right\}$ then,

$$\mathfrak{L}\left\{(f * g)(t)\right\} = F(s)G(s), \tag{1.7}$$

where

$$(f * g)(t) = \int_0^t f(\tau)\, g(t-\tau)\, d\tau.$$

Transform of a polynomial. If $f(t) = a_0 + a_1 t + a_2 t^2 + ... + a_n t^n$ is a polynomial of degree n, then,

$$\mathfrak{L}\left\{f(t)\right\} = \sum_{k=0}^{n} \frac{a_k k!}{s^{k+1}}. \tag{1.8}$$

Transform of infinite series. If

$$f(t) = \sum_{n=0}^{\infty} a_n t^n,$$

converges for $t \geq 0$, with

$$|a_n| \leq \frac{K\alpha^n}{n!},$$

for all n sufficiently large and $\alpha > 0, K > 0$, then

$$\mathfrak{L}\left\{f(t)\right\} = \sum_{n=0}^{\infty} a_n \mathfrak{L}\left\{t^n\right\} = \sum_{n=0}^{\infty} \frac{a_n n!}{s^{n+1}}. \tag{1.9}$$

First Translation or Shifting Property. If $F(s) = \mathfrak{L}\left\{f(t)\right\}$ for $Re(s) > 0$, then

$$F(s-a) = \mathfrak{L}\left\{e^{at} f(t)\right\}, \quad a \in \mathbb{R}, Re(s) > a \tag{1.10}$$

Second Translation or Shifting Property. If $F(s) = \mathfrak{L}\left\{f(t)\right\}$ for $Re(s) > 0$, then

$$\mathfrak{L}\left\{u_a(t) f(t-a)\right\} = e^{-as} F(s), \quad a > 0 \tag{1.11}$$

where $u_a(t)$ is the *unit step function* defined as:

$$u_a(t) = \begin{cases} 1, & \text{if} \quad t \geq a \\ \\ 0, & \text{if} \quad t < a. \end{cases}$$

Change of scale. Let $f \in \mathcal{L}$ and $F(s) = \mathfrak{L}\{f(at)\}$ for $Re(s) > 0$, then

$$\mathfrak{L}\{f(at)\} = \frac{1}{a} F\left(\frac{s}{a}\right). \tag{1.12}$$

1.3 Laplace Transform of some Functions

$f(t)$	$\mathfrak{L}\{f(t)\}$
1	$\frac{1}{s}$
e^{at}	$\frac{1}{s-a}$
$t^n, n \geq 1$	$\frac{n!}{s^{n+1}}$
$\sqrt{t}$	$\frac{\sqrt{\pi}}{2\sqrt{s}}$
$t^n e^{at}, n \geq 1$	$\frac{n!}{(s-a)^{n+1}}$
$u_a(t) = u(t-a)$	$\frac{e^{-as}}{s}$
$\sin at$	$\frac{a}{s^2+a^2}$
$\cos at$	$\frac{s}{s^2+a^2}$
$e^{at} \sinh bt$	$\frac{b}{(s-a)^2-b^2}$
$e^{at} \cosh bt$	$\frac{s-a}{(s-a)^2+b^2}$
$\frac{1}{t} f(t)$	$\int_s^\infty F(u)du$

Table 1.1: *Laplace Transforms - Spiegel (1965)*

1.4 Application to ODEs

As it was mentioned at the beginning of the chapter, the Laplace Transform can be use to solve ODEs. The following example will show how to use the properties of the Laplace Transform to solve an Initial Value Problem (IVP). Later we will deduced a general formula to solve IVPs. Let,

$$\begin{cases} mx'' &= -kx - \beta x', \\ x(0) &= A, \\ x'(0) &= B. \end{cases} \tag{1.13}$$

The second order equation in (1.13) is known as the *Equation of motion with a damping force*, where k is the spring constant, m is the mass and β is the damping constant (See Spiegel (1965)).

Applying the Laplace Transform and its properties to (1.13) we get,

$$\begin{aligned} m\mathfrak{L}\{x''\} &= -k\mathfrak{L}\{x\} - \beta\mathfrak{L}\{x'\} \\ m\left(s^2\mathfrak{L}\{x\} - sx(0) - x'(0)\right) &= -k\mathfrak{L}\{x\} - \beta\left(s\mathfrak{L}\{x\} - x(0)\right) \\ \left(ms^2 + k + \beta s\right)\mathfrak{L}\{x\} &= (ms+\beta)x(0) + mx'(0) \\ \mathfrak{L}\{x\} &= \frac{(ms+\beta)x(0) + mx'(0)}{ms^2 + k + \beta s} \end{aligned}$$

So we obtain:

$$x(t) = \mathfrak{L}^{-1}\left\{\frac{(ms+\beta)x(0) + mx'(0)}{ms^2 + k + \beta s}\right\}. \tag{1.14}$$

1.5 Inverse Laplace Transform

In the preceding section we showed how we can use the properties of the transform to solve an Initial Value Problem. Even though we have a useful table of transforms that can be used to solve ODEs, at some point we might have terms that won't have a "known transform". Thus, we need a general method to obtain the inverse transform. This method is provided by the inversion integral which is usually referred as Bromwich Integral (also Mellin integral). In the Appendix 5 we give a complex analysis background in order to understand and apply this integration formula.

Theorem 1.3. *Let $f(t)$ have a continuous derivative and let $|f(t)| < Me^{\alpha t}$ where M and α are positive constants. Define*

$$\widehat{f}(s) = \mathfrak{L}\{f(t)\} = \int_0^\infty e^{-st} f(t)dt, \quad Re(s) > \alpha.$$

Then

$$f(t) = \mathfrak{L}^{-1}\left\{\widehat{f}(s)\right\} = \frac{1}{2\pi i}\int_{\delta - i\infty}^{\delta + i\infty} e^{st}\widehat{f}(s)ds \tag{1.15}$$

The integral (1.15) above is known as ***Bromwich integral.***

Proof. See the proof at Cohen (2007). □

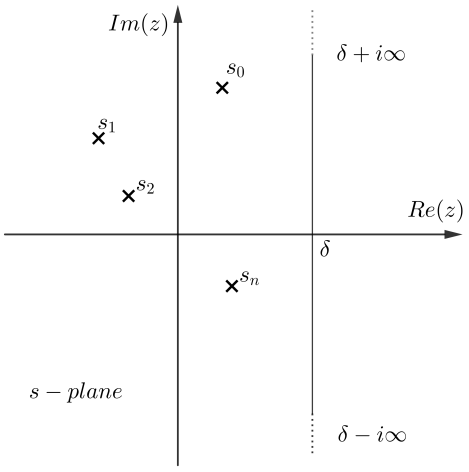

Figure 1.2: *Bromwich integral domain.*

In order to apply the inversion integration formula given by (1.15), we will use complex and residue theory provided in the Appendix 5. The strategy will be to build a close contour that contains the poles of $\widehat{f}$.

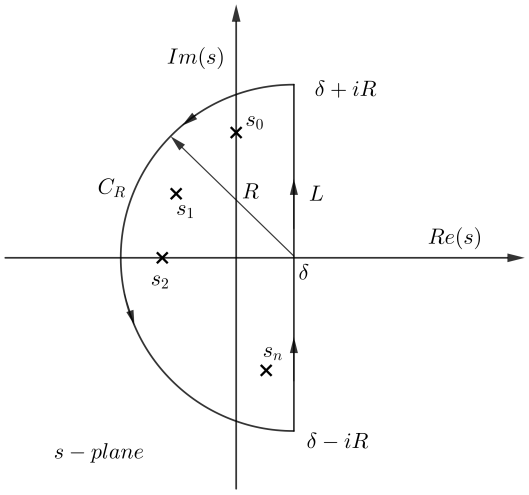

Figure 1.3: *Bromwich closed contour* $C = C_R \cup L$.

Let's consider the contour C, shown in Figure 1.3. Then,

$$\begin{aligned}\int_C e^{st}\widehat{f}(s)ds &= \int_{C_R} e^{st}\widehat{f}(s)ds + \int_L e^{st}\widehat{f}(s)ds \\ &= \int_{C_R} e^{st}\widehat{f}(s)ds + \int_{\delta-iR}^{\delta+iR} e^{st}\widehat{f}(s)ds. \end{aligned} \tag{1.16}$$

The points $s_0, s_1, ..., s_n$ in Figure 1.3 represent a finite number of poles of the function $\widehat{f}$. Since the poles are inside C, then by the Residue Theorem 1.4 we can rewrite (1.16) as

$$2\pi i \sum_{j=0}^{n} Res\left[\widehat{f}(s)e^{st}, s_j\right] = \int_{C_R} e^{st}\widehat{f}(s)ds + \int_{\delta-iR}^{\delta+iR} e^{st}\widehat{f}(s)ds. \tag{1.17}$$

The first integral in (1.17) is going to 0 when $R \to \infty$ due to Jordan's Lemma (See Lemma .1) and also making $R \to \infty$ the second integral becomes the Bromwich integral. Thus,

$$\mathfrak{L}^{-1}\left\{\widehat{f}\right\} = \frac{1}{2\pi i}\int_{\delta-i\infty}^{\delta+i\infty} e^{st}\widehat{f}\,(s)\,ds = \sum_{j=0}^{n} Res\left[\widehat{f}(s)e^{st}, s_j\right]. \tag{1.18}$$

Theorem 1.4 (Residue .6). *Suppose that $f(z)$ is an analytic function on a simply-connected domain D except for a finite number of poles $z_1, z_2, ..., z_k$. Suppose that C is a piecewise smooth positively-oriented simple closed curve not passing through $z_1, z_2, ..., z_k$. Then,*

$$\frac{1}{2\pi i}\int_C f\,(z)\,dz = \sum_{z_j \in C} Res\,[f, z_j].$$

Example 1.4. *Calculate the Inverse Laplace transform of* $\widehat{f}(s) = \frac{1}{s-a}$.

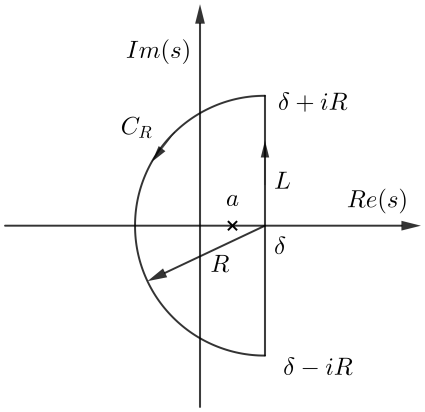

Figure 1.4: *Bromwich close contour for* $\widehat{f}(s) = \frac{1}{s-a}$.

The Laplace transform of f *has one simple pole at* $s = a$ *(Figure 1.4), so:*

$$\begin{aligned} f(t) &= \mathfrak{L}^{-1}\left\{\frac{1}{s-a}\right\} = Res\left[\frac{e^{st}}{s-a}, a\right], \\ &= \lim_{s\to a}(s-a)\left(\frac{e^{st}}{s-a}\right), \\ f(t) &= e^{at}. \end{aligned}$$

It is possible to choose a circle as a contour (Figure 1.5). Because the right side has no poles inside of it, thus the integral over C_{R_2} is equal to zero. Therefore,

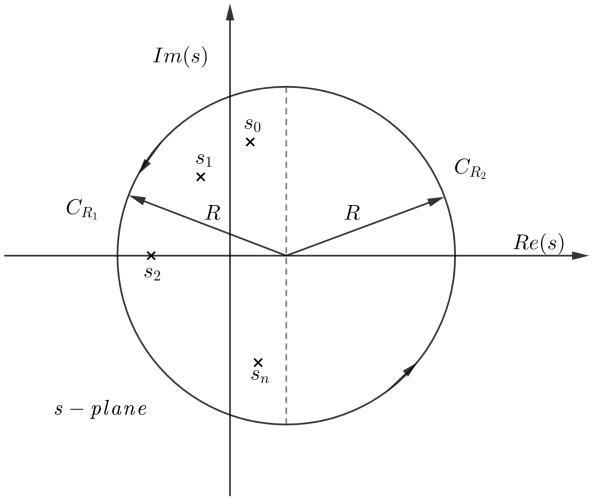

Figure 1.5: *Alternative Bromwich close contour*

$$\mathfrak{L}^{-1}\widehat{f}(s) = \int_{C_{R_1}} e^{st}\widehat{f}(s)\,ds + \int_{C_{R_2}} e^{st}\widehat{f}(s)\,ds = \int_{C_{R_1}} e^{st}\widehat{f}(s)\,ds + 0.$$

Other contours are possible, but we will adopt the circle contour throughout the derivation of the numerical method that follows in the next Chapter.

Chapter 2

Laplace Transform Integration Method

Many physical phenomena are modeled through ODEs. One of the problems while solving these equations are the high frequency components of the solutions. That is why the abilities of the Laplace Transform were explored in different researchs such as Lynch (1985), Lynch (1986), Struylaert and Isacker (1987), Clancy (2010), Clancy and Lynch (2011), Clancy and Lynch (2015). Making some modifications on the inversion formula it is possible to define a numerical scheme that works as a filter of high frequency components. In this chapter we present the formulation of the method based on Laplace Transform Theory provided in the last chapter.

2.1 Numerical Inverse Laplace Transform

The inversion formula for the Laplace Transform is given by:

$$\mathfrak{L}^{-1}\left\{\widehat{f}\right\} = \frac{1}{2\pi i}\int_{\gamma-i\infty}^{\gamma+i\infty} e^{st}\widehat{f}\,(s)\,ds. \tag{2.1}$$

To apply this formula we need to replace the contour in (2.1) with a close contour C^* (See Figure 2.1). We choose a circle centered at the origin and of radius γ (Clancy and Lynch (2011), Clancy (2010)), then:

$$\mathfrak{L}^{-1}\left\{\widehat{f}\right\} = \frac{1}{2\pi i}\int_{C^*} e^{st}\widehat{f}\,(s)\,ds, \tag{2.2}$$

as long as all the poles of $\widehat{f}$ lie inside C^*.

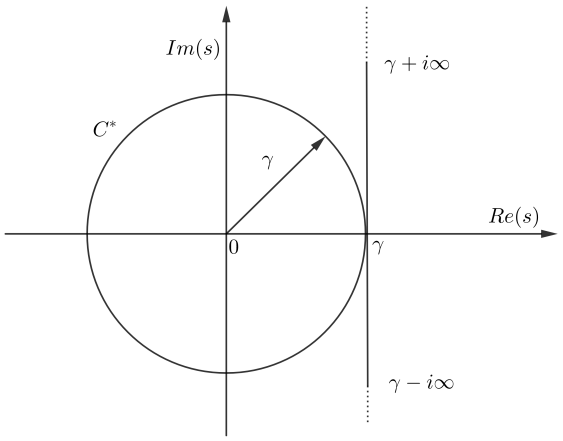

Figure 2.1: *Original contour vs Close contour C^*.*

To apply numerically the formula (2.2), we reduce the integration into a quadrature formula

using the Trapezoidal rule:

$$\mathfrak{L}^{-1}\left\{\widehat{f}\right\} = \frac{1}{2\pi i}\sum_{n=1}^{N} e^{s_n t}\widehat{f}\,(s_n)\,\Delta s_n. \tag{2.3}$$

In equation (2.2), ds represents the length metric element of an arc in C^* and Δs_n is an approximation for it (*see Figure 2.2*):

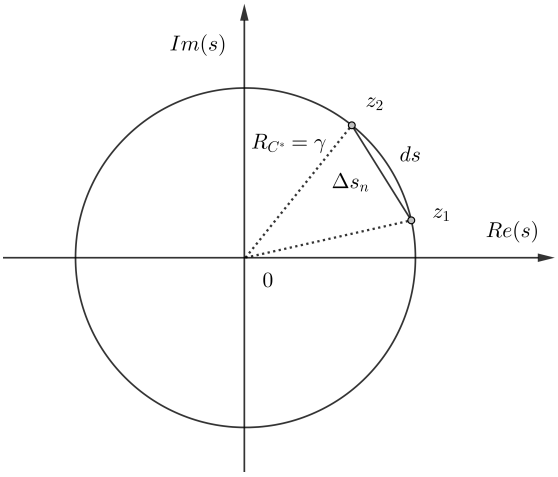

Figure 2.2: *Relation between ds and* Δs_n.

Since our contour is a circle of radius γ, we choose strategic points on C^*. These points are the complex roots of γ (see the Appendix 5), defined as:

$$z_n = \gamma e^{\frac{2i\pi n}{N}} \tag{2.4}$$

where N represents the (even) number of roots we use. So

$$ds \simeq \theta R_{C^*} = \frac{2\pi}{N}\gamma, \tag{2.5}$$

and Δs_n can be calculated as:

$$\begin{aligned}
\Delta s_n &= \frac{2\pi}{N}\left(\frac{z_n - z_{n-1}}{2\sin\left(\frac{\pi}{N}\right)}\right) = \frac{2\pi}{N}\left(\frac{\gamma e^{\frac{2i\pi n}{N}} - \gamma e^{\frac{2i\pi(n-1)}{N}}}{2\sin\left(\frac{\pi}{N}\right)}\right) \\
&= \frac{2\pi}{N}\left(\frac{\gamma e^{\frac{2i\pi n}{N}}\left(1 - e^{-\frac{2i\pi}{N}}\right)}{2\sin\left(\frac{\pi}{N}\right)}\right) \\
&= \frac{2\pi}{N}\left(\frac{\gamma e^{\frac{2i\pi n}{N}}\left(e^{-\frac{i\pi}{N}}e^{\frac{i\pi}{N}} - e^{-\frac{i\pi}{N}}e^{-\frac{i\pi}{N}}\right)}{2\sin\left(\frac{\pi}{N}\right)}\right) \\
&= \frac{2\pi}{N}\left(\frac{\gamma e^{\frac{i\pi(2n-1)}{N}}\left(e^{\frac{i\pi}{N}} - e^{-\frac{i\pi}{N}}\right)}{2\sin\left(\frac{\pi}{N}\right)}\right) \\
&= \frac{2\pi}{N}\left(\frac{\gamma e^{\frac{i\pi(2n-1)}{N}}\left(2i\sin\left(\frac{\pi}{N}\right)\right)}{2\sin\left(\frac{\pi}{N}\right)}\right) \\
&= \frac{2i\pi}{N}\gamma e^{\frac{i\pi(2n-1)}{N}}.
\end{aligned} \tag{2.6}$$

We denoted the exponential term in (2.6) as:

$$s_n = \gamma e^{\frac{i\pi(2n-1)}{N}}. \tag{2.7}$$

Thus:

$$\Delta s_n = \frac{2i\pi}{N} s_n. \tag{2.8}$$

Replacing the value of Δs_n in equation (2.3) we get:

$$\mathfrak{L}^* \left\{ \widehat{f} \right\} = \frac{1}{N} \sum_{n=1}^{N} e^{s_n t} \widehat{f}\,(s_n)\, s_n. \tag{2.9}$$

In addition we replace the exponential term in (2.9) by the truncated Taylor series expansion,

$$e_N^{s_n t} = \sum_{j=0}^{N-1} \frac{(s_n t)^j}{j!}. \tag{2.10}$$

Thus, our discrete approximations defined in (2.9) becomes

$$\mathfrak{L}_N^* \left\{ \widehat{f} \right\} = \frac{1}{N} \sum_{n=1}^{N} e_N^{s_n t} \widehat{f}\,(s_n)\, s_n. \tag{2.11}$$

Clancy and Lynch (2011) obtained the formula (2.11) using an N-sided polygon C_N^* (see Figure 2.3)

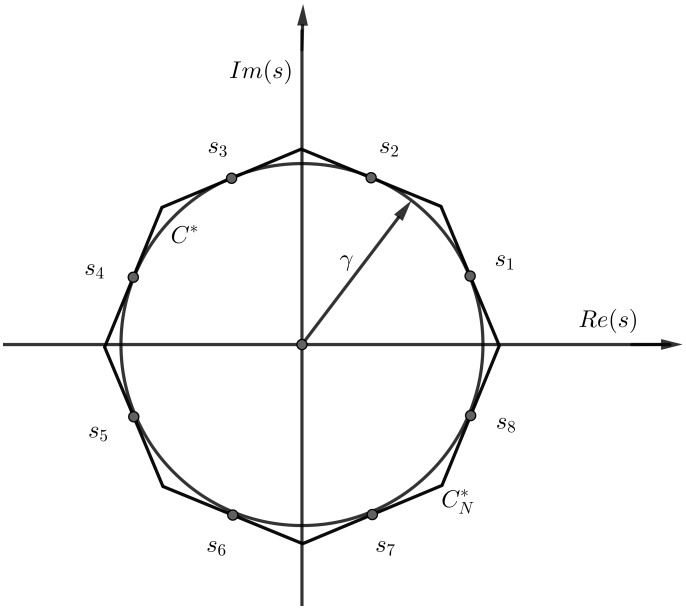

Figure 2.3: *Contour C^* vs N-sided polygon C_N^*.*

with

$$\begin{aligned} s'_n &= \frac{\gamma}{\cos\left(\frac{\pi}{N}\right)} e^{\frac{2\pi i n}{N}}, \quad n = 1, ..., N \\ \Delta s_n &= s'_n - s'_{n-1} = 2i s'_n e^{\frac{-\pi i}{N}} \sin\left(\frac{\pi}{N}\right), \\ s_n &= \gamma e^{\frac{i\pi(2n-1)}{N}} = s'_n e^{\frac{-\pi i}{N}} \cos\left(\frac{\pi}{N}\right), \end{aligned} \tag{2.12}$$

where $s'_n, \Delta s_n, s_n$ represent the vertices, side length and midpoints of C_N^*, respectively. In order to

obtain the formula given in (2.9), Clancy and Lynch (2011) divided the summation in (2.3) by a correction factor to ensure exactness for constants

$$\kappa = \frac{N}{\pi}\tan\frac{\pi}{N}, \tag{2.13}$$

that satisfies

$$\frac{1}{\kappa} = \left(\frac{2\pi i}{N}\right)\left(\frac{s_n}{\Delta s_n}\right). \tag{2.14}$$

In the next section we shall analyze the effects of this replacement.

2.2 Truncated Exponential

Consider the case $f(t) = 1$ and $\widehat{f}(s) = \frac{1}{s}$. We will use the operator defined in (2.9) (and the Taylor Series Expansion of $e^{s_n t}$) to invert $\widehat{f}$. Thus:

$$\begin{aligned}
\mathfrak{L}^*\left(\frac{1}{s}\right) &= \frac{1}{N}\sum_{n=1}^{N} e^{s_n t}\frac{1}{s_n}s_n = \frac{1}{N}\sum_{n=1}^{N} e^{s_n t} \\
&= \frac{1}{N}\sum_{n=1}^{N}\sum_{k=0}^{\infty}\frac{(s_n t)^k}{k!} \\
&= \frac{1}{N}\sum_{n=1}^{N}\sum_{k=0}^{\infty}\frac{\left(\gamma e^{\frac{i\pi(2n-1)}{N}}t\right)^k}{k!} \\
&= \frac{1}{N}\sum_{k=0}^{\infty}\sum_{n=1}^{N}\frac{(\gamma t)^k}{k!}e^{\frac{i\pi(2n-1)k}{N}}.
\end{aligned}$$

If k is a multiple of N, i.e., $k = mN$ with $m \in \mathbb{N}_0 = \mathbb{N}\cup\{0\}$, then:

$$\begin{aligned}
e^{\frac{i\pi(2n-1)k}{N}} &= e^{\frac{i\pi(2n-1)mN}{N}} = e^{i\pi(2n-1)m} \\
&= e^{2imn\pi}e^{-im\pi} = \left(e^{i\pi}\right)^{2mn}\left(e^{-i\pi}\right)^{m} \\
&= (-1)^m. \qquad (*)
\end{aligned}$$

If we define $k = j + mN$ with $j = \{0, 1, ..., N-1\}, m \in \mathbb{N}_0 = \mathbb{N}\cup\{0\}$, then:

$$\mathfrak{L}^*\left(\frac{1}{s}\right) = \frac{1}{N}\sum_{m=0}^{\infty}\sum_{j=0}^{N-1}\sum_{n=1}^{N}\frac{(\gamma t)^{j+mN}}{(j+mN)!}e^{\frac{i\pi(2n-1)(j+mN)}{N}}. \tag{2.15}$$

Analyzing the exponential term in (2.15) :

$$\begin{aligned}
e^{\frac{i\pi(2n-1)(j+mN)}{N}} &= e^{i\pi(2n-1)m}e^{\frac{i\pi(2n-1)j}{N}} \\
&= e^{2imn\pi}e^{-im\pi}e^{\frac{2i\pi nj}{N}}e^{\frac{-i\pi j}{N}} = (1)(-1)^m e^{\frac{2i\pi nj}{N}}e^{\frac{-i\pi j}{N}} \\
&= (-1)^m e^{\frac{2i\pi nj}{N}}e^{\frac{-i\pi j}{N}}.
\end{aligned} \tag{2.16}$$

Now, we can rewrite (2.16):

$$\begin{aligned}\mathfrak{L}^*\left(\frac{1}{s}\right) &= \frac{1}{N}\sum_{m=0}^{\infty}\sum_{j=0}^{N-1}\sum_{n=1}^{N}\frac{(\gamma t)^{j+mN}}{(j+mN)!}(-1)^m e^{\frac{2i\pi nj}{N}}e^{-\frac{i\pi j}{N}} \\ &= \frac{1}{N}\sum_{m=0}^{\infty}(-1)^m\sum_{j=0}^{N-1}\frac{(\gamma t)^{j+mN}}{(j+mN)!}e^{-\frac{i\pi j}{N}}\sum_{n=1}^{N}e^{\frac{2i\pi nj}{N}}. \qquad (2.17)\end{aligned}$$

Analyzing the sum in (2.17), and using geometric summation properties, we conclude that:

$$\begin{aligned}\sum_{n=1}^{N}e^{\frac{2i\pi nj}{N}} &= \sum_{n=1}^{N}\left(e^{\frac{2i\pi j}{N}}\right)^n = e^{\frac{2i\pi j}{N}}\sum_{n=0}^{N-1}\left(e^{\frac{2i\pi j}{N}}\right)^n \\ &= e^{\frac{2i\pi j}{N}}\left(\frac{1-\left(e^{\frac{2i\pi j}{N}}\right)^N}{1-e^{\frac{2i\pi j}{N}}}\right) \\ &= e^{\frac{2i\pi j}{N}}\left(\frac{1-e^{2i\pi j}}{1-e^{\frac{2i\pi j}{N}}}\right).\end{aligned}$$

Notice that we have two cases,

For $j = 0$:

$$\sum_{n=1}^{N}e^{\frac{2i\pi n(0)}{N}} = N. \qquad (**)$$

For $j \neq 0$:

$$\sum_{n=1}^{N}e^{\frac{2i\pi nj}{N}} = 0. \qquad (***)$$

So:

$$\begin{aligned}\mathfrak{L}^*\left(\frac{1}{s}\right) &= \frac{1}{N}\sum_{m=0}^{\infty}(-1)^m\frac{(\gamma t)^{mN}}{(mN)!}e^{-\frac{i\pi(0)}{N}}(N) \\ &\quad +\frac{1}{N}\sum_{m=0}^{\infty}(-1)^m\sum_{j\neq 0}^{N-1}\frac{(\gamma t)^{j+mN}}{(j+mN)!}e^{-\frac{i\pi j}{N}}(0) \\ &= \sum_{m=0}^{\infty}(-1)^m\frac{(\gamma t)^{mN}}{(mN)!} \\ &= 1-\frac{(\gamma t)^N}{N!}+\frac{(\gamma t)^{2N}}{(2N)!}-\frac{(\gamma t)^{3N}}{(3N)!}+\ldots \quad .\end{aligned}$$

If we truncate the exponential in the operator $\mathfrak{L}^*$ defined in (2.9), we have just the contribution of

$m = 0$ and the inversion is exact, i.e.,

$$\mathfrak{L}_N^* \left(\frac{1}{s} \right) = 1, \tag{2.18}$$

and if we use the full exponential we get an $O\left(\frac{(\gamma t)^N}{N!}\right)$ error. Making the same analysis for $\widehat{f}(s) = \frac{1}{s^k}$ we obtain:

$$\mathfrak{L}_N^* \left(\frac{1}{s^k} \right) = \frac{t^{k-1}}{(k-1)!} \quad , for \quad 1 \leq k \leq N,$$

which means that operator $\mathfrak{L}_N^* \left(\frac{1}{s^k}\right)$ defined in (2.11) gives us the exact inversion for polynomials of degree $N-1$. More details about these analysis can be found in Clancy (2010).

2.3 Stability Criteria for Linear IVPs

In this section the stability condition for linear problems. Suppose that we have an linear Initial Value Problem given by,

$$\begin{cases} x'(t) &= i\omega x, \\ x(0) &= 1, \end{cases}$$

whose Laplace Transform and exact solution are given by $\widehat{f}(s)$ and $f(t)$ respectively,

$$\begin{aligned} \widehat{f}(s) &= \tfrac{1}{s-i\omega}, \\ f(t) &= e^{i\omega t}. \end{aligned} \tag{2.19}$$

Applying the operator $\mathfrak{L}^*$ in (2.9) to invert $\widehat{f}(s)$ we have

$$\begin{aligned} \mathfrak{L}^* \left(\frac{1}{s-i\omega} \right) &= \frac{1}{N} \sum_{n=1}^{N} e^{s_n t} \frac{1}{s_n - i\omega} s_n = \frac{1}{N} \sum_{n=1}^{N} e^{s_n t} \left(\frac{s_n}{s_n - i\omega} \right) \\ &= \frac{1}{N} \sum_{n=1}^{N} e^{s_n t} \left(\frac{1}{1 - \frac{i\omega}{s_n}} \right) \\ &= \frac{1}{N} \sum_{n=1}^{N} e^{s_n t} \sum_{p=0}^{\infty} \left(\frac{i\omega}{s_n} \right)^p \quad , \quad for \quad \left| \frac{i\omega}{s_n} \right| < 1 \quad (or \quad |\omega| < |\gamma|). \end{aligned}$$

Suppose that $p = l + mN$ with $l = \{0, 1, ..., N-1\}, m \in \mathbb{N}_0 = \mathbb{N} \cup \{0\}$, then

$$\mathfrak{L}^* \left(\frac{1}{s-i\omega} \right) = \frac{1}{N} \sum_{n=1}^{N} e^{s_n t} \sum_{m=0}^{\infty} \sum_{l=0}^{N-1} \left(\frac{i\omega}{s_n} \right)^{l+mN}. \tag{2.20}$$

Using (2.6) and (∗):

$$\begin{aligned}\left(\frac{i\omega}{s_n}\right)^{l+mN} &= \left(\frac{i\omega}{\gamma}e^{-\frac{i\pi(2n-1)}{N}}\right)^{l+mN}\\ &= \left(\frac{i\omega}{\gamma}\right)^{l+mN} e^{-\frac{i\pi(2n-1)l}{N}} e^{-\frac{i\pi(2n-1)mN}{N}}\\ &= \left(\frac{i\omega}{\gamma}\right)^{l+mN} e^{-\frac{i\pi(2n-1)l}{N}}(-1)^m.\end{aligned}$$

Then:

$$\left(\frac{i\omega}{s_n}\right)^{l+mN} = \left((-1)\left(\frac{i\omega}{\gamma}\right)^{N}\right)^{m} e^{-\frac{i\pi(2n-1)l}{N}}\left(\frac{i\omega}{\gamma}\right)^{l}. \tag{2.21}$$

Replacing (2.21) in (2.20) and using (2.7) and (2.10) we get:

$$\begin{aligned}\mathfrak{L}^*\left(\frac{1}{s-i\omega}\right) &= \frac{1}{N}\sum_{n=1}^{N}\sum_{m=0}^{\infty}\sum_{l=0}^{N-1} e^{s_n t}\left((-1)\left(\frac{i\omega}{\gamma}\right)^{N}\right)^{m} e^{-\frac{i\pi(2n-1)l}{N}}\left(\frac{i\omega}{\gamma}\right)^{l}\\ &= \frac{1}{N}\sum_{m=0}^{\infty}\left((-1)\left(\frac{i\omega}{\gamma}\right)^{N}\right)^{m}\sum_{l=0}^{N-1}\sum_{n=1}^{N} e^{s_n t} e^{-\frac{i\pi(2n-1)l}{N}}\left(\frac{i\omega}{\gamma}\right)^{l}\\ &= \frac{1}{N}\frac{1}{1+\left(\frac{i\omega}{\gamma}\right)^{N}}\sum_{l=0}^{N-1}\sum_{n=1}^{N} e^{s_n t} e^{-\frac{i\pi(2n-1)l}{N}}\left(\frac{i\omega}{\gamma}\right)^{l}\\ &\overset{(2.10)}{=} \frac{1}{N}\frac{1}{1+\left(\frac{i\omega}{\gamma}\right)^{N}}\sum_{l=0}^{N-1}\sum_{n=1}^{N}\sum_{j=0}^{\infty}\frac{(s_n t)^j}{j!} e^{-\frac{i\pi(2n-1)l}{N}}\left(\frac{i\omega}{\gamma}\right)^{l}\\ &\overset{(2.7)}{=} \frac{1}{N}\frac{1}{1+\left(\frac{i\omega}{\gamma}\right)^{N}}\sum_{l=0}^{N-1}\sum_{n=1}^{N}\sum_{j=0}^{\infty}\frac{(\gamma t)^j}{j!} e^{\frac{i\pi(2n-1)j}{N}} e^{-\frac{i\pi(2n-1)l}{N}}\left(\frac{i\omega}{\gamma}\right)^{l}\\ &= \frac{1}{N}\frac{1}{1+\left(\frac{i\omega}{\gamma}\right)^{N}}\sum_{l=0}^{N-1}\sum_{n=1}^{N}\sum_{j=0}^{\infty}\frac{(\gamma t)^j}{j!} e^{\frac{2i\pi n(j-l)}{N}} e^{-\frac{i\pi(j-l)}{N}}\left(\frac{i\omega}{\gamma}\right)^{l}\\ &= \frac{1}{N}\frac{1}{1+\left(\frac{i\omega}{\gamma}\right)^{N}}\sum_{l=0}^{N-1}\sum_{j=0}^{\infty}\frac{(\gamma t)^j}{j!} e^{-\frac{i\pi(j-l)}{N}}\left(\frac{i\omega}{\gamma}\right)^{l}\sum_{n=1}^{N}\left(e^{\frac{2i\pi(j-l)}{N}}\right)^{n}.\end{aligned} \tag{2.22}$$

Observe that the last sum in (2.22) will be different from zero only if $j-l=kN$, with $k=0,1,\ldots$. Writing $j=l+kN$ and using (∗∗) and (∗ ∗ ∗), we get:

$$\begin{aligned}\mathfrak{L}^*\left(\frac{1}{s-i\omega}\right) &= \frac{1}{N}\frac{1}{1+\left(\frac{i\omega}{\gamma}\right)^{N}}\sum_{l=0}^{N-1}\sum_{k=0}^{\infty}\frac{(\gamma t)^{l+kN}}{(l+kN)!} e^{-i\pi k}\left(\frac{i\omega}{\gamma}\right)^{l}\sum_{n=1}^{N}\left(e^{2\pi i k}\right)^{n}\\ &= \frac{1}{N}\frac{1}{1+\left(\frac{i\omega}{\gamma}\right)^{N}}\sum_{l=0}^{N-1}\sum_{k=0}^{\infty}\frac{(\gamma t)^{l+kN}}{(l+kN)!}(-1)^k\left(\frac{i\omega}{\gamma}\right)^{l}N.\end{aligned}$$

Thus,

$$\mathfrak{L}^*\left(\frac{1}{s-i\omega}\right) = \frac{1}{1+\left(\frac{i\omega}{\gamma}\right)^N}\sum_{l=0}^{N-1}(i\omega t)^l\sum_{k=0}^{\infty}(-1)^k\frac{(\gamma t)^{kN}}{(l+kN)!}. \tag{2.23}$$

Separating (2.23) in two parts:

$$\begin{aligned}\mathfrak{L}^*\left(\frac{1}{s-i\omega}\right) &= \frac{1}{1+\left(\frac{i\omega}{\gamma}\right)^N}\left(\sum_{l=0}^{N-1}\frac{(i\omega t)^l}{l!}\right)+\frac{1}{1+\left(\frac{i\omega}{\gamma}\right)^N}\sum_{l=0}^{N-1}(i\omega t)^l\sum_{k=1}^{\infty}(-1)^k\frac{(\gamma t)^{kN}}{(l+kN)!}\\ &= \frac{1}{1+\left(\frac{i\omega}{\gamma}\right)^N}\left(\sum_{l=0}^{N-1}\frac{(i\omega t)^l}{l!}\right)\\ &\quad+\frac{1}{1+\left(\frac{i\omega}{\gamma}\right)^N}\sum_{l=0}^{N-1}(i\omega t)^l\left(-\frac{(\gamma t)^N}{(l+N)!}+\frac{(\gamma t)^{2N}}{(l+2N)!}-\frac{(\gamma t)^{3N}}{(l+3N)!}+\cdots\right). \quad (\star)\end{aligned}$$

Struylaert and Isacker (1985) use the following notation:

$$H_N(\omega) = \frac{1}{1+\left(\frac{i\omega}{\gamma}\right)^N}. \tag{2.24}$$

Then, using (2.24) we can rewrite $(\star)$ as

$$\mathfrak{L}^*\left(\frac{1}{s-i\omega}\right) = H_N(\omega)e_N^{i\omega t}+H_N(\omega)\sum_{l=0}^{N-1}(i\omega t)^l\sum_{k=1}^{\infty}(-1)^k\frac{(\gamma t)^{kN}}{(l+kN)!}. \quad (\diamond)$$

Hence, for the truncated exponential we finally get:

$$\mathfrak{L}_N^*\left(\frac{1}{s-i\omega}\right) = H_N(\omega)e_N^{i\omega t}, \tag{2.25}$$

as reported in Lynch (1986). Notice that the function $H_N(\omega)$ will act as a damping factor when $|H_N(\omega)| \leq 1$. Suppose that $\omega = 2$ and $\gamma = 3$. Then:

$$\begin{aligned}H_2(2) &= \frac{1}{1+\left(\frac{2i}{3}\right)^2} = 1.8 \quad ;\\ H_4(2) &= \frac{1}{1+\left(\frac{2i}{3}\right)^4} = 0.83505... \quad ;\\ H_6(2) &= \frac{1}{1+\left(\frac{2i}{3}\right)^6} = 1.09624... \quad ;\\ H_8(2) &= \frac{1}{1+\left(\frac{2i}{3}\right)^8} = 0.96244... \quad .\end{aligned}$$

Thus, choosing N as a multiple of 4 will guarantee that $|H_N(\omega)| \leq 1$. Our aim is to guarantee stability, so we need the following condition to be satisfied:

$$\left|H_N(\omega)e_N^{i\omega\Delta t}\right| \leq 1. \tag{2.26}$$

Note that:

$$\begin{aligned}\left|e_N^{i\omega\Delta t}\right| &= \left|e^{i\omega\Delta t}+e_N^{i\omega\Delta t}-e^{i\omega\Delta t}\right| \\ &\leq \left|e^{i\omega\Delta t}\right|+\left|e_N^{i\omega\Delta t}-e^{i\omega\Delta t}\right| = 1+\left|\frac{(i\omega\xi)^N}{N!}\right| \quad \xi\in[0,\Delta t]\,.\end{aligned}$$

Therefore,

$$\left|e_N^{i\omega\Delta t}\right| \leq 1+\left|\frac{(i\omega\Delta t)^N}{N!}\right| = 1+\frac{(\omega\Delta t)^N}{N!}. \quad (\star\star)$$

Using (2.24) and $(\star\star)$, we get:

$$\left|H_N(\omega)e_N^{i\omega\Delta t}\right| \leq \left|\frac{1}{1+\left(\frac{i\omega}{\gamma}\right)^N}\right|\left(1+\frac{(\omega\Delta t)^N}{N!}\right).$$

Since we want condition (2.26) to be satisfied, a suficient condition is that

$$\begin{aligned}\left|\frac{1}{1+\left(\frac{i\omega}{\gamma}\right)^N}\right|\left(1+\frac{(\omega\Delta t)^N}{N!}\right) &\leq 1, \\ 1+\frac{(\omega\Delta t)^N}{N!} &\leq \left|1+\left(\frac{i\omega}{\gamma}\right)^N\right| \leq 1+\left(\frac{\omega}{\gamma}\right)^N, \\ 1+\frac{(\omega\Delta t)^N}{N!} &\leq 1+\left(\frac{\omega}{\gamma}\right)^N, \\ \frac{(\omega\Delta t)^N}{N!} &\leq \left(\frac{\omega}{\gamma}\right)^N.\end{aligned}$$

Hence, the method will be stable if:

$$\Delta t \leq \frac{(N!)^{\frac{1}{N}}}{\gamma}. \quad (2.27)$$

Example 2.1. *Let's use $\gamma = 3$ and different values of N on formula (2.27). The Table 2.1 shows the corresponding Δts:*

N	Largest Δt
8	1.25478353
16	2.26682226
24	3.60864540
32	4.26342976
64	8.22469183

Table 2.1: *Time Steps for different values of N and a fix value of γ*

Observe that choosing N sufficiently large should provide means of using a larger Δt, however is not that simple.

2.4 Numerical ODEs

As mentioned in Chapter 1, one of the most important applications of the Laplace Transform is to solve Ordinary Differential Equation systems. Consider the general initial value problem (Clancy and Lynch (2011)):

$$\begin{cases} \frac{d\vec{X}}{dt} &= -L\vec{X} - N\left(\vec{X}\right) \\ \vec{X}(0) &= \vec{X}_0 \end{cases} , \tag{2.28}$$

where L is a linear operator and N a non-linear vector function. The Taylor expansion of the non-linear term $N(\vec{X})$ around $\vec{X}_0$ is given by:

$$N(\vec{X}) = N(\vec{X_0}) + D_X N(\vec{X_0}) \cdot \vec{h} + \frac{1}{2}\vec{h}^t H_X N(\vec{X_0})\vec{h} + ... \quad , \tag{2.29}$$

where $\vec{h} = \vec{X} - \vec{X_0}$, $D_X N(\vec{X_0})$ and $H_X N(\vec{X_0})$ are the Jacobian and Hessian matrices of $N(\vec{X})$ respectively. In order to find the solution of the IVP (2.28) using the Laplace Transform, we use a first order approximation of $N(\vec{X})$:

$$N(\vec{X}) = N(\vec{X_0}) + D_X N(\vec{X_0})\vec{h} + O\left(\left\|\vec{h}\right\|^2\right) \quad , \tag{2.30}$$

where $O\left(\left\|\vec{h}\right\|^2\right)$ contains higher order terms that depends on the norm of $\vec{h}$. The Mean Value Theorem states that:

$$\vec{X}(t) - \vec{X}(t_0) = D_t\vec{X}(\xi_i) \cdot (t - t_0) \quad ,$$

for each $\xi_i \in [t_0, t]$. Then:

$$\begin{aligned} \left\|\vec{h}\right\| = \left\|\vec{X}(t) - \vec{X}(t_0)\right\| &\leq \sup_{\xi_i \in [t_0,t]} \left\|D_t\vec{X}(\xi_i)(t - t_o)\right\| \\ &\leq \sup_{\xi_i \in [t_0,t]} \left\|D_t\vec{X}(\xi_i)\right\| \sup_{\xi_i \in [t_0,t]} \|t - t_0\| \\ &\leq \sup_{\xi_i \in [t_0,t]} \left\|D_t\vec{X}(\xi_i)\right\| \Delta t \end{aligned}$$

Thus:

$$\left\|\vec{h}\right\| = \left\|\vec{X}(t) - \vec{X}(t_0)\right\| \leq c\Delta t, \tag{2.31}$$

where $c = \sup_{\xi_i \in [t_0,t]} \left\|D_t\vec{X}(\xi_i)\right\|$. Thus, using (2.31), equation (2.30) can be written as:

$$N(\vec{X}) = N(\vec{X_0}) + D_X N(\vec{X_0}) \cdot \vec{h} + O\left(\Delta t^2\right). \tag{2.32}$$

Applying the Laplace Transform to (2.28) and replacing (2.32) on it, we obtain:

$$\begin{aligned}
\mathfrak{L}\left\{\frac{d\vec{X}}{dt}\right\} &= -\mathfrak{L}\left\{L\vec{X}+N\left(\vec{X}\right)\right\};\\
s\mathfrak{L}\left\{\vec{X}(t)\right\}-\vec{X}(0) &= -\mathfrak{L}\left\{L\vec{X}(t)\right\}-\mathfrak{L}\left\{N\left(\vec{X}(0)\right)+D_{\vec{X}}N\left(\vec{X}(0)\right)\cdot\vec{h}+O\left(\Delta t^2\right)\right\};\\
s\mathfrak{L}\left\{\vec{X}(t)\right\}-\vec{X}_0 &= -\mathfrak{L}\left\{L\vec{X}(t)\right\}-\mathfrak{L}\left\{N(\vec{X}_0)\right\}-\mathfrak{L}\left\{D_{\vec{X}}N\left(\vec{X}_0\right)\cdot\vec{h}\right\}+\mathfrak{L}\left\{O\left(\Delta t^2\right)\right\};\\
s\mathfrak{L}\left\{\vec{X}(t)\right\}-\vec{X}_0 &= -L\left(\mathfrak{L}\left\{\vec{X}(t)\right\}\right)-N\left(\vec{X}_0\right)\mathfrak{L}\{1\}-D_{\vec{X}}N\left(\vec{X}_0\right)\cdot\mathfrak{L}\left\{\vec{h}\right\}\\
&\quad+\mathfrak{L}\left\{O\left(\Delta t^2\right)\right\};\\
s\mathfrak{L}\left\{\vec{X}(t)\right\}+L\left(\mathfrak{L}\left\{\vec{X}(t)\right\}\right) &= \vec{X}_0-\frac{1}{s}N(\vec{X}_0)-D_{\vec{X}}N\left(\vec{X}_0\right)\cdot\mathfrak{L}\left\{\vec{X}(t)-\vec{X}_0\right\}\\
&\quad+\mathfrak{L}\left\{O\left(\Delta t^2\right)\right\};\\
s\mathfrak{L}\left\{\vec{X}(t)\right\}+L\left(\mathfrak{L}\left\{\vec{X}(t)\right\}\right) &= \vec{X}_0-\frac{1}{s}N(\vec{X}_0)-D_{\vec{X}}N\left(\vec{X}_0\right)\cdot\mathfrak{L}\left\{\vec{X}(t)\right\}\\
&\quad+D_{\vec{X}}N\left(\vec{X}_0\right)\cdot\mathfrak{L}\left\{\vec{X}_0\right\}+\mathfrak{L}\left(O\left(\Delta t^2\right)\right);\\
\left(sI+L+D_{\vec{X}}N\left(\vec{X}_0\right)\right)\cdot\mathfrak{L}\left\{\vec{X}(t)\right\} &= \vec{X}_0-\frac{1}{s}N(\vec{X}_0)+D_{\vec{X}}N\left(\vec{X}_0\right)\cdot\mathfrak{L}\left\{\vec{X}_0\right\}-\mathfrak{L}\left\{O\left(\Delta t^2\right)\right\};\\
\left(sI+L+D_{\vec{X}}N\left(\vec{X}_0\right)\right)\cdot\mathfrak{L}\left\{\vec{X}(t)\right\} &= \vec{X}_0-\frac{1}{s}N(\vec{X}_0)+\frac{1}{s}D_{\vec{X}}N\left(\vec{X}_0\right)\cdot\vec{X}_0-\mathfrak{L}\left\{O\left(\Delta t^2\right)\right\}.
\end{aligned}$$

Assuming that the inverse of $\left(sI+L+D_{\vec{X}}N\left(\vec{X}_0\right)\right)$ exists,

$$\begin{aligned}
\mathfrak{L}\left\{\vec{X}(t)\right\} &= \left(sI+L+D_{\vec{X}}N\left(\vec{X}_0\right)\right)^{-1}\left(\vec{X}_0-\frac{1}{s}N(\vec{X}_0)+\frac{1}{s}D_{\vec{X}}N\left(\vec{X}_0\right)\cdot\vec{X}_0\right)\\
&\quad+\left(sI+L+D_{\vec{X}}N\left(\vec{X}_0\right)\right)^{-1}\mathfrak{L}\left\{O\left(\Delta t^2\right)\right\};\\
X(t) &= \mathfrak{L}^{-1}\left\{\left(sI+L+D_XN\left(X_0\right)\right)^{-1}\left(X_0-\frac{1}{s}N(X_0)+\frac{1}{s}D_XN\left(X_0\right)\cdot X_0\right)\right\}\\
&\quad+\mathfrak{L}^{-1}\left\{\left(sI+L+D_XN\left(X_0\right)\right)^{-1}\left(\mathfrak{L}\left\{O\left(\Delta t^2\right)\right\}\right)\right\};\\
X(t) &= \mathfrak{L}^{-1}\left\{\left(sI+L+D_XN\left(X_0\right)\right)^{-1}\left(X_0-\frac{1}{s}N(X_0)+\frac{1}{s}D_XN\left(X_0\right)\cdot X_0\right)\right\}\\
&\quad+\left(sI+L+D_XN\left(X_0\right)\right)^{-1}\mathfrak{L}^{-1}\left\{\mathfrak{L}\left\{O\left(\Delta t^2\right)\right\}\right\}.
\end{aligned}$$

Thus:

$$\begin{aligned}
X(t) &= \mathfrak{L}^{-1}\left\{\left(sI+L+D_XN\left(X_0\right)\right)^{-1}\left(X_0-\frac{1}{s}N(X_0)+\frac{1}{s}D_XN\left(X_0\right)\cdot X_0\right)\right\}\\
&\quad+\left(sI+L+D_XN\left(X_0\right)\right)^{-1}\left(O\left(\Delta t^2\right)\right). \qquad (2.33)
\end{aligned}$$

Equation (2.33) indicates that the order of accuracy of the method depends on the size of the time step. Clancy (2010) assumed that the non-linear term is slowly varying over time and did a constant approximation for each time step. With this assumption, Clancy and Lynch (2011) obtained the following formula:

$$X(t) = \mathfrak{L}^{-1}\left\{(sI+L)^{-1}\left(X_0 - \frac{1}{s}N(X_0)\right)\right\} - (sI+L)^{-1}\left(O\left(\Delta t\right)\right), \tag{2.34}$$

which has a first order error.
In general, we have to solve IVPs of the form:

$$\begin{cases} X' &= -LX - N\left(X\right); \\ X(t_k) &= X_k. \end{cases} \tag{2.35}$$

Notice that formulas (2.33) and (2.34) require that the initial condition is always defined at $t = 0$. Hence, we need to apply the shift property and rewrite (2.35) using $\tau = t - t_k$:

$$\begin{cases} \tilde{X}' &= -L\tilde{X} - N\left(\tilde{X}\right); \\ \tilde{X}(0) &= \tilde{X}_k; \end{cases} \tag{2.36}$$

where:

$$\begin{cases} \tilde{X}(\tau) &= X(\tau + t_k) = X(t); \\ \tau &= t - t_k. \end{cases} \tag{2.37}$$

So, (2.34) turns into:

$$X\left(t\right) = \mathfrak{L}^{-1}\left\{(sI+L)^{-1}\left(\tilde{X}_0 - \frac{N\left(\tilde{X}_0\right)}{s}\right)\right\}(t - t_k) - (sI+L)^{-1}\left(O(\Delta t)\right). \tag{2.38}$$

Applying the operator $\mathfrak{L}^*$ defined by (2.9), we get:

$$X^*\left(t\right) = \mathfrak{L}^*\left\{\widehat{X}(t)\right\} = \frac{1}{N}\sum_{n=1}^{N}\left[e^{s_n(t-t_k)}\left((s_nI+L)^{-1}\left(\tilde{X}_0 - \frac{N\left(X_0\right)}{s_n}\right) - (sI+L)^{-1}\left(O(\Delta t)\right)\right)s_n\right] \tag{2.39}$$

Then, the numerical scheme is given by:

$$X^*_{k+1} = \frac{1}{N}\sum_{n=1}^{N}\left[e^{s_n(t_{k+1}-t_k)}\left((s_nI+L)^{-1}\left(X^*_k - \frac{N\left(X^*_k\right)}{s_n}\right)\right)s_n\right].$$

Remember that:

$$t_{k+1} - t_k = (k+1)\Delta t - k\Delta t = \Delta t.$$

Thus:

$$X_{k+1}^{*} = \frac{1}{N}\sum_{n=1}^{N}\left[e^{s_n \Delta t}\left((s_n I + L)^{-1}\left(X_k^{*} - \frac{N\left(X_k^{*}\right)}{s_n}\right)\right)s_n\right] \tag{2.40}$$

Summarizing, formula (2.40) gives a numerical scheme that is linearly stable for Δt satisfying (2.27), with exponential convergence on N for linear cases and first order on Δt for non-linear cases.

Chapter 3

Numerical Results

In this chapter we present the numerical results obtained after applying the Laplace Transform Integration Method (LTIM) provided in Chapter 2. In Section 3.1 a linear ODE, whose Laplace transform has a simple pole, is solved. In Section 3.2, as proposed by Lynch (1985), we apply this integration method to remove high frequency components from the approximate solution, i.e., apply this method as a filter under certain conditions. In Section 3.3 we explored the ability of the method to solve a non-linear ODE. Finally, in Section 3.4 we show the stability limitations of the method.

3.1 Linear Case

For the first experiment we considered a simple linear IVP:

$$\begin{cases} \frac{dX}{dt} &= 2iX, \\ X(0) &= 1, \end{cases} \tag{3.1}$$

whose exact solution is:

$$X(t) = e^{2it}. \tag{3.2}$$

and its Laplace transform is given by:

$$\mathfrak{L}(X(t)) = \widehat{X}(s) = \frac{1}{s-2i}, \tag{3.3}$$

3.1.1 Theory Validation: Effect of the Truncated Exponential

In this section, we numerically validate the theory developed in the previous chapter. Recall the formula ($\diamond$):

$$\mathfrak{L}^*\left(\frac{1}{s-i\omega}\right) = H_N(\omega)e_N^{i\omega t} + H_N(\omega)\sum_{l=0}^{N-1}(i\omega t)^l \sum_{k=1}^{\infty}(-1)^k \frac{(\gamma t)^{kN}}{(l+kN)!}, \tag{3.4}$$

Taking $\gamma = 4$ and using different values of N, the largest time step for each N was calculated using (2.27) in order to solve IVP (3.1). Figure 3.1 shows the Error (in $\|\cdot\|_\infty$) made in one time step, we can clearly see the effect of full and truncated exponentials on the approximate solution of (3.1). The decay of the error shows that the truncated exponential guarantees the convergence of the approximate solution to the exact solution up until $N \approx 40$; while with the full exponential, the sum on the right in (3.4) is growing along with the value of N. This produces a larger accuracy error.

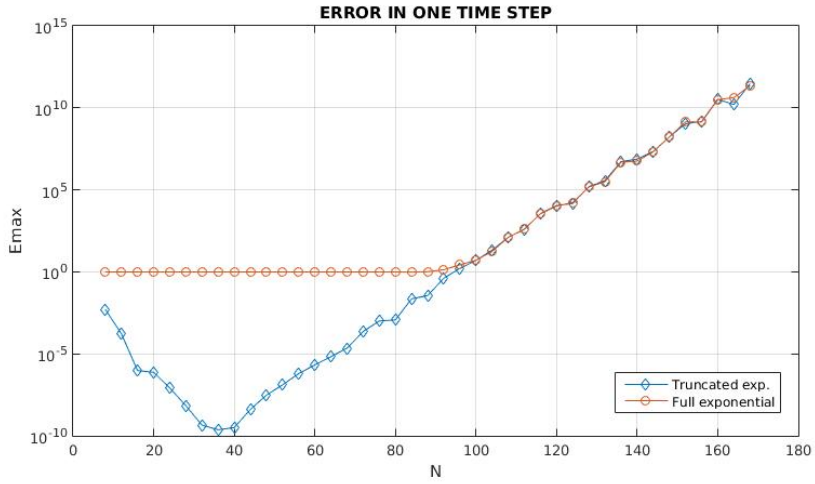

Figure 3.1: *Error Comparison in* $\|\cdot\|_\infty$ *between the full and truncated exponential corresponding to IVP (3.1) using the largest* Δt *for each* N*.*

Observe that, for Δts corresponding to $N \geq 100$ the solution is unstable for both exponentials. This means that, numerically, the stability condition given in Chapter 2 is not enough to guarantee stability. Later, in section 3.4 we discuss this problem and present the stability region for this method. To better appreciate the effect of both exponentials on the approximate solution, we take a smaller time step for each N (80% of the largest Δt) as shown in Figure 3.2.

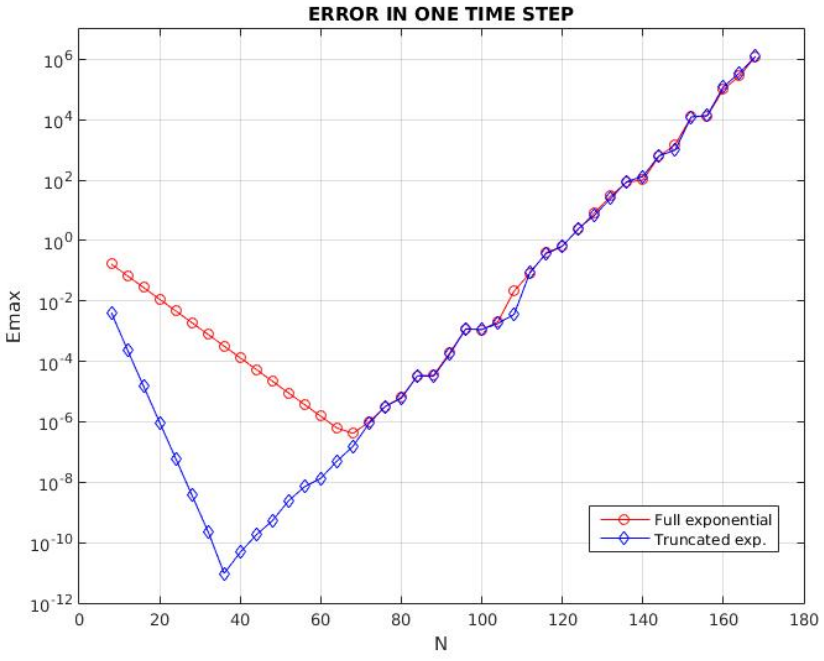

Figure 3.2: *Error Comparison in* $\|\cdot\|_\infty$ *between the full and truncated exponential, using a smaller time step (*80% *of the largest* Δt*).*

Figure 3.3 shows the behavior of the solution of IVP (3.1) for both exponentials in ten time steps. Notice that, the error grows as the approximations process repeats. This result and the effects of varying the values of N, γ, and Δt will be shown in the next section.

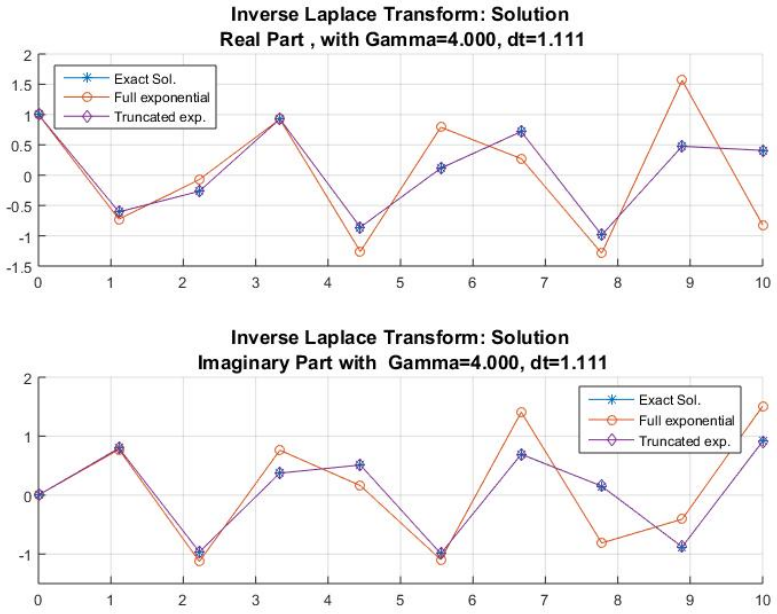

Figure 3.3: *Solution for IVP 3.1 using the full and truncated exponential in 10 time steps and* $N = 12$.

3.1.2 Linear ODEs

The function (3.3) has one simple pole at $s = 2i$ on the imaginary axis. According to the theory (Chapter 1), we will take different radius greater than two otherwise the value of the transform will be zero. Several experiments were made using different values of N, radius γ and time partitions Δt in order to establish a relationship between these parameters and see how they influence the accuracy of the approximate solution. Initially, it is consider $\gamma = 2.1$. The aim of this simulation is to see the behavior of the approximate solution when the contour is very close to the pole of $\widehat{X}$. Choosing values for N and Δt that satisfy the stability condition (2.27) given in Chapter 2 we get the following results.

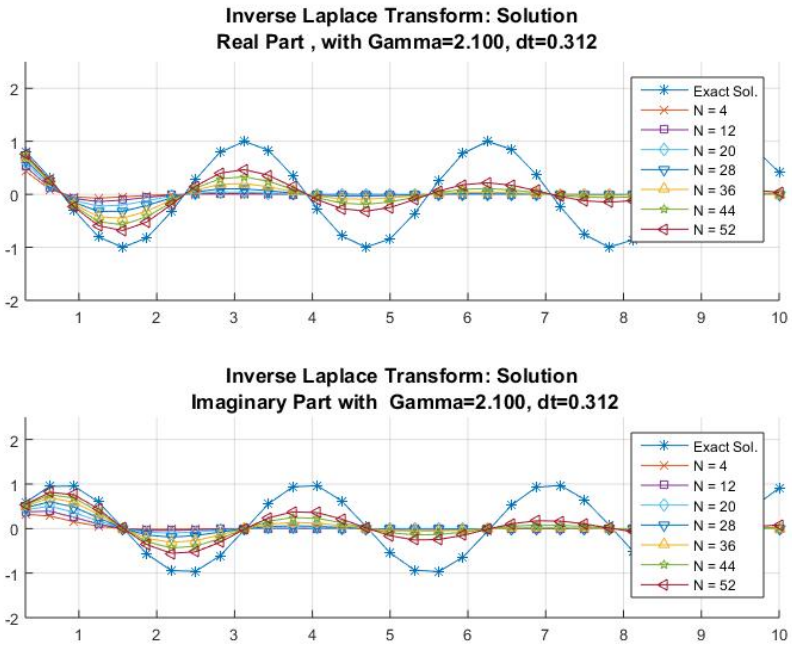

Figure 3.4: *Exact solution vs Approximate solutions using* $\gamma = 2.1$ *for the IVP 3.1.*

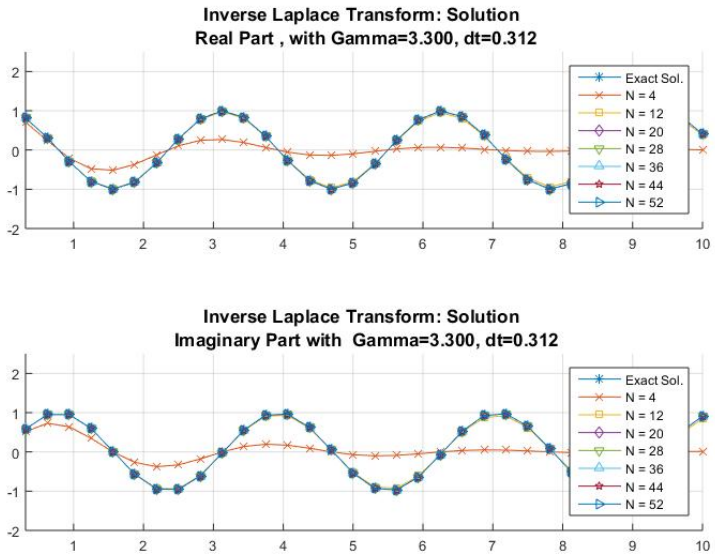

Figure 3.5: *Exact solution vs Approximate solutions using* $\gamma = 3.3$ *for the IVP (3.1).*

Figure 3.4 shows that for a radius of 2.1, no matter how large we choose N, the error is always quite large (no convergence in N). This is largely related to the proximity of the contour to the pole. In Figure 3.5, we can see that the choice of the radius influences the accuracy of the solution. As we get far from the pole we get a better approximation to the exact solution because the influence of the pole is reduced. Also, in both cases, $N = 4$ gets the worst results. Nevertheless, when $\gamma = 3.3$ and $N > 4$, increasing the value of N leads to convergence to the exact solution. In order to see the relation between the parameters we graph, for different values of dt, γ and N, the behavior of the error (in $\|\cdot\|_\infty$) which is the maximum error of all the time steps.

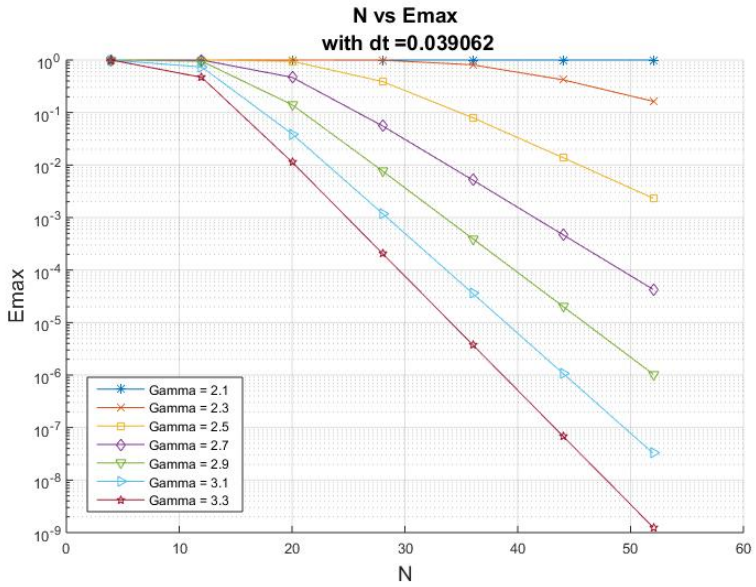

Figure 3.6: *Number of s-points (N) vs Maximum Error taking* $dt = 0.0390625$ *and different values of* γ *for IVP (3.1).*

In Figures 3.6 and 3.7 for a fix dt, we note that the error decays as the value of the radius and N increases. We can also verify that the choice of radius plays an important role in the accuracy of the solution. Each figure shows that the farther from the pole, the smaller the error made.

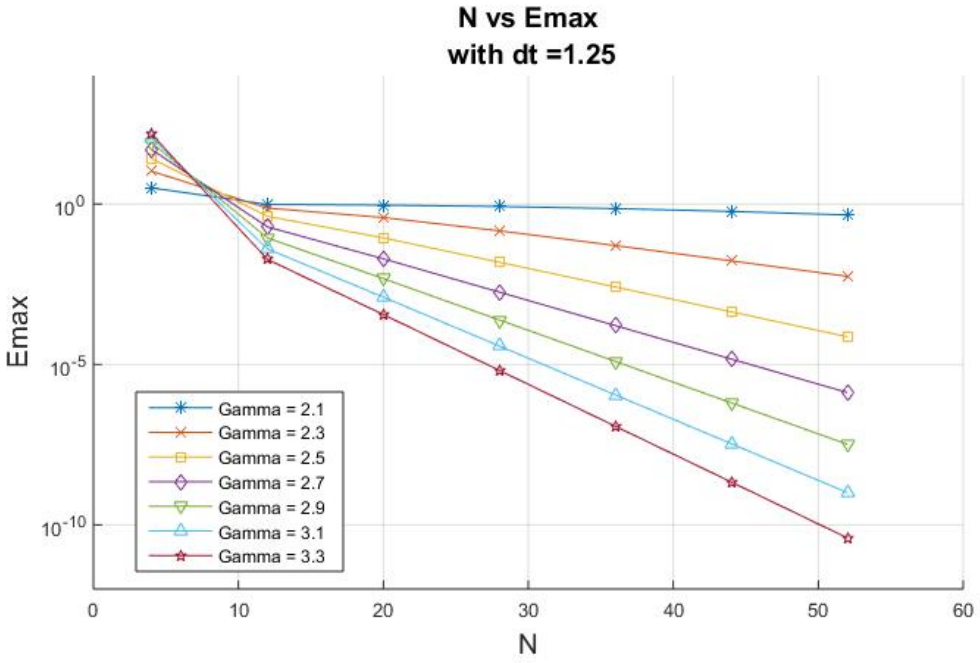

Figure 3.7: *Number of s-points (N) vs Maximum Error taking $dt = 1.25$ and different values of γ for IVP (3.1).*

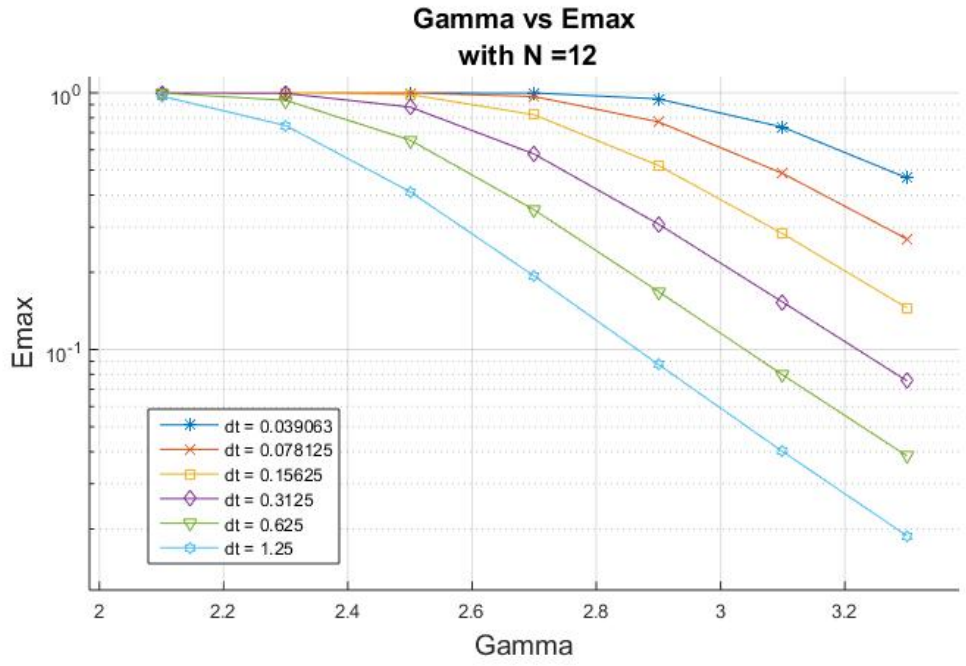

Figure 3.8: *γ vs Maximum Error taking $N = 12$ and different values of dt for IVP (3.1).*

On the other hand, here we fix two values of N and test different values of dt and γ. Figures 3.8 and 3.9 show that the smallest error was obtained for the larger radius. Also we can see that the smallest error corresponds to the largest time step. Observe that, we started with a small error that becomes bigger over time due to the constant repetition of the approximation process. In other words, the smaller time step, the greater accumulated error.

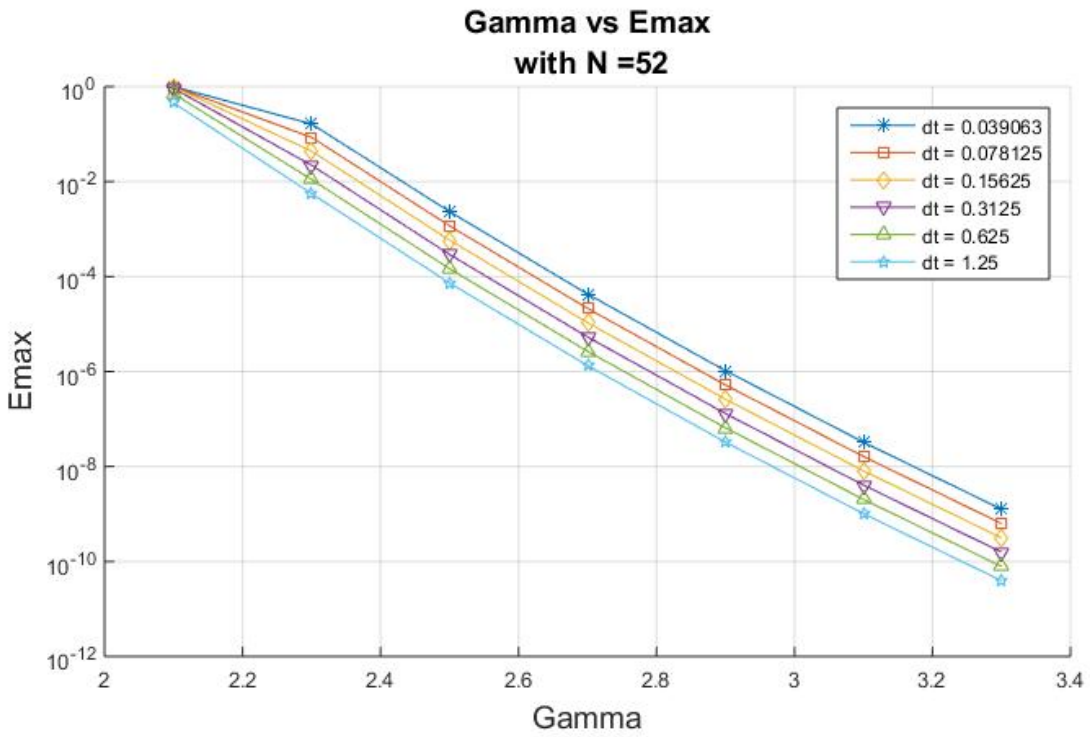

Figure 3.9: *γ vs Maximum Error taking $N = 52$ and different values of dt for IVP (3.1).*

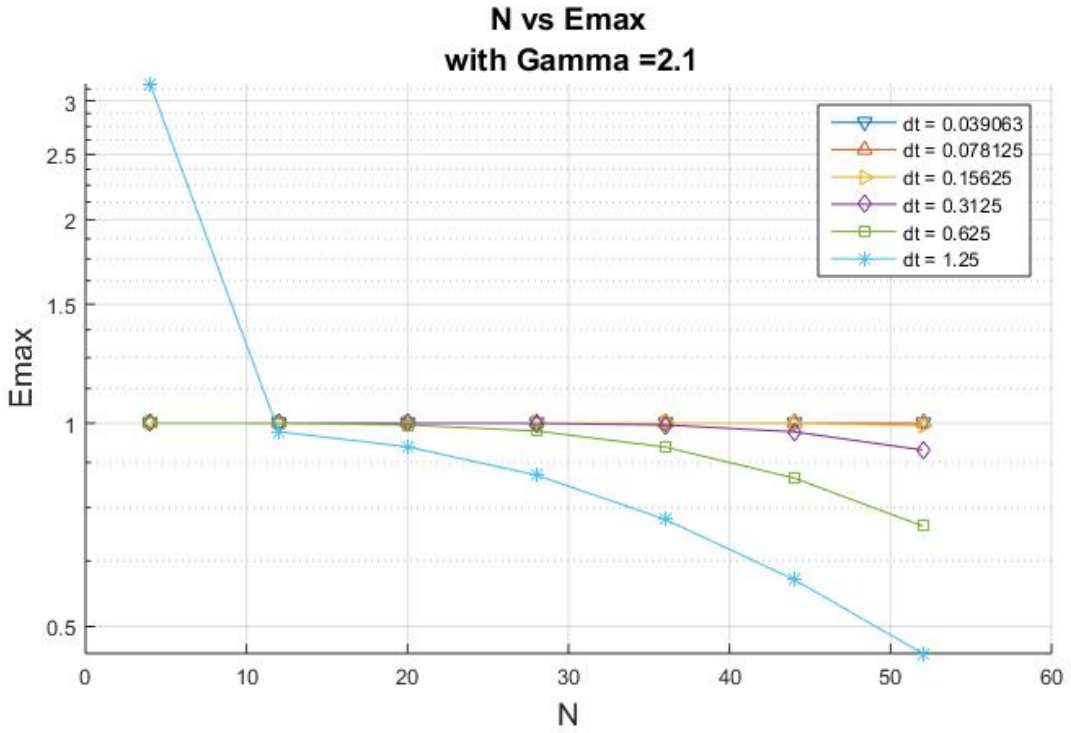

Figure 3.10: *N vs Maximum Error taking $\gamma = 2.1$ and different values of dt for IVP (3.1).*

Now in Figures 3.10 and 3.11, we fix the value of γ and test different values for dt and N. The behavior of the error is the same as in Figures 3.6 - 3.9. The best results are of $\gamma = 3.3$ and $N = 52$. In addition, the accumulated error is smaller for the largest time step.

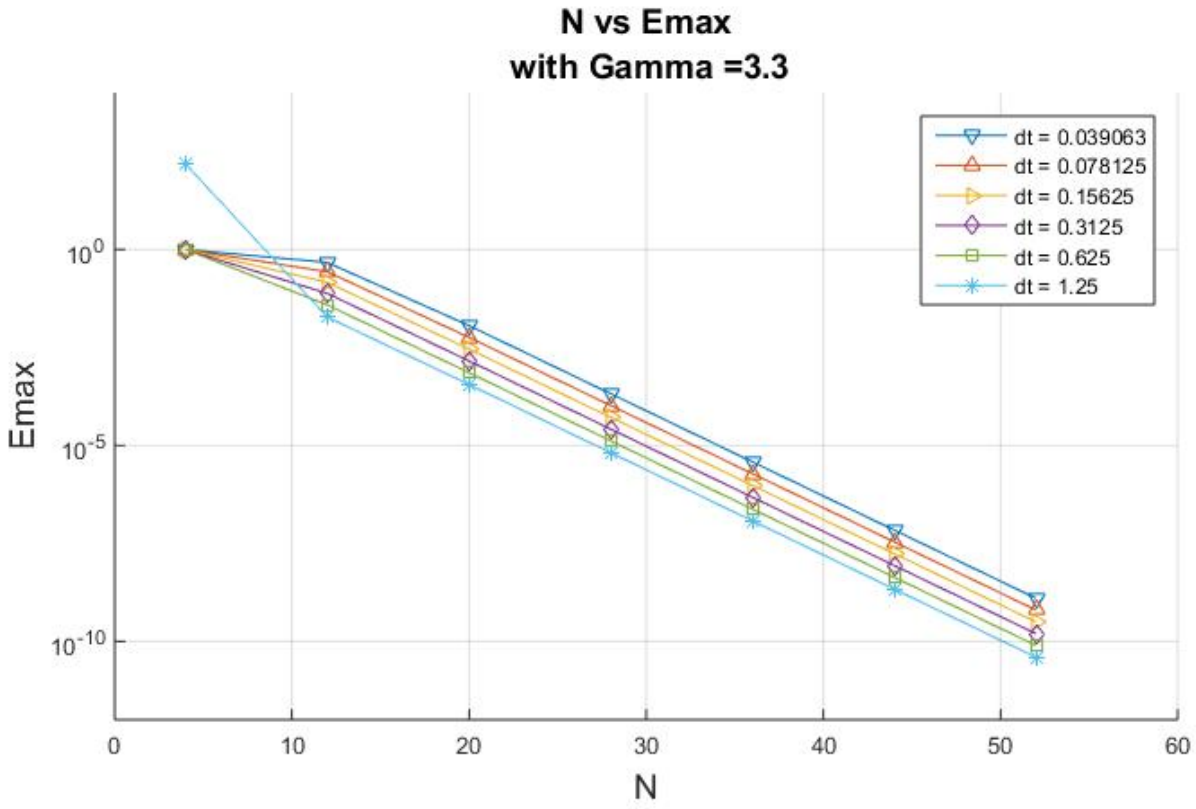

Figure 3.11: *N vs Maximum Error taking $\gamma = 3.3$ and different values of dt for IVP (3.1).*

The Figures 3.6 - 3.11 show a significant decay of the error as the value of N grows. Hence, we calculate the order of that decay. Suppose that:

$$Error = E = O\left(e^{-pN}\right) \approx Ce^{-pN}.$$

Then,

$$\begin{aligned} E_k &= Ce^{-pN_k}, \\ E_{k+1} &= Ce^{-pN_{k+1}}, \end{aligned}$$

where $E_k > E_{k+1}$ and $N_k < N_{k+1}$. So that,

$$\begin{aligned} \frac{E_k}{E_{k+1}} &\approx e^{p(N_{k+1}-N_k)}, \\ \ln\left(\frac{E_k}{E_{k+1}}\right) &\approx p(N_{k+1}-N_k), \\ p &\approx \frac{\ln\left(\frac{E_k}{E_{k+1}}\right)}{N_{k+1}-N_k}. \end{aligned}$$

For different values of N, we get the results listed in Tables 3.1 and 3.2:

	γ						
N	2.1	2.3	2.5	2.7	2.9	3.1	3.3
4							
12	0.000104	0.008324	0.052909	0.131104	0.222516	0.315692	0.406265
20	0.000646	0.052878	0.170346	0.275076	0.360139	0.432946	0.498225
28	0.002589	0.101879	0.213186	0.297726	0.370967	0.438094	0.500729
36	0.006839	0.126127	0.221439	0.299888	0.371533	0.438250	0.500774
44	0.013204	0.135163	0.222857	0.300085	0.371562	0.438255	0.500775
52	0.020458	0.138243	0.223095	0.300103	0.371563	0.438255	0.500771

Table 3.1: *Error Decay Order p for a fix $dt = 0.625$ and different values of γ and N for IVP (3.1).*

From table 3.1 above, observe the difference between the error decay order (in N) for $\gamma = 2.1$ and $\gamma = 3.3$. In the last column of this table, corresponding to $\gamma = 3.3$, see that the value of p is almost constant for each value of N and is approximately 0.5.

	dt					
N	0.0390625	0.078125	0.15625	0.3125	0.625	1.25
4						
12	0.095367	0.163922	0.241102	0.321145	0.406265	1.124570
20	0.464142	0.481873	0.491121	0.495841	0.498225	0.495281
28	0.500071	0.500422	0.500597	0.500685	0.500729	0.500750
36	0.500762	0.500769	0.500772	0.500774	0.500774	0.500775
44	0.500775	0.500775	0.500775	0.500776	0.500774	0.500777
52	0.500779	0.500779	0.500760	0.500799	0.500801	0.500639

Table 3.2: *Error Decay Order p for a fix $\gamma = 3.3$ and different values of dt and N for IVP (3.1).*

For Table 3.2, we fix $\gamma = 3.3$ and test different values for dt and N. See that in the third row the error decay order, associated to $N = 20$ and $N = 28$, is almost the same for all the choices of time step dt. This means that we have the possibility to choose a bigger time step and still get good accuracy.

For the linear case we can conclude that the accuracy of the solution depends more on the choice of the radius γ and the number of s-points N than on the choice of the time step dt. This is due to the way the method was defined. In the absence of the non-linear term, the order of the method does not depend on the size of the time step. It is enough to choose a time step that satisfies the stability condition (2.27) given in Chapter 2.

Finally, as it was mentioned in Chapter 2, the IVP (3.1) is associated to a damping function. The Figure 3.12 shows how this function looks for the different values of γ and N that we tested.

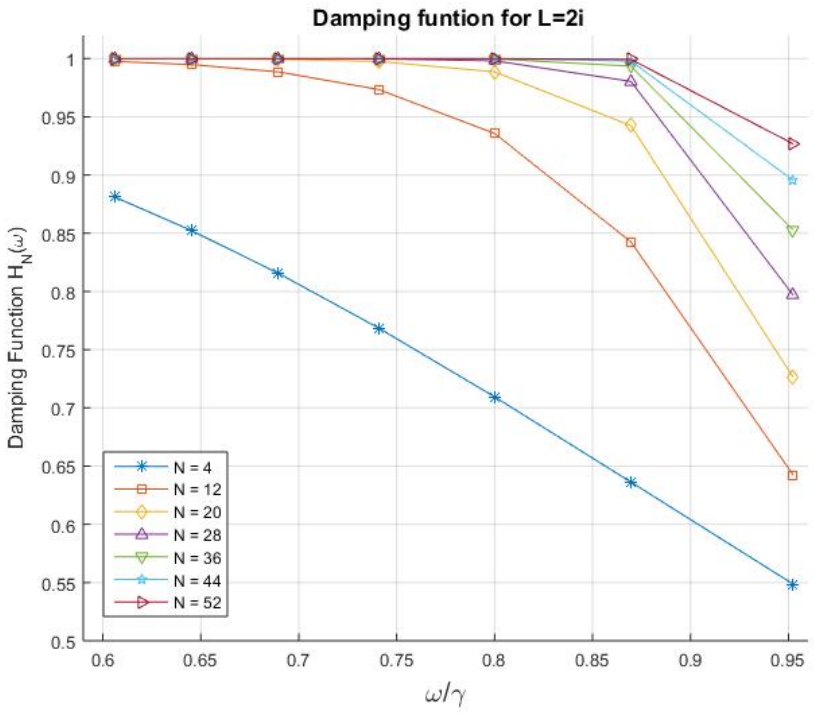

Figure 3.12: *Damping function for the linear case with* $\omega = 2$.

3.2 Filter Case

Many physical problems are modeled using ordinary differential equations whose solutions include high frequency components due to fast waves. In this section, we show the ability of the Laplace Transform to work as a filter under certain considerations. In order to remove these high frequency components we chose a positive number γ such that:

$$|s_l| < \gamma < |s_r|, \tag{3.5}$$

where s_l is the low frequency component and s_r is the high frequency component. Suppose that we have the following IVP:

$$\begin{cases} X'' - 8iX' - 12X = 0, \\ X'(0) = 8i, \\ X(0) = 2. \end{cases} \tag{3.6}$$

The Laplace Transform of this second order ODE is given by:

$$\tilde{X}(s) = \frac{1}{s-2i} + \frac{1}{s-6i}. \tag{3.7}$$

We have two simple poles at $s_1 = 2i$ and $s_2 = 6i$ which represent the low and high frequencies respectively. This means that s_1 and s_2 produce slow and fast oscillations on the solutions of IVP (3.6). Hence, we define the radius as follows:

$$2 < \gamma < 6.$$

The IVP defined in (3.6) can be written as a first order linear system:

$$\begin{cases} \begin{pmatrix} X'_1 \\ X'_2 \end{pmatrix} = \begin{pmatrix} 0 & 1 \\ 12 & 8i \end{pmatrix} \begin{pmatrix} X_1 \\ X_2 \end{pmatrix}, \\ \begin{pmatrix} X_1(0) \\ X_2(0) \end{pmatrix} = \begin{pmatrix} 2 \\ 8i \end{pmatrix}, \end{cases} \tag{3.8}$$

whose exact solution is given by

$$\begin{pmatrix} X_1(t) \\ X_2(t) \end{pmatrix} = \begin{pmatrix} e^{2it} + e^{6it} \\ 2ie^{2it} + 6ie^{6it} \end{pmatrix}, \tag{3.9}$$

and its filtered solution is

$$\begin{pmatrix} X_1^*(t) \\ X_2^*(t) \end{pmatrix} = \begin{pmatrix} e^{2it} \\ 2ie^{2it} \end{pmatrix}. \tag{3.10}$$

3.2.1 Effect of the Truncated Exponential

As we did on Section 3.1, here we present the effect of using the full and truncated exponential while the integration method is acting as a filter.

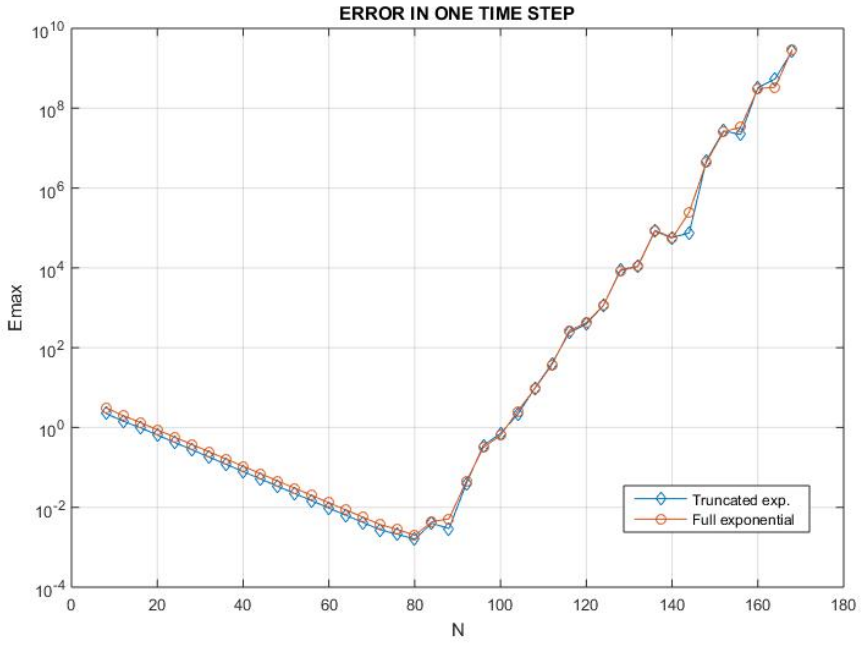

Figure 3.13: *Error Comparison in* $(\|\cdot\|_\infty)$ *between the full and truncated exponential - Filter case.*

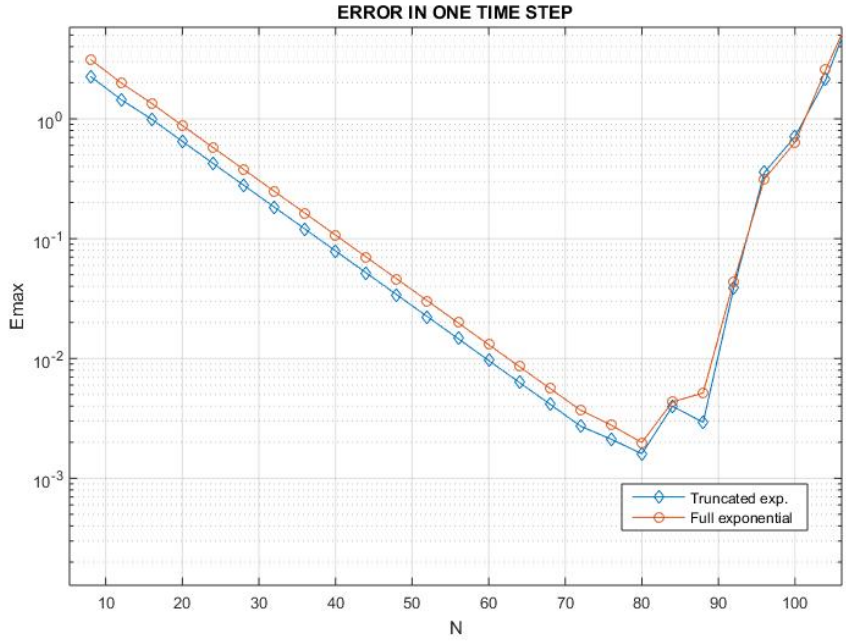

Figure 3.14: *Error Comparison in $\|\cdot\|_\infty$ between the full and truncated exponential - Filter case (Zoom).*

Figures 3.13 and 3.14 show that, although the error made for both exponentials is similar, the truncated exponential continues to give better results than the full exponential. Since in this case the method is being applied as a high frequency filter, the value of the damping function affects the result differently.

Suppose that $\gamma = 4$. Then the Laplace Transform of (3.8) is given by (3.11):

$$\mathfrak{L}^*\left(\frac{1}{s-2i}+\frac{1}{s-6i}\right) = H_N(2)e_N^{2i\Delta t} + H_N(6)e_N^{6i\Delta t} + H_N(2)\sum_{l=0}^{N-1}(2i\Delta t)^l\sum_{k=1}^{\infty}(-1)^k\frac{(4\Delta t)^{kN}}{(l+kN)!}$$

$$+H_N(6)\sum_{l=0}^{N-1}(6i\Delta t)^l\sum_{k=1}^{\infty}(-1)^k\frac{(4\Delta t)^{kN}}{(l+kN)!}. \tag{3.11}$$

Observe that $H_N(2) \longrightarrow 1$ and $H_N(6) \longrightarrow 0$ as the value of N grows. This means that, by choosing a suitable value for gamma and truncating the exponential it is possible to eliminate the high frequency component of the approximate solution, i.e., to obtain the filtered solution. On the other hand, by using the full exponential, we still have the following term:

$$H_N(2)\sum_{l=0}^{N-1}(2i\Delta t)^l\sum_{k=1}^{\infty}(-1)^k\frac{(4\Delta t)^{kN}}{(l+kN)!},$$

as a source of error.

3.2.2 Filtering

In the following figures we will show how the filter works, that is, we will show the filtered function. Since we cut the high frequency component, we only have the contribution of the lowest frequency, i.e, the component with pole of the smallest module.

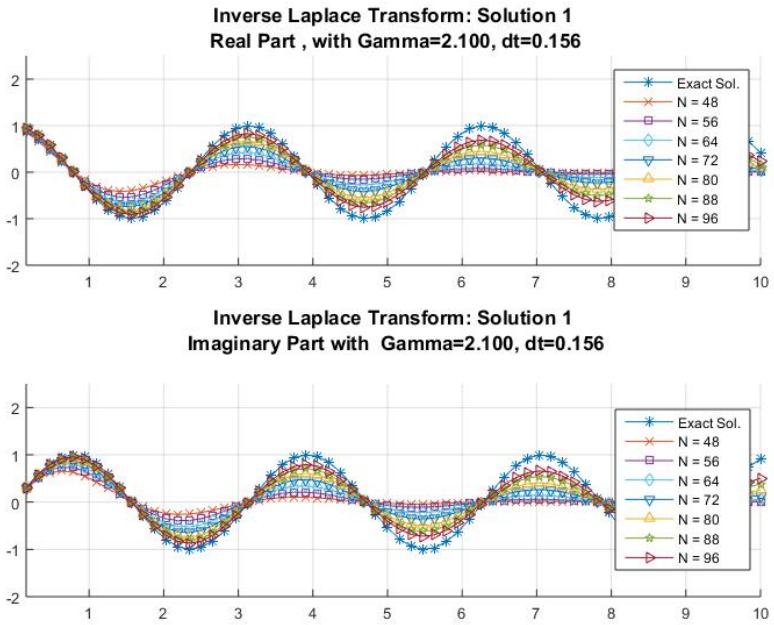

Figure 3.15: *Exact filtered solution X_1^* vs Approximate filtered solutions using $dt = 0.15625$ and $\gamma = 2.1$ for the IVP (3.6).*

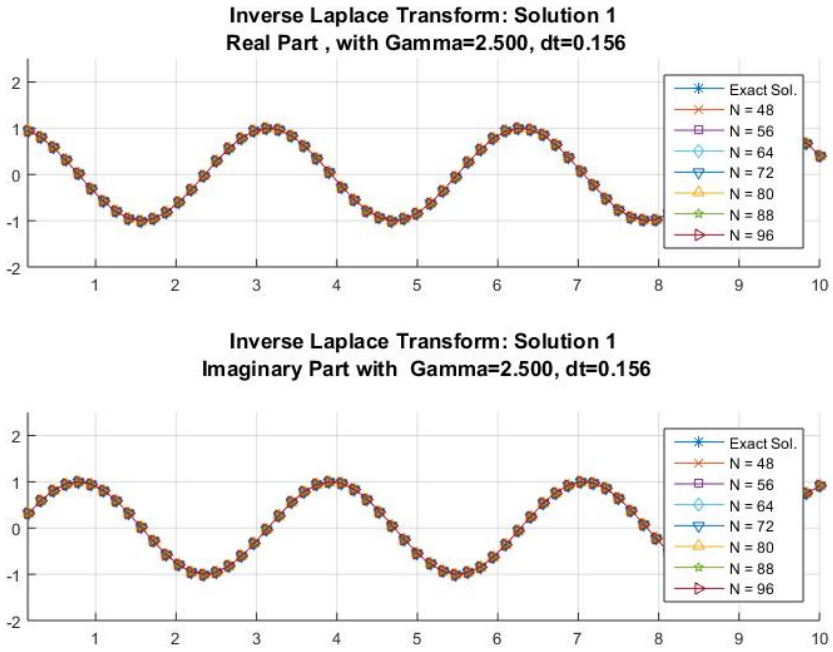

Figure 3.16: *Exact filtered solution X_1^* vs Approximate filtered solutions using $dt = 0.15625$ and $\gamma = 2.5$ for the IVP (3.6).*

Figures 3.15 and 3.16 show the results obtained while approximating the filtered solution X_1^* given in (3.10). As in the first case, with a single pole, the further we get from the smallest pole the better results we get. Here, we have a limitation for the radius, in the following we will see what is the best choice for γ.

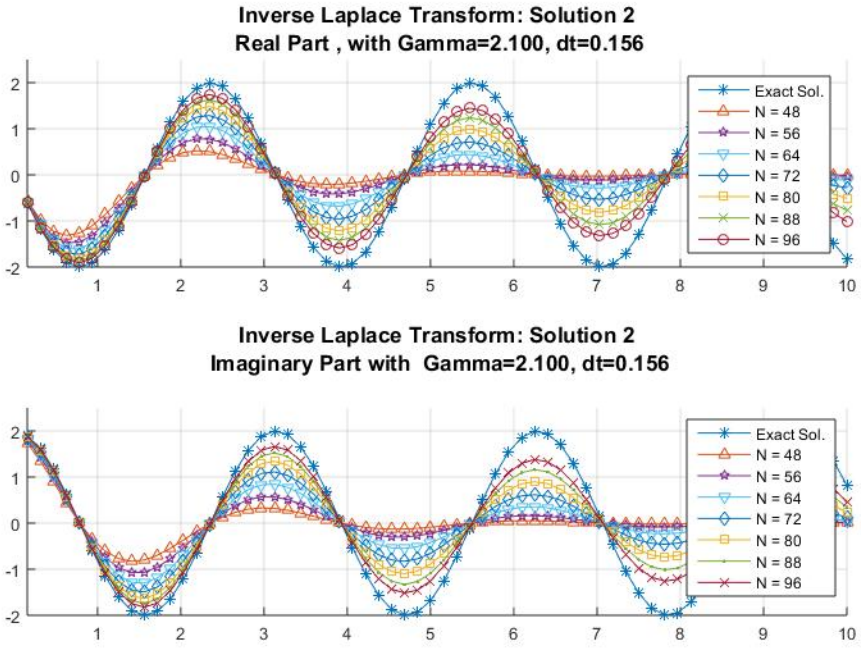

Figure 3.17: *Exact filtered solution X_2^* vs Approximate filtered solutions using $dt = 0.15625$ and $\gamma = 2.1$ for the IVP (3.6).*

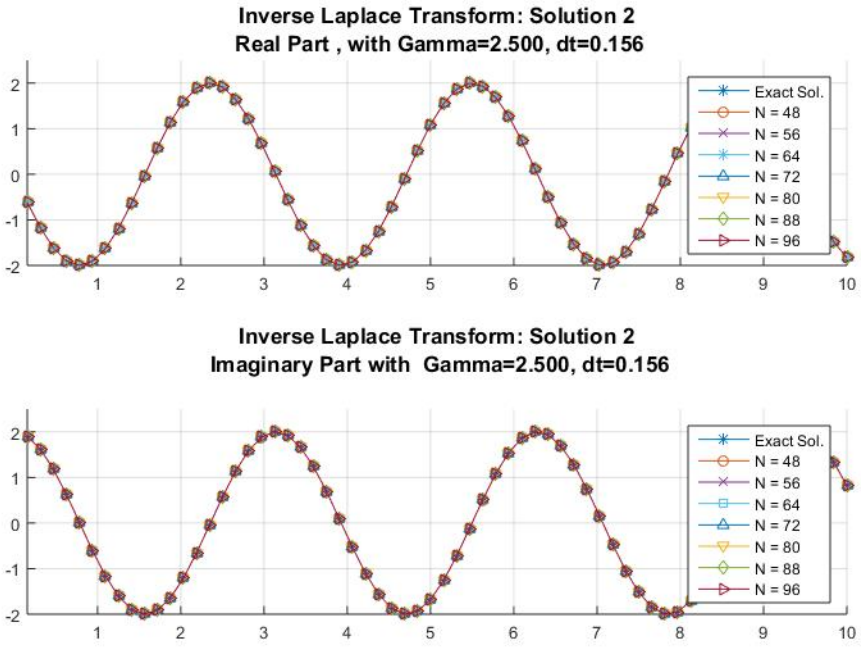

Figure 3.18: *Exact filtered solution X_2^* vs Approximate filtered solutions using $dt = 0.15625$ and $\gamma = 2.5$ for the IVP (3.6).*

Figures 3.17 and 3.18 show the results while approximating the filtered solution X_2^* given in (3.10). Next, we present the graphs showing the behavior of the error for this case. Since the behavior of the error is similar for both solutions we just present the graphs corresponding to the solution X_1^*.

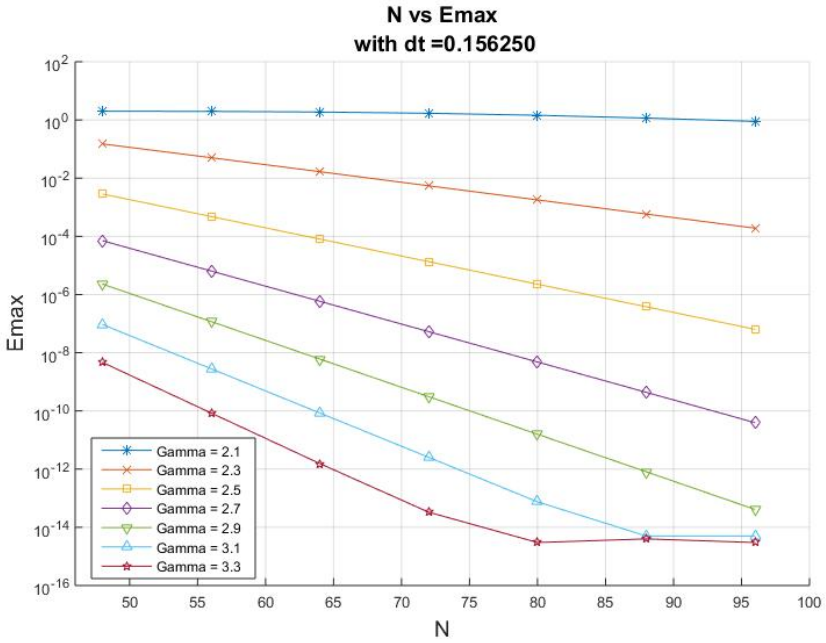

Figure 3.19: *N vs Maximum Error for X_1^* using $dt = 0.15625$ and different values of γ between 2.1 and 3.3 for IVP (3.6).*

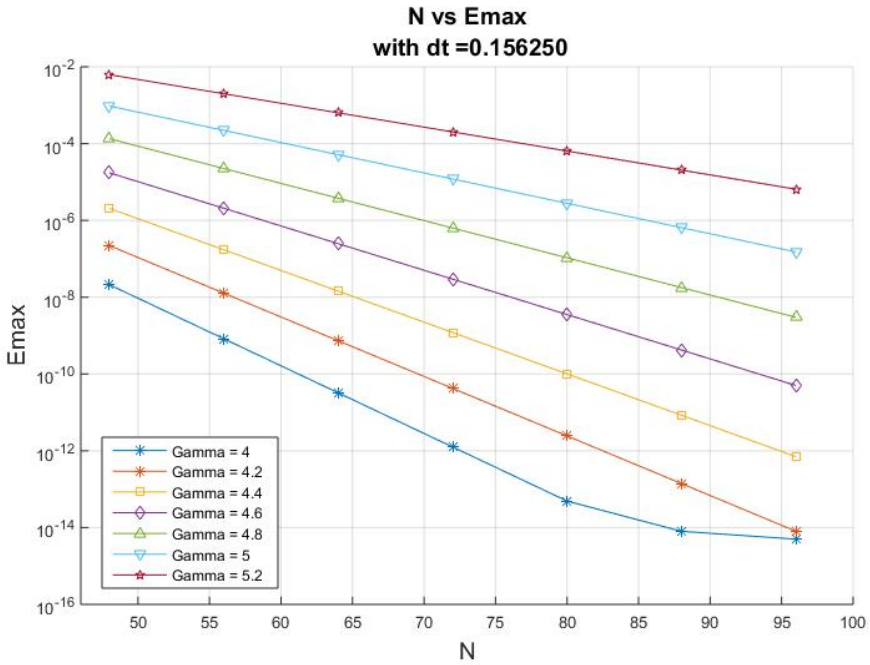

Figure 3.20: *N vs Maximum Error for X_1^* using $dt = 0.15625$ and different values of γ between 4 and 5.2 for IVP (3.6).*

Observe that the simulations were separated in two groups. The first one with γ between 2.1 and 3.3 (Figure 3.19) and the second one with γ between 4 and 5.2 (Figure 3.20). As in the first case, the error decays exponentially for bigger values of N. In addition, notice that for $\gamma = 3.3$ and $\gamma = 4$ we get the smallest error; thus the best choice for the radius is $3.3 \leq \gamma \leq 4$. Figure 3.20 indicates that the error is increasing for $\gamma > 4$, this is because the approach is affected by the high frequency component.

3.3 Non-linear ODEs

Consider the following IVP:

$$\begin{cases} \frac{dX}{dt} &= 2iX + X^2, \\ X(0) &= 0.8 - 0.4i. \end{cases} \tag{3.12}$$

The solution for (3.12) was calculated using algebraic techniques for differential equations :

$$X(t) = \frac{2e^{2it}}{2 + ie^{2it}}. \tag{3.13}$$

As in the linear case, we study the dependence of the stability and accuracy of the approximate solution on the parameters γ, dt and N. We present the results obtained as follows.

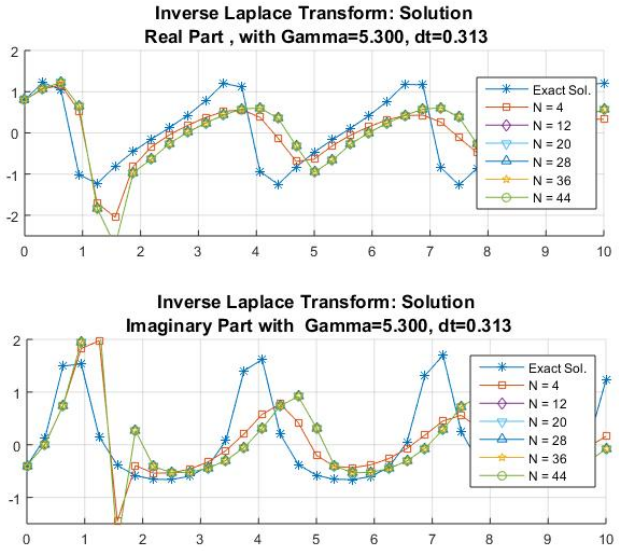

Figure 3.21: *Exact solution vs Approximate solutions using* $dt = 0.3125$ *and* $\gamma = 5.3$ *for IVP (3.12).*

Figure 3.21 shows that the approximate solutions are unstable for the chosen parameters while Figure 3.22 shows stable results for an smaller time step.

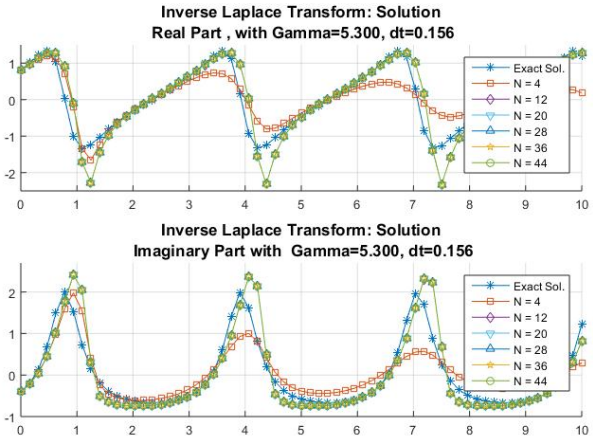

Figure 3.22: *Exact solution vs Approximate solutions using* $dt = 0.15625$ *and* $\gamma = 5.3$ *for IVP (3.12).*

In order to establish the relation of the parameters γ, dt and N, we consider the behavior of the error.

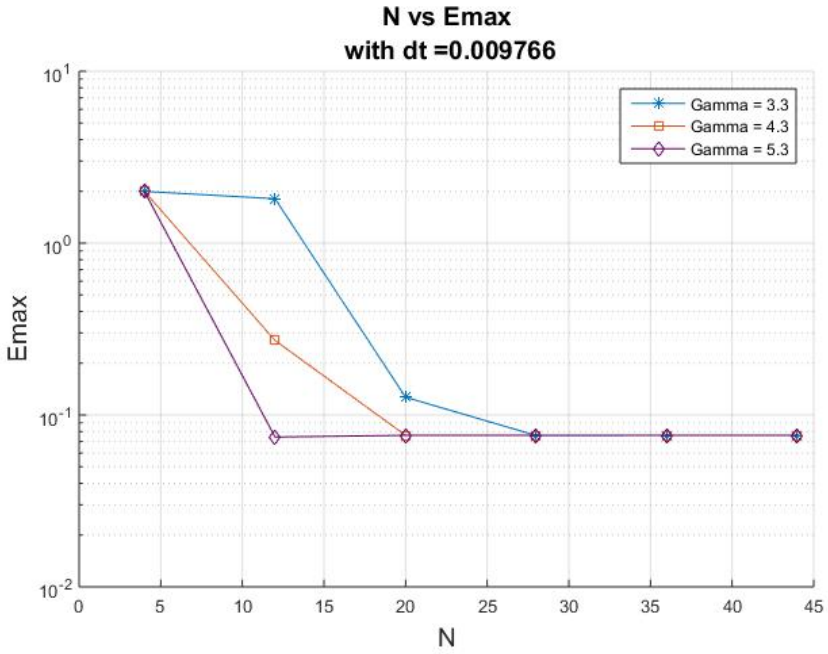

Figure 3.23: *N vs Maximum Error ($\|\cdot\|_\infty$) using $dt = 0.009766$ and different values of γ and N for IVP (3.12).*

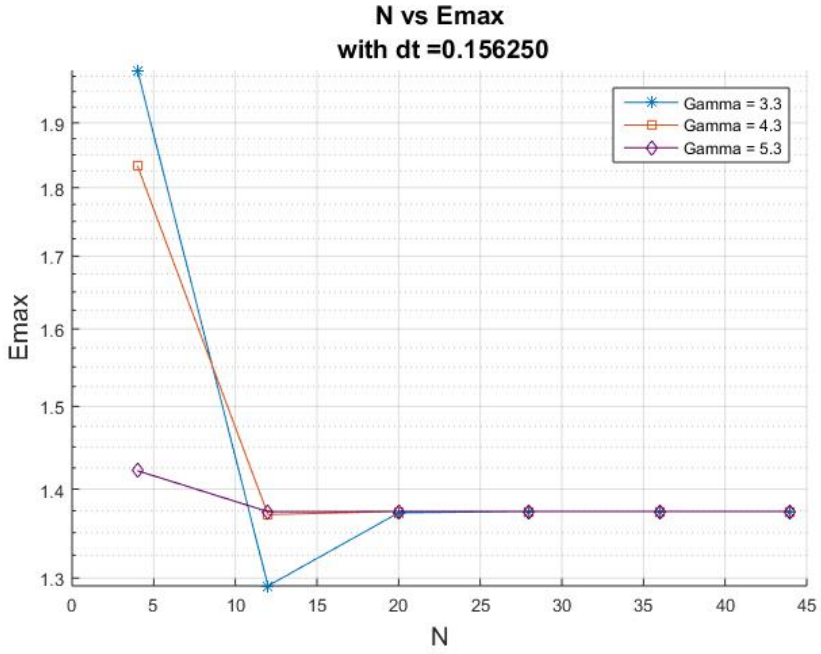

Figure 3.24: *N vs Maximum Error ($\|\cdot\|_\infty$) using $dt = 0.15625$ and different values of γ for IVP (3.12).*

In Figures 3.23 and 3.24 we graph the behavior of the error for a fix dt and different values of γ and N. Observe that the smallest error is obtained with $dt = 0.009766$ and $\gamma = 5.3$, also see that for some large values of N the behavior of the error is constant. This means that the approach is not depending on the value of N, however it is affected by the size of the time step.

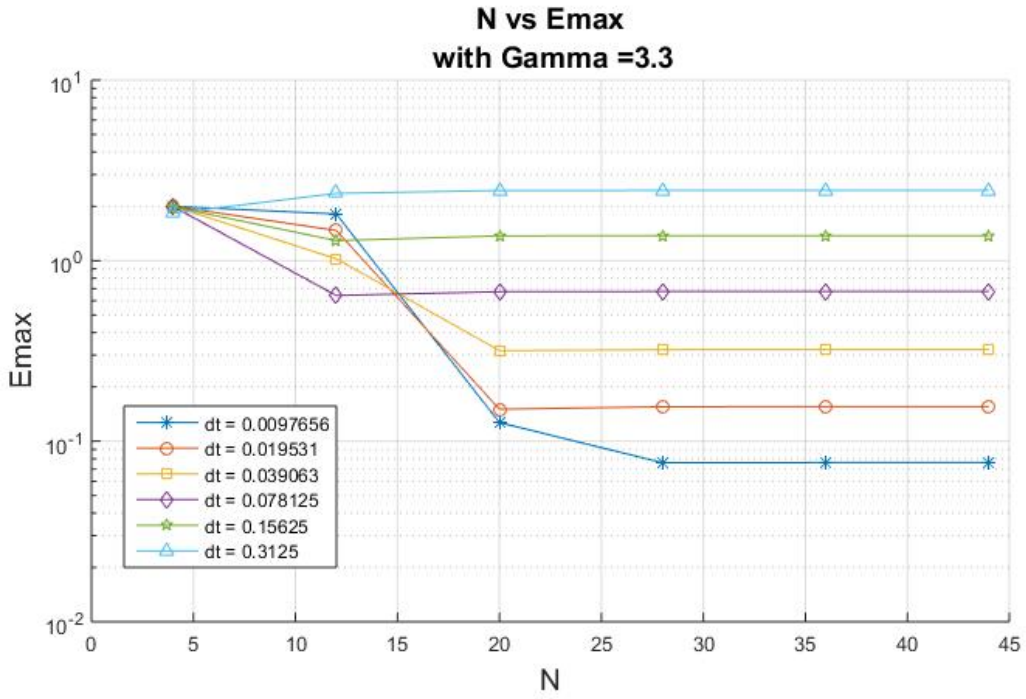

Figure 3.25: *N vs Maximum Error ($\|\cdot\|_\infty$) using $\gamma = 3.3$ and different values of dt and N for IVP (3.12).*

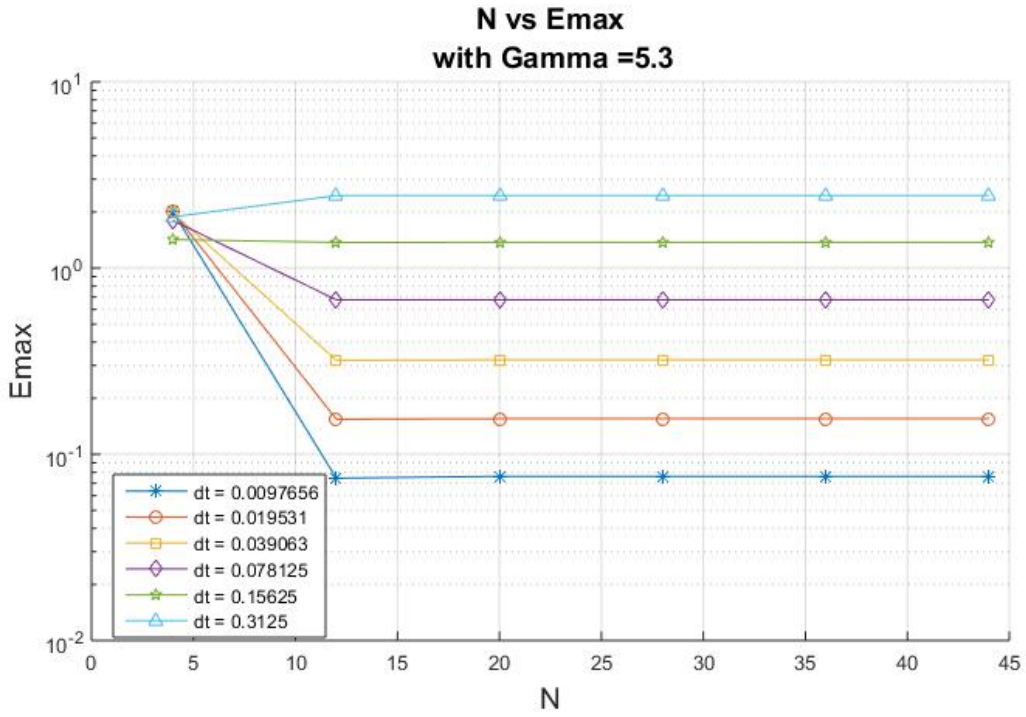

Figure 3.26: *N vs Maximum Error ($\|\cdot\|_\infty$) using $\gamma = 5.3$ and different values of dt and N for IVP (3.12).*

Figures 3.25 - 3.26 indicate that the smallest time step produces the smallest error. Since the approximation of the non-linear term depends on the size of the time step (see Chapter 2), increasing the value of N does not have a significant impact on the accuracy of the solution. It is enough to choose a sufficiently large N.

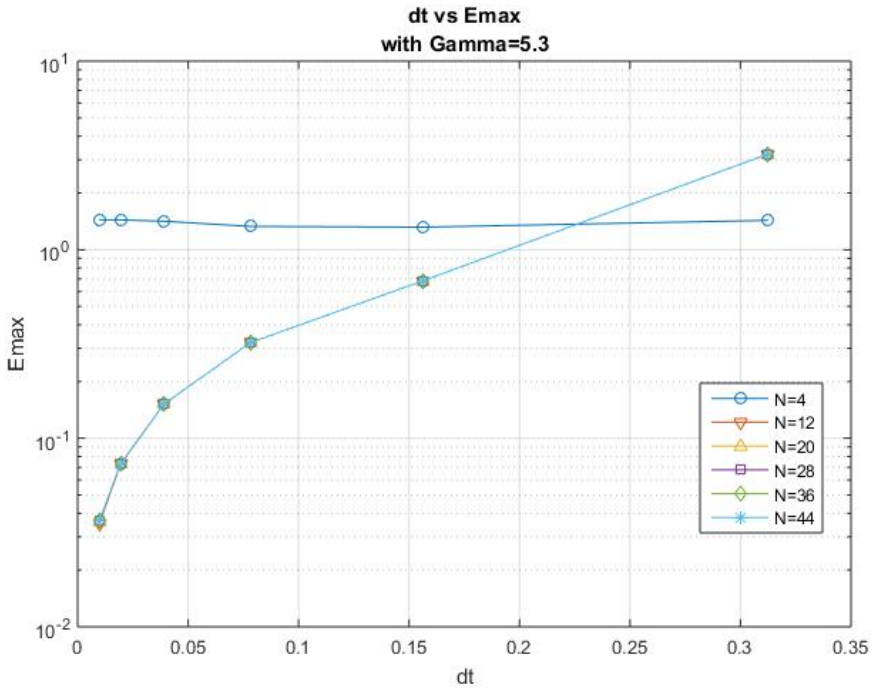

Figure 3.27: *dt vs Maximum Error using* $\gamma = 5.3$ *and different values of dt and N for IVP (3.12).*

For the non-linear case we can conclude that the stability and accuracy of the results depend strongly on the choice of the time step. The bad news is that decay of the error with respect to the time step is of first order (See Table 3.3), which is consistent with the definition of the integration method given by the Equation (2.35) in Chapter 2. In this case, we have a polynomial decay of the error and not exponential as in the linear case. In Table 3.3 we present the order of decay of the error using the time steps that guaranteed stability.

N	dt			
	0.019531	0.0039062	0.078125	0.15625
4				
12	1.0584	1.0542	1.0800	1.0923
20	1.0257	1.0453	1.0780	1.0916
28	1.0257	1.0453	1.0780	1.0916
36	1.0257	1.0453	1.0780	1.0916
44	1.0257	1.0453	1.0780	1.0916

Table 3.3: *Error Decay Order with respect to the time step using* $\gamma = 5.3$ *for IVP (3.12).*

3.4 Stability Limitations of the LTIM

3.4.1 Numerical instability due to roundoff errors

In Section 3.1 we solved an IVP with a small pole and a relation between the parameters γ, dt and N was established. Here we consider the case where a linear IVP has a higher frequency component. Let:

$$\begin{cases} \frac{dX}{dt} &= 100iX, \\ X(0) &= 1, \end{cases} \tag{3.14}$$

be an IVP whose Laplace Transform is given by:

$$\mathfrak{L}\{X(t)\} = \frac{1}{s - 100i}, \tag{3.15}$$

and its exact solution is:

$$X(t) = e^{100it}. \tag{3.16}$$

In order to analyse this case, we chose different values for γ, dt and sufficiently large values for N.

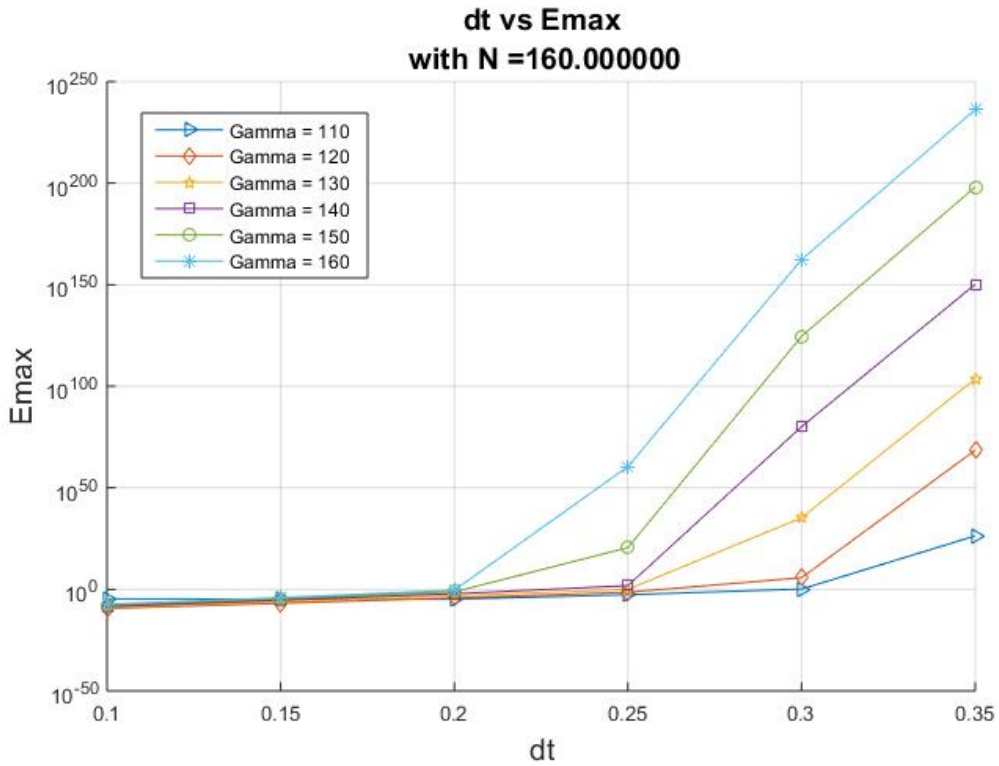

Figure 3.28: *dt vs Maximum Error using $N = 160$ and different values of γ for IVP 3.14.*

Figure 3.28 indicates that for $dt > 0.2$ the error grows too much. The exponential term in the inversion formula has an exponent that is the product of γ and dt. If this is too large, then the computer will not be able to represent it exactly due to round off errors (*See Higham (2002) and Uerberhuber (1997)*). Figure 3.29, shows another perspective of the behavior of the Maximum Error.

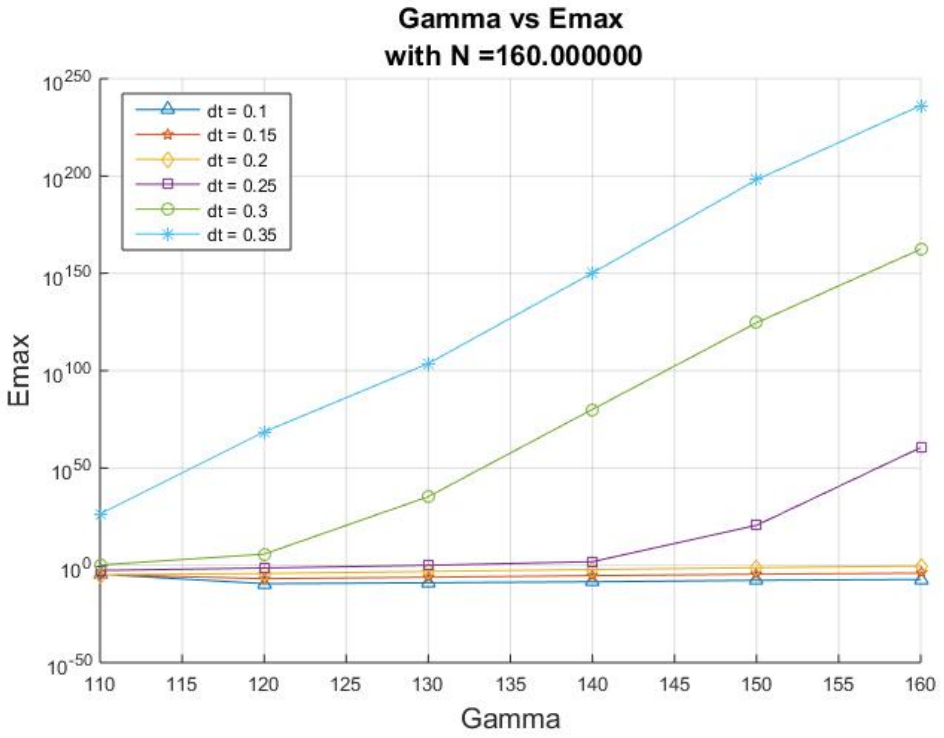

Figure 3.29: *γ vs Maximum Error using $N = 160$ and different values of dt for IVP 3.14.*

Cutting off the errors greater than one (Figures 3.30 and 3.31), is possible to the take a closer look on the error for suitable values of γ and dt.

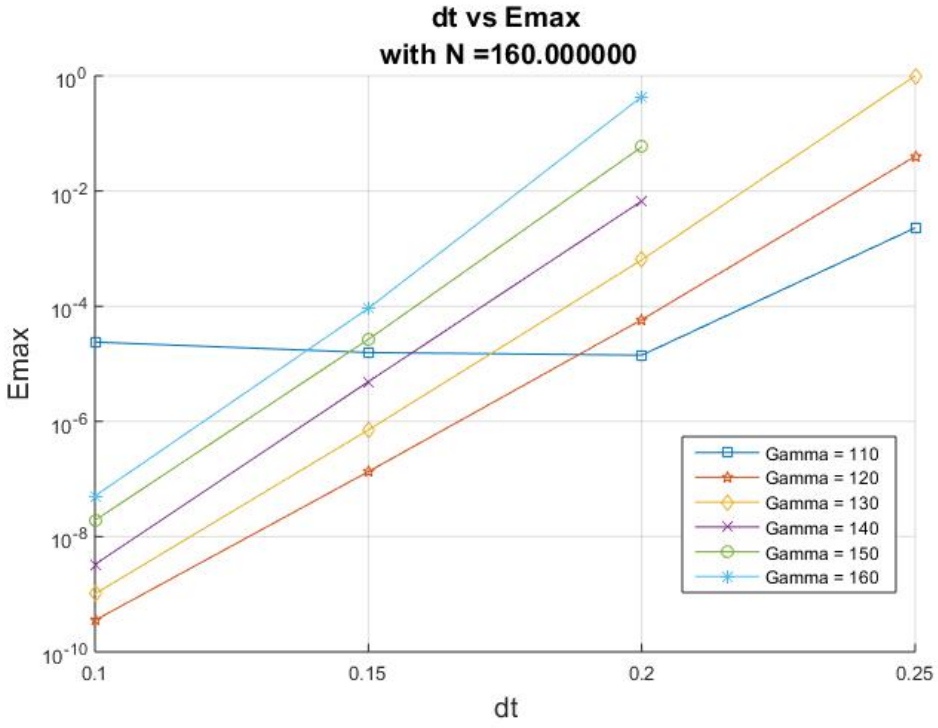

Figure 3.30: *dt vs Maximum Error using $N = 160$ and different values of γ for IVP 3.14.*

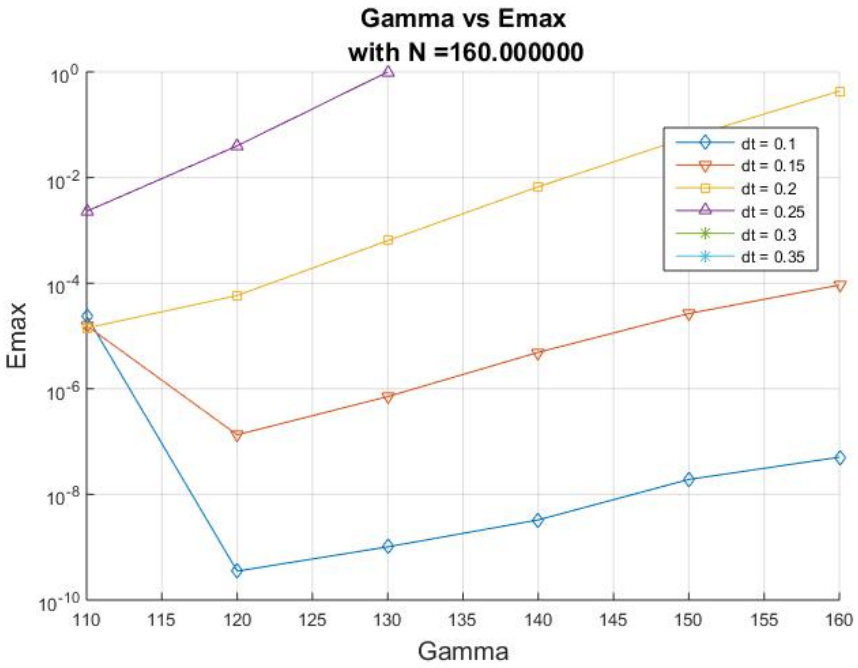

Figure 3.31: *γ vs Maximum Error using $N = 160$ and different values of dt for IVP 3.14.*

Notice that the error curves for $dt = 0.3$ and $dt = 0.35$ did not appear in the Figure 3.31, this is because for any value of γ the error is greater than one. This information is organized in Table 3.4. For each radius γ we show both the analytical (obtained via equation (2.27)) and the largest numerical time step obtained.

γ	Analytical dt	Numerical dt
110	0.5468	0.25
120	0.5012	0.25
130	0.4627	0.25
140	0.4296	0.2
150	0.4009	0.2
160	0.3759	0.2

Table 3.4: *Analytical Numerical dt using $N = 160$ and different values of γ for IVP 3.14.*

Since the bound for the time step depends on the value of γ and N, we might think that, in order to get a bigger time step, we just need to increase the value of N. The problem is that we can not use an exponent that can not be represented by the computer. Thus, the stability condition defined in Chapter 2 will not work in this case. Since we are using double precision, it is possible to make arithmetic operations with sixteen significant digits (see Cheney and Kincaid (2008)). The largest number that we can work with (without round off error problems) is of the form

$$B_1, b_2 b_3 ... b_{16} \times 10^{15}.$$

To obtain the maximum exponent with which arithmetic operations can be performed with the exponential, we perform the following calculation:

$$\begin{aligned} 10^{15} &= e^{m}; \\ 15\log 10 &= m\log e; \\ m &= \frac{15\log 10}{\log e}. \end{aligned}$$

Thus,

$$m \approx 34.5387763949,$$

where $m = sdt$ and s is an s-point. With this result, we plot the numeric stability zone of the LTIM considering N suficiently large, so that the largest analytical stable Δt is larger than the numerical largest Δt.

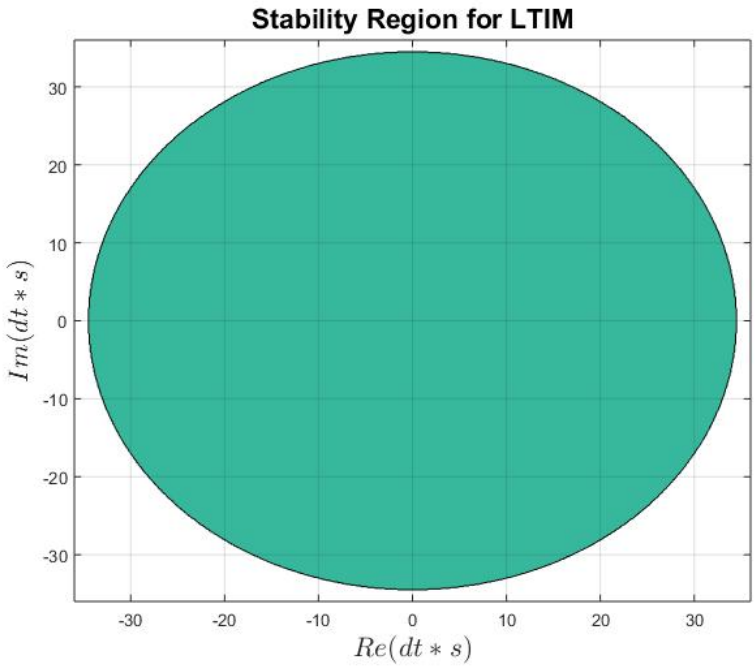

Figure 3.32: *Stability Region of the Laplace Transform Integration Method.*

Chapter 4

Comparison with Fourth Order Runge Kutta Method

4.1 Linear Initial Value Problem

In this section, in order to see the advantages of our method, we compare the LTIM and the Fourth Order Runge Kutta Method (See (Mayers and Süli, 2003)) and solve the linear case given in Section 3.1:

$$\begin{cases} \frac{dx}{dt} &= 2ix, \\ x(0) &= 1, \end{cases} \tag{4.1}$$

where $f(t,x) = 2ix$. The Fourth Runge Kutta (RK4) scheme is given by:

$$\begin{array}{rcl} k_1 &=& dtf(t_n, x_n), \\ k_2 &=& dtf\left(t_n + \frac{dt}{2}, x_n + \frac{dt}{2}k_1\right), \\ k_3 &=& dtf\left(t_n + \frac{dt}{2}, x_n + \frac{dt}{2}k_2\right), \\ k_4 &=& dtf\left(t_n + dt, x_n + dtk_3\right), \\ x_{n+1} &=& \frac{1}{6}dt\left(k_1 + 2k_2 + 2k_3 + k_4\right). \end{array} \tag{4.2}$$

The stability zone of RK4 is given by the following condition (see Figure 4.1):

$$\left|1 + \lambda dt + \frac{(\lambda dt)^2}{2} + \frac{(\lambda dt)^3}{6} + \frac{(\lambda dt)^4}{24}\right| \leq 1. \tag{4.3}$$

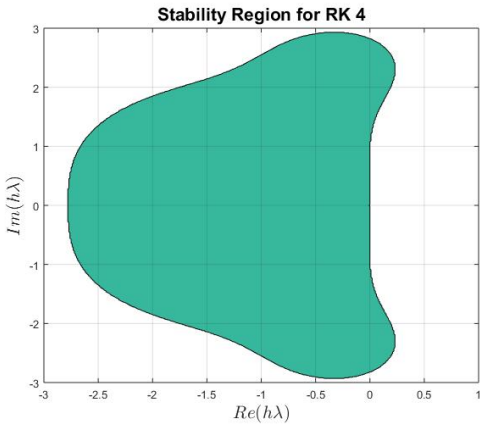

Figure 4.1: *Stability Region of the Fourth Order Runge Kutta Method.*

For IVP (4.1) we have that $\lambda = 2i$. Thus, the largest time step for this method is

$$dt \leq 1.25965.$$

The numerical scheme given by (4.2) indicates that for each iteration it is necessary to do execute four evaluations of the function f. In the case of the Laplace Transform Integration Method, we execute N evaluations per time iteration.

If we take $dt = 1.25$ and $[0, 10]$ as the time domain, we have 8 iterations in time, which means we need to make 32 evaluations of the function f for the RK4 and $8N$ evaluations for LTIM. As mentioned in Chapter 2, the size of the time step depends on the value of N and γ. Thus, for $dt = 1.25$ the value of N is approximately 12.

Method	Evaluations	Max. Error
LTIM	96	0.0983
RK4	32	1.1110

Table 4.1: *Fourth Order Runge Kuta vs Laplace Transform Integration Method I.*

Table 4.1 shows that the RK4 needs fewer evaluations than LTIM, but the RK4 method is not as accurate as the LTIM. Now, observe Table 4.2.

Method	Time step	Evaluations	Max. Error
LTIM	1.25	96	0.0983
	1.25	256	1.8542×10^{-5}
RK4	1.25	32	1.1110
	0.4	100	0.0665
	0.05	800	1.6665×10^{-5}

Table 4.2: *RK4 vs LTIM, Time step comparison II.*

In Table 4.2, increased values of N produced a more accurate result for LTIM. On the other hand, in order to get an error of size 10^{-5} with RK4 we had to reduce the size of time step. This restricts even more the choice of the time step. If we want to increase the accuracy of the method we have to increase in number of stages, which increases the computational cost. One of the aims of this work is to take as large time steps as possible.

Method	N	Time step	Evaluations	Max. Error
LTIM	92	10	92	0.0257
RK4	-	0.4	100	0.0665

Table 4.3: *RK4 vs LTIM, Time step comparison III.*

Table 4.3 shows that with the LTIM is possible to take a larger time step with an smaller error than with RK4. Notice also, that the LTIM needed fewer evaluations and the time step is 25 times larger than the one used for RK4. Thus, for the linear case, the Laplace Transform Integration Method is more efficient than the Fourth Runge Kutta Method.

4.2 Non-linear Initial Value Problem

4.2.1 Swinging Spring System

In this section we apply the Laplace Integration Method to the Lynch's Swinging Spring Model (Lynch, 1996), given by:

$$\begin{cases} \dot{\theta} &= \frac{p_\theta}{mr^2}, \\ \dot{p_\theta} &= -mgr\sin\theta, \\ \dot{r} &= \frac{p_r}{m}, \\ \dot{p_r} &= \frac{p_\theta^2}{mr^3} - k(r-l_0) + mg\cos\theta, \end{cases} \tag{4.4}$$

where m is the mass of the bob, l_0 is the unstretched length of the spring, k is the elasticity or stiffness of the spring, g is the gravity force, θ and r represent the angle and radius respectively and, p_θ and p_r represent their velocities.

This model is of mathematical interest because for an appropriate choice of parameters, the elastic oscillations have much higher frequency than the rotation or libration of the bob. Lynch (1996) considered the elastic oscillations to be analogues of the high frequency waves in atmosphere. Likewise, he considered the low frequency rotational motions to correspond to the rotational or Rossby-Haurwitz waves. Figure 4.2 shows a geometric representation of a swinging spring.

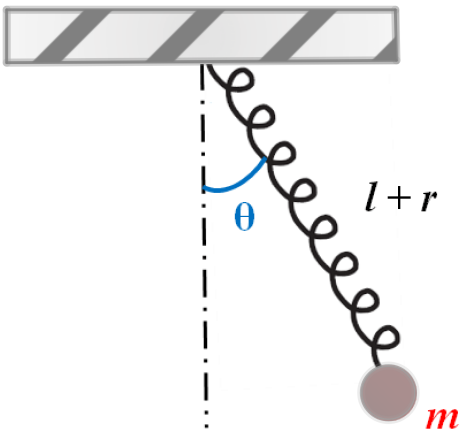

Figure 4.2: *Swinging Spring Pendulum.*

To solve this model, we linearize the system given by Equation (4.4) with $X = \begin{pmatrix} \theta & p_\theta & r & p_r \end{pmatrix}^t$:

$$J_{\vec{X}} = \begin{pmatrix} 0 & \frac{1}{mr^2} & -\frac{2p_\theta}{mr^3} & 0 \\ -mgr\cos\theta & 0 & -mg\sin\theta & 0 \\ 0 & 0 & 0 & \frac{1}{m} \\ -mg\sin\theta & \frac{2p_\theta}{mr^3} & -\frac{2p_\theta^2}{mr^4} - k & 0 \end{pmatrix}. \tag{4.5}$$

The equilibrium point is of the form:

$$X_e = \begin{pmatrix} 0 & 0 & l_0 + \frac{mg}{k} & 0 \end{pmatrix}^t. \tag{4.6}$$

Thus, evaluating (4.5) in (4.6) we get:

$$J_{\vec{X_e}} = \begin{pmatrix} 0 & \frac{1}{mr^2} & 0 & 0 \\ -mgr & 0 & 0 & 0 \\ 0 & 0 & 0 & \frac{1}{m} \\ 0 & 0 & -k & 0 \end{pmatrix}. \tag{4.7}$$

Using matrix (4.7), it is possible to write system (4.4) in the form:

$$\dot{X} = -LX - N(X).$$

The chosen parameters for the simulations are:

$$m = 1kg, \quad l_0 = 1m, \quad g = \pi^2 ms^{-2}, \quad k = 100\pi^2 kgs^{-2}, \tag{4.8}$$

and the initial condition is:

$$X_0 = \begin{pmatrix} -\frac{1}{2} & 0 & 1.01 & 0 \end{pmatrix}^t. \tag{4.9}$$

Figures 4.3 and 4.4 show the reference solution for the system (4.4) with initial data (4.8) and (4.9):

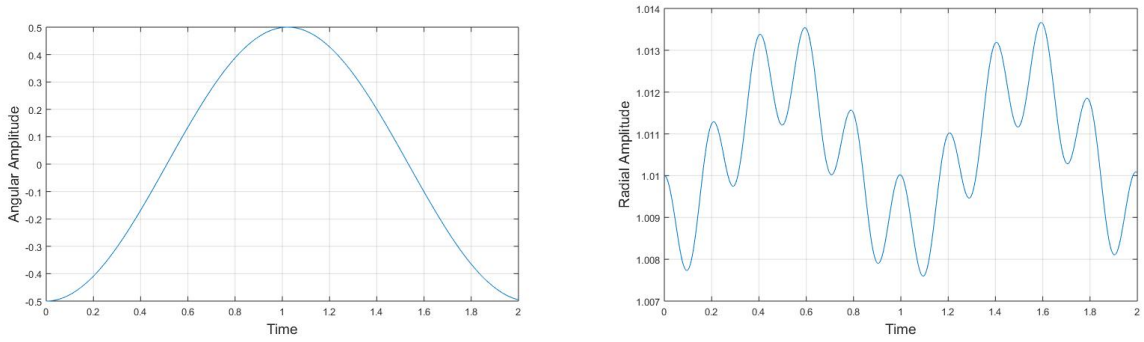

Figure 4.3: *On the left: Angular Amplitude. On the right: Radial Amplitude.*

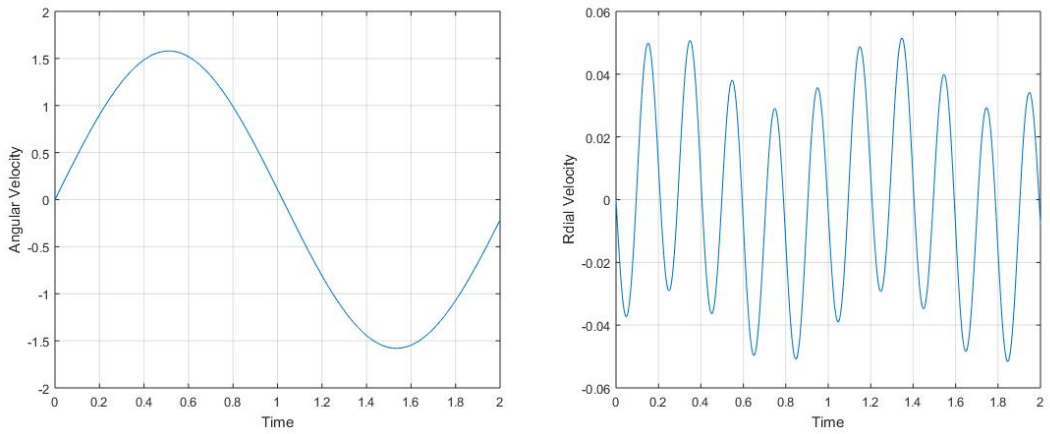

Figure 4.4: *On the left: Angular Velocity. On the right: Radial Velocity.*

In order to make the comparison between Laplace Transform Integration Method and The Fourth Order Runge Kutta, two different sets of time steps were considered.

RK4	
Δt	Total Evaluations
0.001953125	4086
0.0078125	1024
0.03125	256
0.125	64
0.25	32

LTIM	
Δt	Total Evaluations
0.03125	2560
0.0625	1280
0.125	640
0.25	320
0.5	160

Table 4.4: *On the left: Time steps and number of evaluations for Rk4. On the right: Time steps and number of evaluations for LTIM using* $\gamma = 40$ *and* $N = 40$.

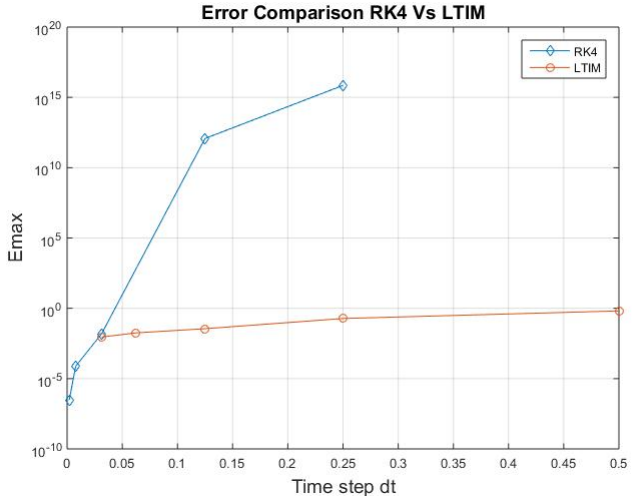

Figure 4.5: *Error Comparison RK4 vs LTIM.*

Figure 4.5 presents the Error curves for each method. As we can see, the LTIM was able to perform numerical operations with larger time steps than the RK4. Considering just the time steps for which the RK4 worked, observe that, the error for LTIM is not as small as the one for RK4. However, it is still acceptable. Cutting off the errors for which RK4 does not work (See Figure 4.6), we get a closer view of both curves:

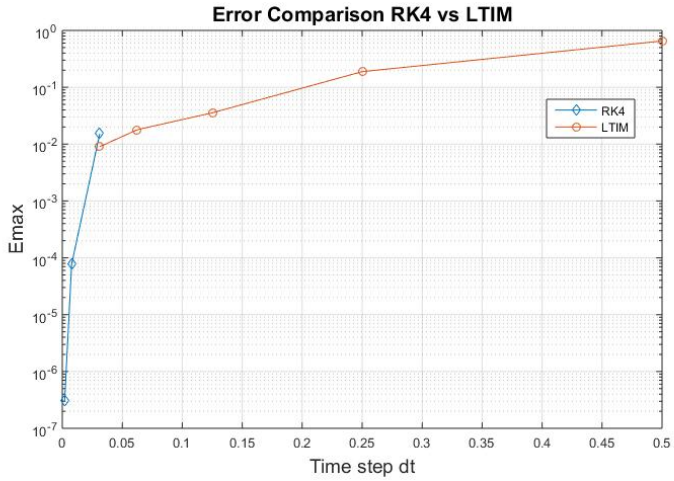

Figure 4.6: *Error Comparison RK4 vs LTIM - Zoom.*

Naturally, being a non-linear problem the accuracy of the RK4 (fourth order) is far greater than the first order accuracy LTIM on the non-linearities.

Chapter 5

Conclusions

Many physical phenomena are modeled through systems of differential equations. Generally, these systems are difficult to solve (or do not have solution), so we have to appeal to numerical methods. Weather forecast models, for example, include solutions with very fast oscillations that interfere with the stability of the approximate solutions. Due to this inconvenience, we are always looking for more efficient methods. Our work aimed to study an alternative numerical method to solve systems of ordinary differential equations that allows larger time step without losing stability and accuracy. In this case, the numerical method was based on the Inverse Laplace Transform. By making some modifications on the contour of the Bromwich integral it was possible to develop a method that can filter high frequency components from the solutions.

From the experiments we saw that, for linear cases, stability can be guaranteed only by choosing a time step that satisfies the stability condition (2.27) given in Chapter 2 and does not exceed the stability zone defined in Chapter 3. Choosing a suitable time step, the accuracy of the approximate solutions depends on the choice of N and γ. The behavior of the error showed a significant decay as the value of N increased, i.e., we have spectral convergence in N. The same results were observed while applying the method as a filter. In addition, we could verify that the truncated exponential guarantees the convergence of the approximate solution to the exact solution.

On the other hand, for non-linear cases, the approximate solution is strongly affected by the non-linear part. The behavior of the error indicated that the accuracy and stability of the solution depends on the choice of Δt. This is a consequence of the order of approximation of the non-linear term.

When comparing the Laplace Transform Integration Method with the Fourth Order Runge Kutta method, we showed that the first method was able to perform numerical operations with larger time steps maintaining stability and an acceptable error. In addition, unlike RK4, in the LTIM each evaluation of the numerical scheme is independent of each other. This means that we can do the calculations in parallel which would reduce the computation time.

Since the numerical scheme includes an exponential term, the main limitation that this method faced was instability due to round off errors. In order to control this problem, an stability region (that depends on the value of γ and Δt) was defined.

As future work plans, we want to apply this method of integration to physical problems that are modeled through partial differential equations. In this work, we have used an approach that has first order error with respect to non-linearities. Improving the approximation of the non-linear term will make this method more accurate for larger time step sizes. One option would be to use some known method of differences to approximate the non-linear term separately, such as predictor-corrector methods. Another option would be to apply the exponential integrator methods (See Hochbruck and Ostermann (2010), Cox and Matthews (2002), Pope (1963)). We would like to

explore another integration contours different from the circle, this with the aim of improving the accuracy of the method and expanding its stability zone.

Bibliography

Ablowitz and Fokas(2003) Marks J. Ablowitz and Athanassios S. Fokas. *Complex Variables: Introduction and Applications*, 2nd Edition. Cambrigde University Press, New York. Cited in pag.

Ahmad and Javidi(2013) Bashir Ahmad and Mohammad Javidi. *Numerical Solution of Fractional Partial Differential Equations by Numerical Laplace Inversion Techniques. Springer - Advances in Difference Equations*, 375:1–18. Cited in pag.

Ahmad and Ambrosetti(2014) Shair Ahmad and Antonio Ambrosetti. *A textbook on Ordinary Differential Equations*, 2nd Edition. Springer, Switzerland. Cited in pag.

Al *et al.***(2016)** Nawfal Al, Lubomir Brancik and Zubaidi Smith. *Comparative Study on One-Dimensional Numerical Inverse Laplace Transform Methods for Electrical Engineering. ElectroRevue*, 18:1–7. Cited in pag.

Ashan(2012) Mahmud Ashan. *Numerical Solution of the Advection - Diffusion Equation Using Laplace Transform Finite Analytic Method. International Jouernal of River Basin Management*, 10:2:177–188. Cited in pag.

Aydin and Kizilkan(2012) Kemal Aydin and Glünur Kizilkan. *Step size strategies for the numerical integration of systems of Differential Equations. Journal of Computational and Applied Mathematics*, 236:3805–3816. Cited in pag.

Bellman(1966) Richard Bellman. *Numerical Inversion of the Laplace Transform: Applications to Biology, Economics, Engineering and Physics.* American Elsevier Publishing Company, INC. University of Southern California. Cited in pag.

Bishop and Isaacson(2003) Herbert Bishop and Eugene Isaacson. *Introduction to Numerical Analysis.* Cambridge, New York. Cited in pag.

Burlish and Stoer(2002) R. Burlish and J. Stoer. *Introduction to Numerical Analysis*, 3rd Edition. Springer. Cited in pag.

Busch *et al.***(2014)** Kurt Busch, Abdullah Demirel, Marlis Hochbruck and Jens Niegemann. *Efficient Multiple Time-Stepping Algorithms of Higher Order. Journal of Computational Physics*, Preprint:1–7. Cited in pag.

Cheney and Kincaid(2008) Wan Cheney and David Kincaid. *Numerical Mathematics and Computing*, 6th Edition. Thomson Brookscole. Cited in pag.

Clancy(2010) Colm Clancy. *A Filtering Laplace Transform Integration Scheme for Numerical Weather Prediction.* PhD Thesis, University College Dublin. Cited in pag.

Clancy and Lynch(2011) Colm Clancy and Peter Lynch. *Laplace Transform Integration of the Shallow Water Equations. Part 1: Eulerian formulation and Kelvin waves. Quarterly Journal of Royal Metereological Society*, pages 1–7. Cited in pag.

Clancy and Lynch(1994) Colm Clancy and Peter Lynch. *Improving the Laplace Transform Integration Method. Quarterly Journal of the Royal Metereological Society*, 142:1196–1200. Cited in pag.

Clancy and Lynch(2015) Colm Clancy and Peter Lynch. *Notes and Correspondence Improving the Laplace Transform Integration Method. Royal Metereological Society*, 142:1196–1200. Cited in pag.

Cohen(2007) Alan Cohen. *Numerical Methods for Laplace Transform Inversion.* Springer. Cited in pag.

Coiffer(2011) Jean Coiffer. *Fundamentals of Numerical Weather Prediction.* Cambrigde University Press. Cited in pag.

Cox and Matthews(2002) S. M. Cox and P. C. Matthews. *Exponential Time Differencing for Stiff Systems. Journal of Computational Physics*, 176:430–455. Cited in pag.

Craig and Thompson(1994) I. J. D. Craig and A. M. Thompson. *Why Laplace Transforms are Difficult to Invert Numerically. Computers in Physics*, 8:648–654. Cited in pag.

Davies(1999) Alan Davies. *The Solution of Differential Equations Using Numerical Laplace Transforms. International*, 30:1:65–79. Cited in pag.

Deng(2015) Yuefan Deng. *Lectures, Problems and Solutions for Ordinary Differential Equations.* World Scientific Publishing. Stony Brook University, USA. Cited in pag.

Griffiths and Highman(2010) David F. Griffiths and Desmond J. Highman. *Numerical Methods for Ordinary Differential Equations, Initial Value Problems.* Springer, London. Cited in pag.

Groove(1991) A. C. Groove. *An Introduction to the Laplace Transform and Z-Transform.* Prentice Hall International, United Kingdom. Cited in pag.

Higham(2002) Nicholas J. Higham. *Accuracy and Stability of Numerical Algorithms*, 2nd Edition. SIAM. Cited in pag.

Hochbruck and Ostermann(2010) Marlis Hochbruck and Alexander Ostermann. *Exponential integrators.* Technical report, Cambridge University, United Kingdom. Cited in pag.

Howie(2003) Jonh Mackintosh Howie. *Complex Analysis.* Springer, London. Cited in pag.

Jose(2004) Figueroa O'Farrill Jose. *Mathematical Techniques.* University of London. Cited in pag.

Kreiszig(2011) Erwin Kreiszig. *Advanced Engineering Mathematics*, 10th Edition. Laurie Rosatone. Cited in pag.

Langer(1954) Rudolph E. Langer. *A First Course in Ordinary Differential Equations.* John Wiley and Sons, University of Winsconsin. Cited in pag.

Li *et al.***(2010)** Chen Yan Li, Yan Quan and Hu Sheng. *Applications of Numerical Inverse Laplace Transform Algorithms in Fractional Calculus. Franklin Insitute*, 348:315–330. Cited in pag.

Logemann and Ryan(2013) Harmut Logemann and Eugene P. Ryan. *Ordinary Differential Equations: Analysis, Qualitative Theory and Control.* Springer, London. Cited in pag.

Lynch(1985) Peter Lynch. *Initialization of the Barotropic Limited-Area Model Using the Laplace Transform Technique. American Metereological Society*, 113:1338–1344. Cited in pag.

Lynch(1986) Peter Lynch. *Numerical Forecasting using Laplace Transforms Theory and Applications to the Data Assimilation.* Technical Report 48, Irish Metereological Service, Glasnevin Hill, Dublin. Cited in pag.

Lynch(1996) Peter Lynch. *The Swinging Spring: A Simple Model of Atmospheric Balance. Proceedings of the Symposium on the Mathematics of Atmosphere-Ocean Dynamics, Isaac Newton Institute.* Cited in pag.

Mayers and Süli(2003) David Mayers and Endre Süli. *Introduction to Numerical Analysis.* Cambridge, University of Oxford. Cited in pag.

Ngounda(2009) Edgard Ngounda. Numerical methods for integrating lineal parabolic partial differential equations. Master's Thesis, Applied Mathematics, Department of Mathematical Sicences. University of Stellenbosch, South Africa. Cited in pag.

Pope(1963) David A. Pope. *An Exponential Method of Numerical Integration of Ordinary Differential Equations. Communications of the ACM*, 6:491–493. Cited in pag.

Rahman and Thohura(2013) Azad Rahman and Sharaban Thohura. *Numerical Approach for Solving Stiff Differential Equations: A Comparative Study. Global Journal of Science Frontier Research Mathematics and Decision Sciences*, 13:7–18. Cited in pag.

Randall(2013) David A. Randall. *An Instroduction to Numerical Modeling of the Atmosphere, Class Notes.* Department of Atmospheric Science,Colorado State University. Cited in pag.

Rani *et al.***(2019)** Dimple Rani, Vinod Mishra and Carlo Cattani. *Numerical Inverse Laplace Transform for Solving a Class of Fractional Differential Equations. Simmetry*, 11:1–20. Cited in pag.

Sawant(2018) L. S. Sawant. *Applications of Laplace Transform in Engineerig Fields. International Reasearch Journal of Engineering and Technology (IRJET)*, 5:3100–3105. Cited in pag.

Schiff(1999) Joel L. Schiff. *Laplace Transform, Theory and Applications.* Springer, New York. Cited in pag.

Smith(1966) M. G. Smith. *The Laplace Transform: Theory and Applicarions.* Springer, London. Cited in pag.

Spiegel(1965) Murray R. Spiegel. *Theory and Problems of Laplace Transforms.* McGraw Hill, Rensselaer Polytechnic Institute. Cited in pag.

Struylaert and Isacker(1987) W. Struylaert and J. Van Isacker. *Laplace Transform Applied to a Baroclinic Model. Royal Metereological Society*, pages 247–253. Cited in pag.

Struylaert and Isacker(1985) W. Struylaert and J. Van Isacker. *Numerical Forecasting using Laplace Transforms.* Technical Report A-115, Royal Belgian Meteorological Institute, Belgium. Cited in pag.

Uerberhuber(1997) Christoph W. Uerberhuber. *Numerical Computation 1: Methods, Software and Analysis.* Springer, Berlin. Cited in pag.

Complex Analysis Review

In this part we present an overview of the theory of complex analysis, which is required to understand and apply complex integration formulas. More details about complex analysis theory can be found at Schiff (1999), Spiegel (1965), Howie (2003), Ablowitz and Fokas (2003), Jose (2004), Kreiszig (2011).

.1 Complex numbers

We will use Euler's notation for the imaginary unit number:

$$i^2 = -1.$$

A complex number is an expression of the form:

$$z = x + iy,$$

where x represents the real part of z, $Re(z)$, and y represents the imaginary part of z, $Im(z)$. The set $\mathbb{C}$ of complex numbers is naturally identified with the plane $\mathbb{R}^2$, and is often referred as *Argand Plane* (see Figure 1).

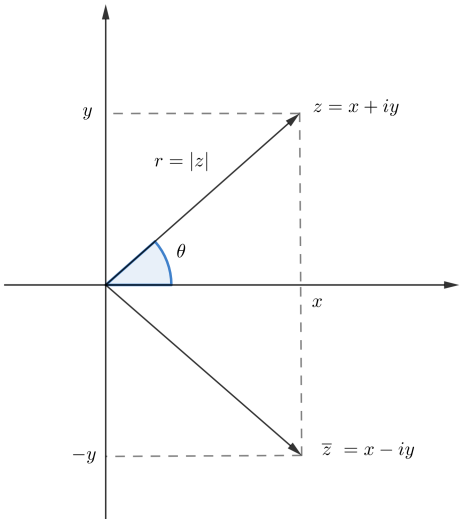

Figure 1: *Argand Plane.*

Definition .1. *The complex number $\overline{z} = x - iy$ is called the **complex conjugate** of $z = x + iy$.*

Points in the complex plane can also be represented using polar coordinates:

$$x = rcos\theta;$$
$$y = rsin\theta.$$

Then

$$z = r\cos\theta + i(r\sin\theta) = r(\cos\theta + i\sin\theta), \tag{1}$$

where $r = |z| = \sqrt{x^2 + y^2}$, and θ is the angle of z (also called ***argument of*** z, $\theta = arg(z)$).

We can rewrite equation (1) as

$$z = re^{i\theta}, \quad 0 \leq \theta < 2\pi, \tag{2}$$

Euler's formula (exponential version of a complex number). The expression (2) represents any point on a circle of radius r (see Figure 2).

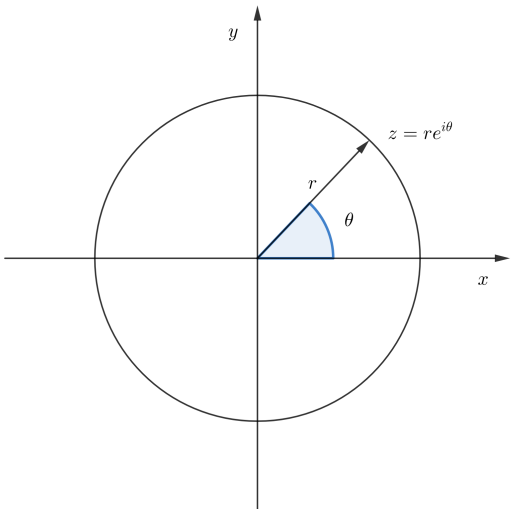

Figure 2: *Complex circle of radius r.*

Let $z_1 = x_1 + iy_1$ and $z_2 = x_2 + iy_2$ two non-null complex numbers. The following algebraic operations are defined.

Addition and subtraction. The sum (subtraction) of complex two numbers is a complex number.

$$z_1 \pm z_2 = (x_1 \pm x_2) + i\,(y_1 \pm y_2)$$

Product. The product of complex two numbers is a complex number.

$$z_1 z_2 = (x_1 x_2 - y_1 y_2) + i\,(x_1 y_2 + x_2 y_1)$$

Division.

$$\frac{z_1}{z_2} = \frac{x_1 + iy_1}{x_2 + iy_2} . \frac{x_2 - iy_2}{x_2 - iy_2} = \frac{z_1 \overline{z_2}}{|z_2|^2}$$

Some useful results concerning complex numbers are mentioned below.

Triangular Inequality. Let $z_1 = x_1 + iy_1$ and $z_2 = x_2 + iy_2$ two non-null complex numbers. Then

$$||z_1| - |z_2|| \leq |z_1 + z_2| \leq |z_1| + |z_2|\,.$$

Moivre's Formula. For any complex number z (and in particular, for any real number) and

for any integer n it is verified that

$$z^n = \left(re^{i\theta}\right)^n = r^n e^{i\theta n}.$$

Roots of a complex number. Let $z = re^{i\theta} = r(\cos\theta + i\sin\theta)$ and $\omega = \rho e^{i\phi} = r(\cos\phi + i\sin\phi)$. Suppose that it is required to solve the equation $z^n = \omega$ with

$$\begin{aligned} z^n &= r^n e^{in\theta} = r^n(\cos\theta n + i\sin\theta n), \\ \omega &= \rho e^{i\phi} = r(\cos\phi + i\sin\phi). \end{aligned} \tag{3}$$

then

$$z^n = r^n(\cos\theta n + i\sin\theta n) = \rho e^{i\phi} = r(\cos\phi + i\sin\phi) = \omega. \tag{4}$$

Thus

$$\begin{aligned} r^n &= \rho, \\ \theta n &= \phi + 2k\pi, \quad k = 0, 1, ..., n-1, \end{aligned}$$

or equivalently

$$\begin{aligned} r &= \rho^{1/n}, \\ \theta &= \tfrac{\phi+2k\pi}{n}, \quad k = 0, 1, ..., n-1. \end{aligned} \tag{5}$$

By (2) and (5):

$$\begin{aligned} z^{1/n} &= \rho^{1/n}\left(\cos\left(\tfrac{\phi+2k\pi}{n}\right) + i\sin\left(\tfrac{\phi+2k\pi}{n}\right)\right), \\ z^{1/n} &= \rho^{1/n} e^{i\left(\frac{\phi+2k\pi}{n}\right)}, \end{aligned} \tag{6}$$

for $n \in \mathbb{N}$. This means z has ***n-distinct roots***.

Example .1. *For $n = 4$ the roots of $z = 1$, are given by:*

$$z^{1/4} = e^{i\left(\frac{0+2k\pi}{4}\right)}, \quad k = 0, 1, 2, 3,$$

that is:

$$\begin{aligned} z_1 &= 1 \\ z_2 &= e^{i\left(\frac{\pi}{2}\right)} = i \\ z_3 &= e^{i\pi} = -1 \\ z_4 &= e^{i\left(\frac{3\pi}{2}\right)} = -i \end{aligned} \tag{7}$$

The n-roots of a complex number z represent the vertices of an inscribed regular polygon on the complex plane (see Figure 3).

.2 Complex functions

A complex valued function $w = f(z)$ of a complex variable assigns to each independent variable z one or more dependent variables w. If there is only one such value w, then the function $f(z)$ is called ***single-valued***; otherwise $f(z)$ is ***multiple valued*** (Schiff (1999)).

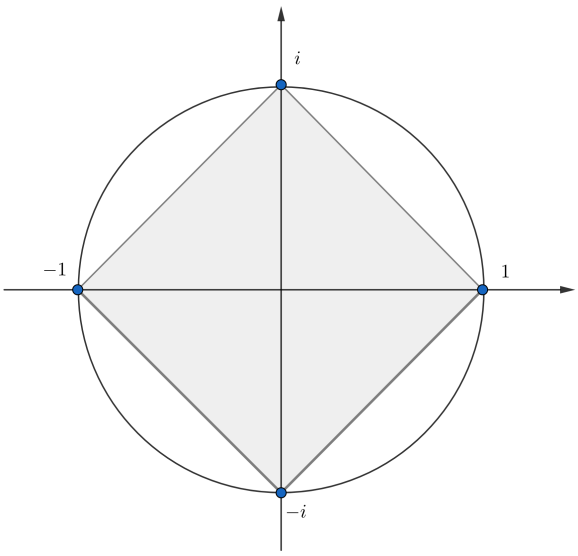

Figure 3: *Roots of the unity - Example .1*

Let $z = x + iy$ and $w = u + iv$. Then we can write:

$$w = f(z) = u(x, y) + iv(x, y),$$

where $u = u(x, y)$ and $v = v(x, y)$ are real valued functions that represent the real and imaginary parts of $f(z)$.

Example .2.

$$\begin{aligned} f(z) &= z^2 + 1 = (x^2 - y^2) + 1 + 2ixy \\ g(z) &= e^{iz} = e^{-y}\cos x + ie^{-y}\sin x \end{aligned}$$

where f, g are single valued complex functions.

Let $z \in \mathbb{C}$. Some important complex functions are listed bellow.

Power series.

$$f(z) = \sum_{k=0}^{n} a_k z^k$$

Rational functions

$$f(z) = \frac{\sum_{k=0}^{n} a_k z^k}{\sum_{j=0}^{m} a_j z^j}$$

Taylor series

$$f(z) = \sum_{k=0}^{\infty} a_k (z - z_0)^k,$$

which is convergent only if $L = \lim_{k\to\infty} \left|\frac{a_{k+1}}{a_k}\right|$ exists. Thus f converges for $|z - z_0| < \frac{1}{L}$ *(radius of convergence)*.

Exponential function

$$e^z = \sum_{k=0}^{\infty} \frac{z^k}{k!}$$

Trigonometric functions

$$\sin z = \frac{e^{iz} - e^{-iz}}{2i}$$

$$\cos z = \frac{e^{iz} + e^{-iz}}{2}$$

Hyperbolic functions

$$\sinh z = \frac{e^{z} - e^{-z}}{2}$$

$$\cosh z = \frac{e^{z} + e^{-z}}{2}$$

Trigonometric identities

$$i \sin z = \sinh iz \qquad \sin iz = i \sinh z$$

$$\cos z = \cosh iz \qquad \cos iz = \cosh z$$

Complex logarithm. Let $z = x + iy$ and $w = u + iv$. The complex number w, such $e^w = z$ is called *logarithm of* z, i.e:

$$w = \log z.$$

Notice:

$$\begin{aligned} x + iy &= z = e^w \\ &= e^{u+iv} = e^u e^{iv} \\ &= e^u(\cos v + i \sin v). \end{aligned}$$

Then:

$$\begin{aligned} x &= e^u \cos v, \\ y &= e^u \sin v. \end{aligned} \tag{8}$$

To obtain $R = |z|$:

$$\begin{aligned} |z| &= \sqrt{x^2 + y^2} \\ &= \sqrt{e^{2u}(\cos^2 v + \sin^2 v)} = \sqrt{e^{2u}} \\ &= e^u. \end{aligned}$$

Thus $u = \ln |z|$, which is a real value logarithm. From (8) we have that $arg(z) = v$ is the

angle of z. So:

$$w = u + iv = \log z \to \log z = \ln|z| + iarg(z).$$

However, $\theta + 2k\pi$ also works as an angle:

$$\log z = \ln|z| + i(arg(z) + 2k\pi), \quad \forall k \in \mathbb{Z}, \theta \in [0, 2\pi). \tag{9}$$

For $k = 0$, (9) is called ***principal value or principal logarithm***. Complex logarithm is a classic example of a multivalued function (see Figure 4).

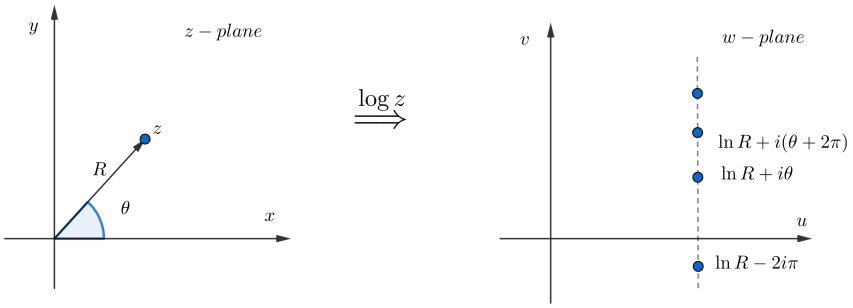

Figure 4: *Complex logarithm.*

Example .3. *Calculate the principal value of* $z = 1 - \sqrt{3}i$*:*

$$\log(1 - \sqrt{3}i) = \ln|1 - \sqrt{3}i| + iarg(1 - \sqrt{3}i).$$

We know that $\theta = arg(z) = \arctan(\frac{y}{x})$*. Then:*

$$arg(z) = \arctan\left(\frac{-\sqrt{3}}{1}\right) = \arctan(-\sqrt{3}) = \frac{5\pi}{3}.$$

Thus,

$$\log(1 - \sqrt{3}i) = \ln 2 + \frac{5i\pi}{3}.$$

.3 Analytic functions and Cauchy Riemann conditions

Definition .2 (Schiff (1999))**.** *A complex function* $f(z)$ *defined on a connected open domain* D *is differentiable at a point* $z_0 \in D$ *if the limit*

$$\frac{df}{dz}(z_0) = f'(z_0) = \lim_{z \to z_0} \frac{f(z) - f(z_0)}{z - z_0}$$

exists.

If $f(z)$ is differentiable at all points of some neighbourhood $|z - z_0| < r$ then $f(z)$ is said to be ***analytic*** at z_0. Since analytic functions are differentiable, they are continuous.

Definition .3 (Cauchy - Riemann conditions (Schiff (1999)))**.** *Let* $f(z) = u(x, y) + iv(x, y)$ *an analytic function. The real and imaginary parts (*u *and* v*), cannot be arbitrary functions, have to satisfy the following property:*

$$u_x = v_y, \quad u_y = -v_x. \tag{10}$$

As a consequence of (10), a non-constant analytic function $f = u + iv$ cannot have $v \equiv 0$, for Cauchy Riemann conditions would imply that u is a constant function, which is a contradiction.

Theorem .1. *If $f(z) = u(x,y)+iv(x,y)$ is single valued and defined in a domain D and u_x, u_y, v_x, v_y are continuous and satisfy (10), then $f(z)$ is analytic in D.*

Proof. See Kreiszig (2011). □

Remark .1 (Characterization of Analytic Functions (Schiff (1999))). *A function $f(z)$ is analytic at z_0 if and only if its Taylor series*

$$f(z) = \sum_{n=0}^{\infty} \frac{f^n(z_0)}{n!}(z - z_0)^n$$

converges to the function in a neighbourhood of z_0.

Theorem .2. *Let $f(t)$ be piecewise continuous on $[0, \infty)$ and of exponential order α ($f \in \mathcal{L}$). Then:*

$$F(s) = \mathfrak{L}\{f(t)\},$$

is an analytic function in the domain $Re(s) > \alpha$.

Proof. See Schiff (1999). □

Example .4. *The function $f(z) = (z - z_0)^n$ is not analytic for $n = -1, -2, -3, ...$*

.4 Integrals in the complex plane

Definition .4 (Schiff (1999)). *A **Contour** C is a continuous curve that is piecewise smooth, that is, there is a subdivision $\alpha = t_0 < t_1 < ... < t_n = \beta$ and $z = z(t)$ is smooth on each subinterval $[t_{k-1}, t_k]$, $k = 1, 2, .., n$ with $n \in \mathbb{N}$. The points $z(\alpha)$ and $z(\beta)$ are the initial and final points, and if $z(\alpha) = z(\beta)$ then the contour is called **closed** (see Figure 5).*

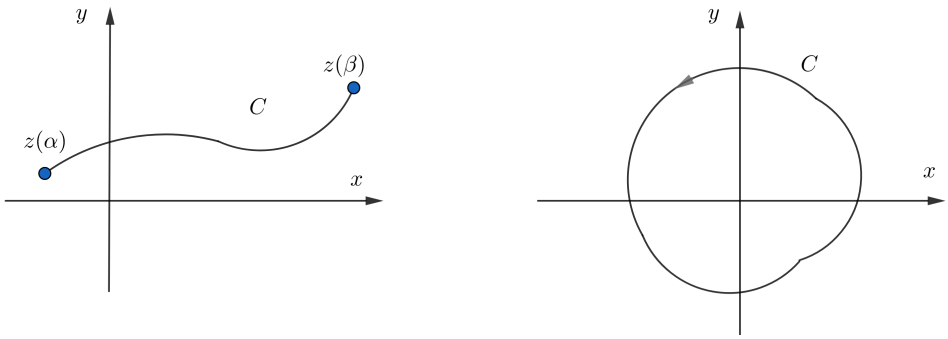

Figure 5: *On the left an example of a simple contour, on the right an example of a closed simple contour.*

Definition .5. *If the contour C does not cross itself, it is called **simple** (see Figure 5).*

Theorem .3. *If C is a curve joining z_0 and z_1 in a simple, closed connected region where $f(z)$ is analytic, then the integral*

$$\int_C f(z)dz$$

is independent of the path (see figure (6)).

Proof. See Kreiszig (2011). □

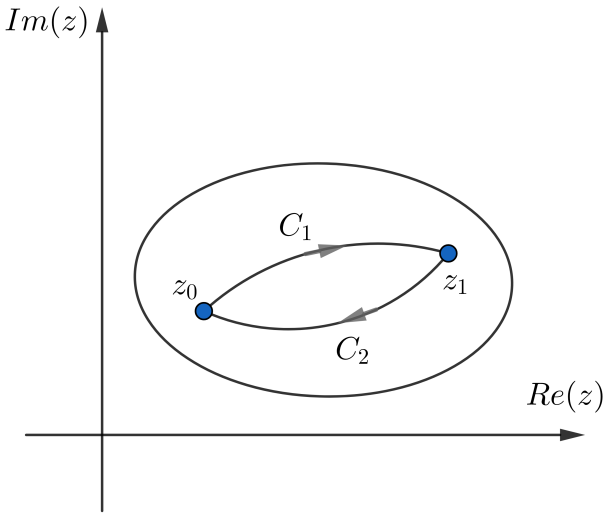

Figure 6: *Independence of the path, $C = C_1 + C_2$.*

Theorem .4 (Cauchy - Goursat)**.** *Let $f(z)$ be analytic in a simply connected domain D. Then for any closed contour C in D,*

$$\int_C f(z)dz = 0. \tag{11}$$

Proof. Since $f(z)$ is a complex function:

$$\int_C f(z)dz = \int_C (u+iv)\,(dx+idy) = \int_C (udx - vdy) + i\int_C (vdx + udy).$$

By the Green's theorem:

$$\iint_D (-v_x - u_y)\,dxdy + i\iint_D (u_x - v_y)\,dxdy.$$

since f is an analytic function it satisfies the Cauchy Riemann conditions given in (10). Then:

$$\int_C f(z)dz = 0.$$

□

Corolary .1 (Principle of deformation of the paths)**.** *Let C_1 and C_2 be two closed simple contours positively oriented (counterclockwise), where C_2 is inside C_1. If $f(z)$ is analytic in the closed region formed by those contours and the points between them, then:*

$$\int_{C_1} f(z)dz = \int_{C_2} f(z)dz.$$

(See figure 7).

Example .5. *Let $f(z) = (z-a)^n$, which is not analytic for $n = -1, -2, ...$ Nevertheless its integral over close contours has nice properties.*

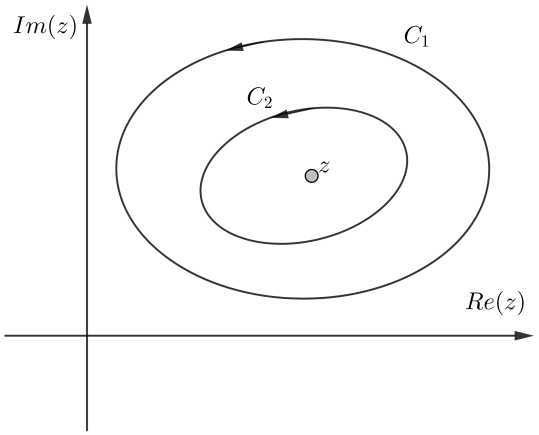

Figure 7: *Deformation of the paths.*

Case 1: *For* $n = -2, -3, \cdots$ *and* $n > 0$*:*

$$\int_C (z-a)^n dz = \left[\frac{(z-a)^{n+1}}{n+1}\right]_{z_0}^{z_1} = 0.$$

Since $f(z)$ *is analytic for these values of* n*, the integral is equal to zero due to theorem (.4).*

Case 2: *For* $n = -1$*:*

$$\int_C (z-a)^{-1} dz = \left[\log(z-a)\right]_{z_0}^{z_1} \neq 0,$$

because $\log(z-a)$ *is a multivalued function. In order to calculate the value of the integral, we deform* C *into a circle of radius* R *and use the polar form of a complex number. Let's take:*

$$\begin{aligned} z - a &= Re^{i\theta}, \\ dz &= iRe^{i\theta} d\theta. \end{aligned}$$

So,

$$\begin{aligned} \int_C (z-a)^{-1} dz &= \int_0^{2\pi} \frac{iRe^{i\theta}}{Re^{i\theta}} d\theta \\ &= \int_0^{2\pi} i d\theta \\ &= 2\pi. \end{aligned}$$

From cases 1 *and* 2 *we have:*

$$\int_C (z-a)^{-n} dz = \begin{cases} 0 & , \quad n \neq -1 \\ 2\pi & , \quad n = -1 \end{cases}. \tag{12}$$

Theorem .5 (Cauchy integral formula)**.** *Let* $f(z)$ *be analytic within and on a simply closed contour* C*. If* z_0 *is any interior point in* C*, then*

$$\left[\frac{d^n f}{dz^n}\right]_{z=z_0} = \frac{n!}{2\pi i} \int_C \frac{f(z)}{(z-z_0)^{n+1}} dz. \tag{13}$$

In particular, for $n = 0$

$$f(z_0) = \frac{1}{2\pi i}\int_C \frac{f(z)}{z - z_0}dz. \tag{14}$$

Proof. To derive equation (14) we write:

$$\int_C \frac{f(z)}{z - z_0}dz = \int_C \frac{f(z_0)}{z - z_0}dz + \int_C \frac{f(z) - f(z_0)}{z - z_0}dz.$$

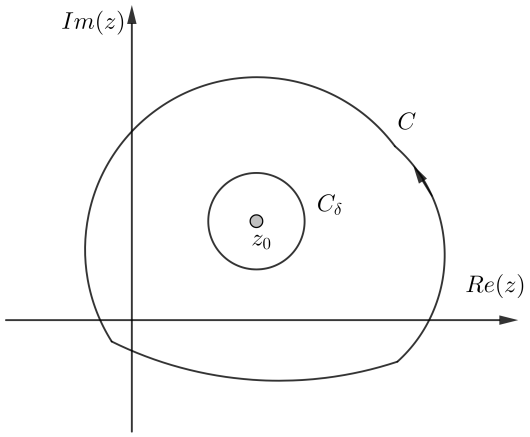

Figure 8: *Contour* C *deformed into a circle* C_δ.

To show that the second integral on the right side is zero we going to deform C into a circle C_δ of radius δ (Figure 8).

Since $f(z)$ is analytic around z_0, it is possible to choose a δ such that $|f(z) - f(z_0)| < \epsilon$ on C_δ. So:

$$\left|\int_C \frac{f(z) - f(z_0)}{z - z_0}dz\right| \leq \int_C \left|\frac{f(z) - f(z_0)}{z - z_0}\right| dz \leq \int_C \frac{\epsilon}{z - z_0}dz,$$

and by the result (12) obtained in Example .5:

$$\left|\int_C \frac{f(z) - f(z_0)}{z - z_0}dz\right| \leq 2\pi i\epsilon.$$

Letting $\epsilon \to 0$,

$$\int_C \frac{f(z) - f(z_0)}{z - z_0}dz = 0.$$

Then:

$$\int_C \frac{f(z)}{z - z_0}dz = \int_C \frac{f(z_0)}{z - z_0}dz + 0 = f(z_0)\int_C \frac{1}{z - z_0}dz$$

$$\overset{(12)}{=} 2\pi f(z_0)$$

Hence:

$$f(z_0) = \frac{1}{2\pi i}\int_C \frac{f(z)}{z - z_0}dz.$$

The proof of (13) can be found in Kreiszig (2011).

□

Definition .6 (Schiff (1999)). *A power series is an infinity series of the form:*

$$\sum_{n=0}^{\infty} a_n (z - z_0)^n = a_0 + a_1(z - z_0) + a_2(z - z_0)^2 + \cdots \tag{15}$$

where z is a complex variable and $z_0, a_0, a_1, \cdots$ are fixed complex numbers.

The power series given by equation (15) has a radius of convergence $R \geq 0$:

For $R = 0$, (15) converges only for $z = z_0$;

For $0 < R < \infty$, (15) converges absolutely for $|z - z_0| < R$;

For $|z - z_0 \leq R_0 < R$, (15) converges uniformly;

For $|z - z_0| > R$, (15) diverges;

For $R = \infty$, (15) converges for all $z \in \mathbb{C}$.

The value of R is given by

$$R = \frac{1}{\lim_{n\to\infty} \sqrt[n]{|a_n|}}$$

or by

$$R = \lim_{n\to\infty} \left| \frac{a_n}{a_{n+1}} \right|,$$

whenever the limit exists.

Theorem (.1) shows that an analytic function can be represented by a Taylor series, but in cases where this series can not be applied, an alternative option is to use Laurent Series.

Definition .7. *A Laurent series, around a point z_0, is defined as*

$$f(z) = \sum_{n=1}^{+\infty} a_{-n}(z - z_0)^{-n} + \sum_{n=0}^{+\infty} a_n (z - z_0)^n \tag{16}$$

or

$$f(z) = \sum_{n=-\infty}^{\infty} a_n (z - z_0)^n, \tag{17}$$

where

$$a_n = \frac{1}{2\pi i} \int_C \frac{f(z)}{(z - z_0)^{n+1}} dz. \tag{18}$$

*The first sum in (16) is called **principal part** while the second sum is called **analytic part**.*

A Laurent series converges in the annulus $0 < |z - z_0| < R$ (see Figure 9), where:

$$\begin{aligned} R &= \left(\underset{n\to\infty}{limsup} \sqrt[n]{|a_n|} \right)^{-1}; \\ r &= \underset{n\to\infty}{limsup} \sqrt[n]{|a_{-n}|}. \end{aligned} \tag{19}$$

Analytic functions have very useful properties in complex integration, so it is important to study also those points at which a function ceases to be analytic.

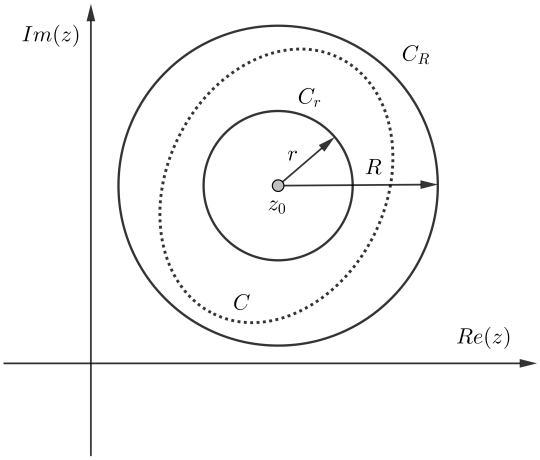

Figure 9: *Annulus of convergence for Laurent series.*

Definition .8. *A **singularity** z_0 of a function $f(z)$ is a point at which $f(z)$ is not analytic.*

Definition .9. *A function has an **isolated singularity** in $z = z_0$ if f is not analytic in z_0, and there is a $R > 0$ such that f is analytic in a punctured disk $D = \{z \in \mathbb{C}, 0 < |z - z_0| < R\}$.*

Isolated singularities can be of three types.

Removable. A function f has a removable singularity at z_0 if and only if

$$\exists \lim_{z \to z_0} f(z) \Rightarrow \lim_{z \to z_0} (z - z_0) f(z) = 0.$$

Or equivalently, if and only if $a_n = 0$ for all $n > -1$, where a_n is the coefficient of Laurent expansion of f given by (18).

Pole. Let D be such that $a \in D$, f analytic in D. The function f has a pole on z_0 of order m if and only if there is a positive integer m and an analytic function $g : D \to \mathbb{C}$ with $g(a) \neq 0$ such that

$$f(z) = \frac{g(z)}{(z - z_0)^m}.$$

Or equivalently, if and only if $a_{-n} \neq 0$ and $a_n = 0$ for all $n \leq -(n + 1)$, where a_n is the coefficient of Laurent expansion of f given by (18). If $m = 1$ then the pole is called **simple pole**.

Essential. An essential singularity z_0 is an isolated singularity that is not removable and is not a pole. Or equivalently, z_0 is an isolated singularity if and only if $a_n \neq 0$ for infinite negative values of n

Definition .10. *Let f be an analytic function and z_0 an isolated singularity of f. The **residue** of f is given by the coefficient a_{-1} from its Laurent expansion.*

$$Res[f, z_0] = a_{-1}$$

In general, Laurent series is used to calculate the residues of a function. However, in cases where the singularity is a pole, there are simpler procedures that can be applied.

If f has a pole of order m in z_0, the residue is obtain using:

$$\begin{aligned} m = 1 \quad &: \quad Res\left[f, z_0\right] = \lim_{z \to z_0} \left(z - z_0\right) f\left(z\right); \\ m > 1 \quad &: \quad Res\left[f, z_0\right] = \tfrac{1}{(m-1)} \lim_{z \to z_0} \tfrac{d^{m-1}}{dz_0{}^{m-1}} \left[\left(z - z_0\right)^m f\left(z\right)\right]. \end{aligned} \tag{20}$$

Theorem .6 (Residue). *Suppose that $f(z)$ is an analytic function on a simply-connected domain D except for a finite number of poles $z_1, z_2, ..., z_k$. Suppose that C is a piecewise smooth positively-oriented simple closed curve not passing through $z_1, z_2, ..., z_k$. Then,*

$$\frac{1}{2\pi i} \int_C f\left(z\right) dz = \sum_{z_j \in C} Res\left[f, z_j\right].$$

Proof. See Kreiszig (2011). □

Lemma .1 (Jordan's Lemma). *Let f be continuous for large $R = |z|$, and assume that $f(z) \to 0$ as $z \to \infty$. Then, provided $t > 0$, we have:*

$$\lim_{R \to \infty} \int_{C_R} f\left(z\right) e^{tz} dz = 0$$

where C_R denotes a semicircular contour with $\theta \to a + Re^{i\theta}$, $\frac{\pi}{2} < \theta < \frac{3\pi}{2}$ (see Figure 10).

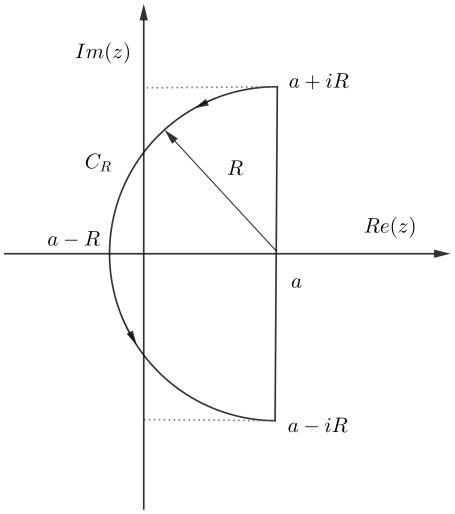

Figure 10: *Semicircle C_R*

Proof. Let $\epsilon > 0$. Because $f(z) \to 0$ as $z \to \infty$, there exists $k > 0$ such that $|z| \geq k$ implies $|f(z)| \leq \epsilon$. This means that $|f(z)| \leq \epsilon$ whenever $|z - a| \geq k + |a|$, because $|z| + |a| \geq |z - a|$. For $R \geq k + |a|$, we have:

$$\begin{aligned}
\left|\int_{C_R} f(z)\, e^{tz} dz\right| &\leq \int_{C_R} \left|f(z)\, e^{tz} dz\right| \\
&\leq \epsilon \int_{C_R} \left|e^{tz}\right| |dz|, \quad |z-a| = R \geq k + |a| \\
&= \epsilon \int_{C_R} e^{tRe(z)} |dz| = \epsilon \int_{\frac{\pi}{2}}^{\frac{3\pi}{2}} e^{ta} e^{tR\cos\theta} R d\theta, \quad z = a + Re^{i\theta} \\
&= 2\epsilon R e^{ta} \int_{\frac{\pi}{2}}^{\pi} e^{tR\cos\theta} d\theta, \quad by \quad symmetry \\
&= 2\epsilon R e^{ta} \int_0^{\frac{\pi}{2}} e^{-tR\sin\theta} d\theta \\
&\overset{(*)}{\leq} 2\epsilon R e^{ta} \int_0^{\frac{\pi}{2}} e^{\frac{-2tR\theta}{\pi}} d\theta \\
&= 2R e^{ta} \epsilon \left[\frac{-\pi}{2tR} e^{\frac{-2tR\theta}{\pi}}\right]_0^{\frac{\pi}{2}} \\
&= \frac{e^{ta}\pi\epsilon}{t}\left(1 - e^{-tR}\right) \\
&\leq \frac{e^{ta}\pi\epsilon}{t}.
\end{aligned}$$

Since $t > 0$ is fixed, this final quantity can be made as small as desired. □

$(*)$ Jordan's inequality states that:

$$\frac{2}{\pi}\theta \leq \sin\theta \leq \theta \quad for \quad \theta \in \left[0, \frac{\pi}{2}\right].$$